Aus dem Institut für Medizinische Immunologie
der Medizinischen Fakultät Charité – Universitätsmedizin Berlin

DISSERTATION

Paralysis of pulmonary immunity after stroke by neurohumoral mechanisms

zur Erlangung des akademischen Grades
Doctor of Philosophy (PhD)

vorgelegt der Medizinischen Fakultät
Charité – Universitätsmedizin Berlin

von

Sandra Jagdmann

Datum der Promotion: 04.03.2022

TABLE OF CONTENTS

LIST OF ABBREVIATIONS

ACh	acetylcholine
ACTH	adrenocorticotrophic hormone
AM	alveolar macrophages
ANOVA	analysis of variance
BAL	bronchoalveolar lavage
BALF	bronchoalveolar lavage fluid
CFU	colony forming units
CNS	central nervous system
CRH	corticotropin-releasing hormone
DC	dendritic cell
EDTA	ethylenediaminetetraacetic acid
ELISA	enzyme-linked immunosorbent assay
FCS	fetal calf serum
GC	glucocorticoid
G-CSF	granulocyte colony-stimulating factor
GM-CSF	granulocyte-macrophage colony-stimulating factor
HMGB1	high mobility group box 1
HPA	hypothalamic-pituitary-adrenal
IFN-γ	interferon γ
IL	interleukin
IM	interstitial macrophages
i.n.	intranasal
i.p.	intraperitoneal
IP-10	IFN-γ-induced protein 10
i.t.	intratracheal
KO	knockout
LPS	lipopolysaccharide
LTA	lipoteichoic acid
MCAo	middle cerebral artery occlusion

miRs	MicroRNAs
nAChR	nicotinic acetylcholine receptor
NK cell	natural killer cell
PBMC	peripheral blood mononuclear cells
PBS	phosphate-buffered saline
PVN	paraventricular nucleus
qRT-PCR	quantitative reverse transcriptase polymerase chain reaction
RPMI	roswell park memorial institute
SAP	stroke-associated pneumonia
s.c.	subcutaneous
STAT1	signal transducer and activator of transcription 1
SNS	sympathetic nervous system
TF	transcription factor
TFEC	transcription factor EC
TGF- β	transforming growth factor β
tRFs	transfer RNA fragments
zbp1	Z-DNA-binding protein 1

ZUSAMMENFASSUNG

Bakterielle Pneumonien gehören zu den schwerwiegendsten Komplikationen nach Schlaganfall, deren zugrundeliegenden pathophysiologischen Mechanismen nur unzureichend verstanden sind. Eine Überaktivierung des autonomen und insbesondere auch des cholinergen Systems nach Schädigung des zentralen Nervensystems (ZNS) trägt maßgeblich zu einer schnell einsetzenden, temporären Immunsuppression und damit zur Entwicklung von Schlaganfall-assoziierten Pneumonien (SAP) bei. Der α7 nikotinerge Acetylcholinrezeptor (nAChR) wurde im experimentellen Schlaganfall als wichtiger Mediator der beeinträchtigten Immunantwort in einer spontanen SAP identifiziert. Da *in vitro* Versuche auf eine Beteiligung von nicht-α7nAChR an einer pulmonalen Immunsuppression hinwiesen, wurde in der **ersten Studie** die Rolle von den in der Lunge exprimierten α2, α5, α7 und α9/10nAChR in einem Mausmodell der Aspirations-induzierten Pneumokokken-Pneumonie nach Schlaganfall untersucht. Die Abwesenheit verschiedener nAChR hatte keinen Einfluss auf die Rekrutierung von Leukozyten in Lunge und Milz sowie die pulmonale pro- und anti-inflammatorische Zytokinantwort und führte letztlich nicht zur verbesserten Beseitigung des Erregers, was dafürspricht, dass nAChR die gestörte Immunantwort gegen Pneumokokken nach Schlaganfall nicht vermitteln. Das cholinerge System kann auf der Ebene der Acetylcholinsynthese, des Transportes, der Freisetzung, der kognaten Rezeptoren, aber auch durch die Regulation der Expression der zugrundeliegenden Gene mittels kleiner RNAs beeinflusst werden. In der **zweiten Studie** wurden daher kleine RNAs im Blut von Schlaganfallpatienten untersucht und eine Verringerung der Mikro-RNAs (miRs) und einen Anstieg der Transfer-RNA-Fragmente (tRFs) zwei Tage nach Schlaganfall nachgewiesen. Die Schlaganfall-induzierten tRFs enthielten komplementäre Motive zu aktiven Transkriptionsfaktoren in Monozyten, die unter anderem cholinerge Gene und Inflammation regulieren. Diese Befunde sprechen dafür, dass tRFs eine fundamentale Rolle in der Regulation der Immunantwort nach Schlaganfall spielen. Neben der cholinergen Überaktivierung kommt es auch zu einer Stimulation des sympathischen Nervensystems, was unter anderem zu einem IFN-γ-Defizit und damit zu einer gestörten bakteriellen Abwehr führt. In der **dritten Studie** wurde die intratracheale IFN-γ Administration bei SAP im Mausmodell getestet. Die pulmonale IFN-γ Behandlung hatte keinen negativen Einfluss auf die Infarktreifung und kann daher in Bezug auf mögliche negative pro-inflammatorische Effekte im ZNS als sicher betrachtet werden. Trotz einer Verbesserung der Lungenzell-Funktionalität in den IFN-γ behandelten Schlaganfall-Mäusen konnten spontane Pneumonien sowie Aspirations-induzierte Pneumokokken-Pneumonien nicht verhindert werden. Obwohl diese Arbeit im experimentellen Schlaganfall-Modell keinen Nachweis dafür erbringen konnte, dass durch eine cholinerge Blockade oder durch gezielte pulmonale Zytokin-Therapie die SAP verhindert werden kann, bieten die Ergebnisse eine Grundlage für neue Therapieansätze. Basierend auf den hier vorgelegten Daten könnten Kombinationstherapien mit verschiedenen Immunstimulatoren oder die Manipulation kleiner RNAs zur Behandlung der SAP sinnvolle Optionen darstellen.

ABSTRACT

Bacterial pneumonias belong to the most serious complications after stroke whose underlying pathophysiological mechanisms are poorly understood. Overactivation of the autonomic, especially the cholinergic system, after central nervous system (CNS) injury contributes to a rapid onset of temporary immunosuppression and thus to the development of stroke-associated pneumonia (SAP). The α7 nicotinic acetylcholine receptor (nAChR) was identified in the experimental stroke model as an important mediator of the impaired immune response against spontaneous SAP. Since *in vitro* experiments indicated that non-α7nAChRs contribute to pulmonary immunosuppression, the **first study** investigated the role of α2, α5, α7 and α9/10nAChRs, expressed in the lung, in a mouse model of an aspiration-induced pneumococcal pneumonia after stroke. The absence of different nAChRs did not affect leukocyte recruitment to the lung and spleen, as well as pro- and anti-inflammatory cytokine responses in the lung and ultimately did not improve pathogen clearance, suggesting that nAChRs do not mediate the impaired immune response to pneumococci after stroke. The cholinergic system can be influenced at the level of acetylcholine synthesis, the transport, the release, the cognate receptors, but also by the regulation of the expression of underlying genes using small RNAs. In the **second study,** small RNAs in the blood of stroke patients were analyzed and demonstrated a decrease of microRNAs (miRs) and an increase of transfer RNA fragments (tRFs) two days after stroke. The stroke-induced tRFs contained complementary motifs to active transcription factors in monocytes regulating, among others, cholinergic genes and inflammation, suggesting that tRFs play a fundamental role in the regulation of the immune response after stroke. Besides cholinergic overactivation, the sympathetic nervous system is also activated after stroke, resulting, among others, in an IFN-γ-deficit and thus to an impaired bacterial defense. In the **third study**, intratracheal IFN-γ treatment of SAP was tested in a mouse model. Pulmonary IFN-γ administration had no negative effect on infarct maturation and can therefore be considered safe with respect to possible negative pro-inflammatory effects in the CNS. Despite an enhanced lung cell functionality in the IFN-γ treated stroke mice, both spontaneous infections and aspiration-induced pneumococcal pneumonias were not prevented. Although this work failed in an attempt to prevent SAP in the experimental stroke model by cholinergic blockade or by pulmonary cytokine therapy, the data provide basis for new therapeutic approaches. Combination therapy with different immunostimulators or manipulation of small RNAs to treat SAP would be conceivable here.

1 INTRODUCTION

1.1 Stroke-associated pneumonia – the most severe medical complication

Stroke is an infarction or hemorrhage in the brain [1]. The global burden of disease study of 2017 showed that 6.2 million people died as a consequence of a stroke, making it the second leading cause of death after ischemic heart diseases [2]. Patients, who survive, often suffer from moderate or severe disabilities [3]. Medical complications and the resulting long-term care as well as rehabilitation after stroke lead to rising healthcare costs, which demand stroke prevention and reduction of stroke related disability [4].

Up to 85% of all stroke patients suffer from medical complications, including neurological-recurrent stroke, epileptic seizure, infections, mobility related-falls, falls with serious injury, pressure sores, thromboembolism, pain, psychological-depression, anxiety, emotionalism, dysphagia, fever, incontinence and confusion [5,6]. Therein, pneumonia is the most severe medical complication, occurring in up to 33% of all stroke patients [7,8]. Dysphagia and aspiration were identified as significant risk factors for the development of SAP [9,10]. It was shown that dysphagia occurs in up to 78% and aspiration, due to impaired swallowing, in up to 30% of all stroke patients, resulting in an enormous increased risk to suffer from pneumonia [11-13]. Nevertheless, not all patients who aspirate develop pneumonia [10,14]. It has become clear that these risk factors may not be sufficient to induce pulmonary infections after stroke. Previous experiments have shown that CNS injuries like stroke result in secondary immunosuppression due to overactivation of stress pathways, which was identified as an independent risk factor contributing to SAP [7].

1.2 Stroke-induced immunosuppression by activating neurohumoral stress pathways

The CNS can influence the immune system through soluble mediators, such as high mobility group box 1 (HMGB1), directly released from damaged tissue [15], but also due to the activation of the three stress pathways: the hypothalamic-pituitary-adrenal (HPA)-axis, the sympathetic nervous system (SNS) and the cholinergic signaling [7]. Clinical studies demonstrated that stroke is linked with an activation of the HPA-axis in the hyperacute phase. Blood analysis of stroke patients showed initial increased levels of adrenocorticotrophic hormone (ACTH) and cortisol. In a second phase, a rapid ACTH decrease mediated by a negative feedback mechanism was observed. In contrast, high cortisol levels in blood persisted due to prolonged activation of the adrenal gland by ACTH [16-18]. On the one hand, stroke causes physiological stress, resulting in the direct or indirect activation of the HPA-axis by different regions of the brain, including hippocampus, amygdala and bed nucleus of the stria terminalis [19]. On the other hand, pro-inflammatory cytokines, released in the brain after stroke, can directly

activate the paraventricular nucleus (PVN) of the hypothalamus, leading to an increased secretion of the corticotropin-releasing hormone (CRH). Subsequently, CRH stimulates the release of ACTH by the anterior pituitary following glucocorticoid (GC) secretion by the adrenal cortex. GC suppresses immunity by inhibiting pro-inflammatory cytokines (interleukin (IL) -1, IL-6, tumor necrosis factor (TNF)-α, IL-12), chemokines (IL-8), prostaglandins and nitric oxide. Additionally, GC stimulates anti-inflammatory mediators, including IL-10 and transforming growth factor β (TGF-β) and induces apoptosis of immune cells. Furthermore, GC downregulates the expression of major histocompatibility complex class II, diminishes antigen presentation to lymphocytes by monocytes/macrophages/dendritic cells (DCs), promotes development of regulatory T cells, as well as differentiation of Th2 cells and induces lymphopenia in blood and spleen. The hypothalamus does not only induce immunosuppression by activating the pituitary-adrenal pathway, but also by activating the SNS and the cholinergic signaling [7,20-22].

The SNS is another stress pathway, which is activated by stroke. Inflammation or injury stimulate preganglionic sympathetic fibers, coming from the grey matter or the lateral horn of the spinal cord and synapse with the postganglionic sympathetic fibers in the ganglia of the sympathetic chain [23]. Postganglionic nerve fibers release catecholamines, including adrenaline, noradrenaline and dopamine, among others, into the blood, the primary, as well as the secondary lymphoid organs and modulate immune cell function [24]. Among others, catecholamines act on β-adrenergic receptors, which are expressed on almost all leukocytes resulting in an initial increase of blood lymphocytes and granulocytes originating from marginal pool and peripheral reservoirs. Findings in animals have shown that persistent increased catecholamine concentrations in the blood induce apoptosis of lymphocytes, reduce TNF-α, IL-1β and IL-12 secretion, diminish natural killer cell (NK cell) activity and lead to atrophy of spleen, thymus and lymph nodes. Furthermore, it was shown that catecholamines inhibit the expression of interferon (IFN)-γ and IL-2 by Th1 cells and stimulate the expression of IL-4 and IL-5 [7,20].

Besides the SNS, the cholinergic signaling also interacts with the immune system and plays a key role in the regulation and control of inflammation. In brief, damaged tissue activates the afferent limb stimulating preganglionic parasympathetic fibers in the brainstem nuclei or sacral spinal cord, which synapse with postganglionic fibers near different organs, including the eye, heart, lung, stomach, intestine, gallbladder, pancreas and kidney [23]. Efferent parasympathetic nerve fibers, including the efferent vagus nerve, innervate most of the thoracic and abdominal organs [25,26], release acetylcholine (ACh) to the cells of the effector organs and induce anti-inflammatory signaling via different nAChRs. In addition, non-neuronal cells such as lymphocytes, DCs, macrophages and the airway epithelium produce and secret ACh and thus actively contribute to cholinergic signaling in homeostasis and disease [27,28]. *In vitro* studies showed that nicotine or ACh diminish TNF-α, IL-1, IL-6 and IL-18, but not the anti-inflammatory IL-10 response to endotoxin by human macrophages.

Experiments in mice could confirm the anti-inflammatory effect of cholinergic signaling: Vagotomy in rats raised TNF-α levels in serum and liver in response to intravenously applied endotoxin and vagus nerve stimulation diminished TNF-α levels in serum, liver and heart and prevented shock of animals treated with a lethal dose of endotoxin [26,29]. This anti-inflammatory pathway was shown to be regulated and potentiated by miRs. Lipopolysaccharide (LPS) induced miR-132, targeting and inhibiting acetylcholinesterase transcription [30]. LPS stimulation of RAW264.7 cells resulted in an increase of miR-124 via the α7nAChR diminishing IL-6 and TNF-α production [31].

It is well known that the cholinergic anti-inflammatory pathway plays a pivotal role in the control of inflammation in different diseases, including sepsis and ischemic stroke [32,33]. Experiments in mice demonstrated that brain ischemia led to a rapid increase of the cholinergic signaling. Vagotomy prevented pulmonary infection after experimental stroke, suggesting that increased cholinergic signaling contributes to the development of spontaneous SAP. [33]. Findings in patients confirmed the important role of the cholinergic activation in the development of SAP. Patients showed significantly increased ACh production by blood lymphocytes 24 h after stroke onset compared to healthy controls. Lymphocytes of stroke patients with pneumonia produced significantly higher ACh levels compared to stroke patients without pneumonia. Additionally, regression analysis demonstrated a positive correlation between ACh production and infarct volume or infarct severity with pneumonia [34].

1.3 The role of nicotinic acetylcholine receptors in the modulation of the immune system

Cholinergic signaling occurs via acetylcholine receptors, which are activated by the endogenous neurotransmitter ACh and are divided into muscarinic and nAChRs. nAChRs are fast excitatory ligand-binding ion channels and are composed of α-subunits (α1-10) and β-subunits (β1-4) [35]. Different combinations of α- and β-subunits can form heteromeric receptors with 5 subunits. Exclusively, the α7 and α9 subunit can form homomeric receptors, whereas the α9 subunit is also capable of forming a heteromeric receptor with the α10 subunit [27]. Due to the high calcium permeability, nAChRs contribute to the regulation of second messenger signaling pathways, including the PI3-kinase/AKT pathway, activation of transcriptional systems and proteolytic processes. nAChRs are expressed by neuronal, as well as non-neuronal cells such as lymphocytes, DCs and macrophages [35]. Especially the α2, α5, α6, α7, α9 and α10 subunits are detectable on immune cells [27]. *In vitro* and *in vivo* studies demonstrated that immune cell function is mediated by its own non-neuronal cholinergic signaling via the α7nAChR. Mice lacking the α7nAChR showed significantly increased pro-inflammatory cytokine secretion compared to WT littermates in response to ovalbumin immunization and LPS application [36,37]. Stimulation of the α7nAChR on macrophages resulted in significantly diminished TNF-α production and release [37]. Agonists of the α7nAChR prevented the activation of the NF-κB pathway and inhibited HMGB1 secretion [38]. The important role of the α7nAChR in the control and regulation

of inflammation sparked the interest to investigate the α7nAChR in the development and pathogenesis of different diseases. Experiments in mice have exhibited that stimulation of the α7nAChR results in a reduction of brain edema after experimental stroke and a neuroprotective effect on stroke, due to reduction of inflammation and oxidative stress [39,40]. In contrast, the α7nAChR was shown to mediate immunosuppression in the lung after experimental stroke, contributing to the development of spontaneous pneumonia, mainly caused by Gram-negative bacteria. But *in vitro* experiments have demonstrated that cholinergic stimulation results in impaired IL-6 secretion by macrophages isolated from WT mice, as well as from α7nAChR knockout (KO) mice, suggesting a contribution of non-α7nAChR to the cholinergic anti-inflammatory pathway [33].

1.4 Immunomodulatory treatment as a novel treatment option of stroke-associated pneumonia?

Besides the antibiotic therapy immediately after diagnosis of the pulmonary infection in stroke patients [13], the prevention of aspiration, standardized swallow screening and oral care are also pivotal measures in the treatment of SAP [41]. In addition, prophylactic antibiotic treatment to prevent SAP was tested in different clinical studies with contradictory results [42]. Finally, 2 phase III trials demonstrated that prophylactic antibiotic treatment neither prevents SAP nor improves stroke outcome [43,44]. The long-lasting immunosuppression after stroke and the growing emergence of antibiotic-resistant bacteria raised the interest on immunomodulatory therapy for the treatment of SAP. Cytokine immunotherapy was already tested for different diseases in mouse models, as well as in human trials with promising results. Patients with a sepsis-associated immunosuppression treated with granulocyte-macrophage colony-stimulating factor (GM-CSF) or IFN-γ, as well as patients with postoperative immunosuppression treated with GM-CSF showed a reconstituted immune function and an improved clinical course [45-47]. The administration of granulocyte colony-stimulating factor (G-CSF), IFN-γ, IL-12 and GM-CSF to prevent and treat pneumonia resulted in an enhanced pathogen clearance, dependent on the type of application and bacteria species. Despite possible complications, such as unsolicited systemic effects or dose-limiting toxicity, the cytokine treatment represents a mechanistically reasonable therapeutic approach for the treatment of SAP [48]. Subcutaneous (s.c.) administration of GM-CSF was already tested in an experimental mouse model of spontaneously developing infections after stroke and showed increased peripheral and pulmonary leukocyte numbers, an improved peripheral cytokine responses and diminished bacterial burden in the bronchoalveolar lavage fluid (BALF) [49]. An i*n vivo* study demonstrated that stroke induces impaired IFN-γ production in blood and visceral organs, as well as apoptosis of IFN-γ producing immune cells in lymphatic organs [22]. Since the pulmonary IFN-γ levels are also significantly diminished after experimental stroke [50], a local pulmonary administration of IFN-γ might be a suitable treatment option to prevent or treat SAP.

1.5 Importance and aims of the PhD thesis

Despite preventive antibiotic treatment, the overall frequency of SAP remained unchanged over the last decades [51]. Also the administration of β-blocker to reverse adrenergic immunosuppression did not guarantee the prevention of pulmonary infections after stroke [7,20]. Further therapeutic approaches for the prevention and treatment of SAP remain scarce. Therefore, it is important to identify and investigate further factors contributing to SAP and to develop new therapeutic strategies. The aim of this work was to better understand underlying mechanisms resulting in cholinergic immunosuppression after stroke, as well as to evaluate a pulmonary cytokine therapy in a mouse model of SAP.

1. The first aim of this PhD project was to analyze the role of the α2, α5, α7 and α9/10nAChRs, expressed in the lung, in an impaired immune response against an aspiration-induced pneumococcal pneumonia after experimental stroke and thus to identify possible target structures for new therapeutic concepts to reverse cholinergic immunosuppression after stroke.

2. The second study aimed to investigate if LPS-induced pro-inflammatory cytokine secretion in human monocytes is regulated by the cholinergic system and if tRFs play a role in this inflammation control. The data were analyzed comparatively with the investigation of changes in the levels of small RNAs in the blood of stroke patients. Finally, this study aimed to identify potential therapeutic targets to manipulate the gene regulation of the cholinergic system after stroke.

3. The third aim was to reconstitute lung antibacterial defense after stroke by local pulmonary IFN-γ administration and therefore to prevent spontaneous pneumonia, as well as to improve bacterial clearance in an aspiration-induced pneumococcal pneumonia model after stroke.

2 METHODS

2.1 Animals and housing

Experiments were performed in accordance with the European directive on the protection of animals used for scientific purposes and the respective German legislation after approval by the relevant authority, Landesamt für Gesundheit und Soziales (LAGESO), Berlin, Germany. Mice were placed in cages with chip bedding and environmental enrichment on a 12 h light/dark cycle with ad libitum access to food standard chow and water. Analysis of nAChR expression in brain and lung, as well as IFN-γ treatment was performed by using 12-weeks-old male C57BL/6J mice (The Jackson Laboratory, Bar Harbor, Maine, USA). To investigate the impact of nAChRs on post-stroke pneumococcal pneumonia, 12-to-20-weeks-old male mice lacking the α2, α5, α7 and α9/10nAChR and WT littermates were used (information about the mouse strains are described in study 1 [52]). Since all strains carry the C57BL/6JCrl background, mixed WT littermates of all strains served as a control.

2.2 Expression analysis of nicotinic acetylcholine receptors

Total RNA from lung and brain tissue was isolated using Trizol (Roth, Karlsruhe, Germany). RNA was incubated with DNase (Promega, Fichtburg, MA, USA) followed by purification with Phenol-Chloroform to remove genomic DNA and reverse transcribed using ProtoScript® II Reverse Transcriptase (New England Biolabs, Ipswich, UK). The mRNA expression of genes was analyzed using a LightCycler 480 (Roche, Mannheim, Germany) and the LightCycler-FastStart-DNA-Master-SYBR-Green-I-Kit (Roche, Mannheim, Germany) according to the manufacturer's guidelines with the thermal protocol described in study 1 [52]. Target gene expression was normalized to β-actin as housekeeping gene. Primer were used as described in table 1. Analysis was performed using 7500 Software v2.3 (Life Technologies, Carlsbad, California, USA).

PRIMER	FORWARD SEQUENCE	REVERSE SEQUENCE
mChrnaalpha2	TGGATGGGCTGCAGAGAGACAGG	GGTCCTCGGCATGGGTGTGC
mChrnaalpha5	ATCAACATCCACCACCGCTC	CTTCAACAACCTCGCGGACG
mChrnaalpha7	TCCGTGCCCTTGATAGCACA	TCTCCCGGCCTCTTCATGCG
mChrnaalpha9	CGGACGCGGTGCTGAACGTC	AGACTCGTCATCGGCCTTGTTGT
mChrnaalpha10	ACCCTCTGGCTGTGGTAGCG	GCACTTGGTTCCGTTCATCCATA

Table 1: Primer used for quantitative Reverse Transcriptase Polymerase Chain Reaction (qRT-PCR).

2.3 Experimental stroke

Middle cerebral artery occlusion (MCAo) was performed as described elsewhere [53]. In brief, animals were anesthetized with isoflurane (Abott, Wiesbaden, Germany) in a 1:2 mixture oxygen/nitrous oxide. A silicon-coated filament (Docol Corporation, Sharon, USA) was introduced over the common carotid artery and the internal carotid artery into the circle of Willis blocking the origin of the middle cerebral artery for 60 min.

2.4 Analysis of infarct size

Brains were removed, frozen in 2-Methylbutan (Carl Roth, Karlsruhe, Germany) on dry ice and cut into 25 µm thick cryosections. Infarct size was determined by hematoxylin staining according to Harris. Total area of contralateral hemisphere (HA_{contra}) and area of not injured part of the ipsilateral hemisphere (HAN_{ipsi}) were measured in 5 sections at defined regions using SigmaScan Pro 5 (Systat Software GmbH, Erkraht, Germany) as follows:

$$A = A_{section1} + 2 * A_{section2} + 2 * A_{section3} + 2 * A_{section4} + A_{section5}.$$

Infarct size was calculated with the following equation:

$$\%\ \text{Infarct size} = \frac{HA_{contra} - HAN_{ipsi}}{HA_{contra}} * 100.$$

2.5 Aspiration-induced pneumonia model with *S. pneumoniae*

Spontaneously developing infections were prevented by antibiotic treatment (marbofloxacin, 5.0 g/kg BW, Vétoquinol GmbH, Ravensburg, Germany) applied intraperitoneally (i.p.) one day before and on the day of MCAo. Animals were anesthetized i.p. with midazolam (5.0 mg/kg BW, Roche Pharma AG, Grenzach-Whylen, Germany) and medetomidin (0.5 mg/kg BW, Orion Corporation, Espoo, Finland). nAChR KO mice and WT littermates were infected intratracheally (i.t.). To this end, a bronchoscope was inserted until the bifurcation of the trachea and a *S. pneumoniae* (D39 serotype 2, Rockefeller University, New York, NY, USA) suspension (2000 colony forming units (CFU)/50 µl) was applied [52,54]. To investigate the effect of IFN-γ treatment on an aspiration-induced pneumococcal pneumonia, C57BL/6J mice were infected intranasally (i.n.) with a suspension of 10,000 CFU/20 µl (PN36, NCTC 7978, serotype 3). Anesthesia was antagonized s.c. with flumazenil (0.5 mg/kg BW, Inresa, Freiburg, Germany) and atipamezol (5.0 mg/kg BW, Orion Corporation, Espoo, Finland).

2.6 IFN-γ treatment

Mice were anesthetized and antagonized as described for the pneumococcal infection. IFN-γ (PeproTech GmbH, Hamburg, Germany) diluted in solvent or solvent only (phosphate-buffered saline (PBS), Gibco® life technologiesTM, Waltham, Massachusetts, USA) were applied bronchoscopy-guided in the bifurcation of the trachea as established in our laboratory [54].

2.7 Microbiological analysis

Bronchoalveolar lavage (BAL) was performed as described elsewhere [55]. Lungs were dissected and homogenized in 500 µl PBS. Blood collection was performed from the abdominal aorta. Lung homogenate, BALF and blood were plated on Columbia-Agar plates (BD Bioscience, Heidelberg, Germany) or LB-Agar and incubated at 37°C for 18 h. Bacterial colonies were counted to calculate the CFUs per ml tissue/liquid.

2.8 Analysis of leukocytes in lung and spleen by flow cytometry

Single cell suspensions from spleen and lung were prepared as described elsewhere [22,33]. $2x10^6$ cells were stained for 20 min in the dark with anti-mouse monoclonal antibodies (Biolegend, San Diego, USA or BD Bioscience, Heidelberg, Germany) listed in table 2. Cell phenotyping was performed on LSRII flow cytometer using FACS Diva software (BD Bioscience, Heidelberg, Germany) and Flowjo software 9.6.6 (Tree Star Inc, San Carlos, California, USA).

	MARKER	FLUOROCHROME
Lymphoid panel	CD45	PerCP
	CD11b	APC Cy7
	NK1.1	PE
	CD19	FITC
	CD3	APC
	CD4	A700
	CD8	PB
Myeloid panel	CD45	PerCP
	Gr1	PE
	Cd11b	PE-Cy7
	F480	APC
	Siglec F	APC-Cy7
	CD11c	PB

Table 2: List of antibodies used for flow cytometry.

2.9 Analysis of leukocytes in blood and BALF

Blood was collected in ethylenediaminetetraacetic acid (EDTA) tubes and analyzed with an animal blood counter (Scil Vet abc, Scil veterinary excellence, Viernheim, Germany). Cytocentrifugation of BAL cells was performed to prepare cytospins. Macrophages, neutrophils and lymphocytes became visible by May-Grünwald-Giemsa staining. Cells per ml BALF were calculated.

2.10 Analysis of cytokines in BALF and plasma and permeability of the alveolar-capillary barrier

BAL was performed as described elsewhere [55]. Cytokine concentrations were measured in BALF and plasma using a commercially available Milliplex Map Kit (Merk Millipore, Darmstadt, Germany). To investigate the permeability of the alveolar-capillary barrier, albumin concentrations were measured in plasma and BALF using an enzyme-linked immunosorbent assay (ELISA) (Bethyl Laboratories Inc., Montgomery, AL, USA).

2.11 Isolation and *ex vivo* stimulation of lung and BAL cells

BAL (100,000 cells/ml) and lung cells ($2x10^6$ cells/ml) were isolated and stimulated with 1 µg/ml LPS (O55:B5, Sigma) in roswell park memorial institute (RPMI) medium (Biochrom GmbH, Berlin, Germany) with 10% fetal calf serum (FCS), 10% L-alanyl-L-glutamine and 100 U/ml penicillin/streptomycin (Biochrom GmbH, Berlin, Germany) for 12 h at 37°C. TNF-α and IL-6 concentrations were measured by using a commercially available ELISA (eBioscience, San Diego, USA).

2.12 Isolation of human monocytes and *ex vivo* stimulation

The study was approved by the ethics committee of the Charité-Universitätsmedizin Berlin (MG Cohort: EA1/281/10). Peripheral blood mononuclear cells (PBMCs) from healthy donors were purified by density gradient centrifugation over Ficoll (Biocoll separating solution, Biochrom) and underwent magnetic cell separation to isolate untouched monocytes by a commercially available Pan Monocyte Isolation Kit (Miltenyi Biotec). Monocytes ($2x10^6$ cells/ml) were stimulated with LPS (1 ng/ml, 0127:B8; Sigma), LPS and nicotine (300 µM, Sigma) or nicotine in RPMI medium with 1% penicillin-streptomycin (Biochrom), 2 mM L-glutamine (Biochrom), and 10% autologous serum for 6 h, 12 h and 18 h at 37°C. TNF-α concentrations in culture supernatant were determined by using a commercial DuoSet ELISA kit (R&D Systems).

2.13 Statistics

Data were analyzed using Prism 6.0 Software (GraphPad, San Diego, CA, USA) or R (version 3.4.1). Values are shown as scatter dot plots with mean ± standard deviation (SD), box plots with whiskers minimum to maximum or bars. *P*-values of less than 0.05 were considered statistically significant. One-tailed Mann-Whitney test, One-way analysis of variance (ANOVA), two-way ANOVA and Pearson Correlation was performed as indicated in the legends in the of the publications listed in the appendix.

3 RESULTS

3.1 Study 1: The role of nicotinic acetylcholine receptors in stroke-associated pneumonia

3.1.1 α2, α5, α7, α9 and α10nAChRs are expressed in the lung of naïve mice

We hypothesized that additional nAChRs besides the α7nAChR might be involved in the cholinergic pulmonary immunosuppression [33]. Therefore, the expression of different nAChRs in whole lung tissue homogenate, isolated from naïve C57BL/6J mice was investigated. Brain tissue served as a positive control. We found that α2, α5, α7, α9 and α10nAChRs are expressed in the lung, suggesting a role in cholinergic pulmonary immunosuppression (***8.1 Selected publications: Study 1, Figure 1***) [52].

3.1.2 Impaired bacterial clearance in pneumococcal pneumonia after experimental stroke does not involve α2, α5, α7 and α9/10nAChRs

We previously demonstrated that the clearance of an induced pneumococcal pneumonia with *S. pneumoniae* strain D39 is impaired after experimental stroke [56]. To investigate the effect of different nAChRs on the course of an induced pneumococcal infection after stroke, a pneumococcal suspension of 2000 CFU was applied at the bifurcation of the trachea of α2, α5, α7, α9/10nAChR KO MCAo mice and WT MCAo littermates, three days after stroke. Naïve mice without MCAo surgery were also infected and served as controls. CFU in lung, BALF and blood, as well as infarct size were determined one day after infection (**Figure 1**). Microbiological analysis of the lung showed that out of 15 naïve mice, 12 naïve mice were able to completely clear the induced infection. Three naïve mice demonstrated slight infections without any clinical symptoms, suggesting near complete bacterial clearance. In contrast, 40 out of 43 MCAo mice showed severe pulmonary infections. Bacterial burden in lungs from α2, α7, α9/10 KO MCAo and WT MCAo mice was significantly increased compared to naïve WT mice. Microbiological analysis of BALF one day after infection revealed similar results. Additionally, α9/10 KO MCAo mice showed significantly increased bacterial burden in blood compared to naïve WT mice. However, bacterial burden in lung, BALF and blood and infarct size did not significantly differ between any type of MCAo nAChR KO mice and MCAo WT mice using MCAo WT littermates as reference group (***8.1 Selected publications: Study 1, Figure 2***) [52].

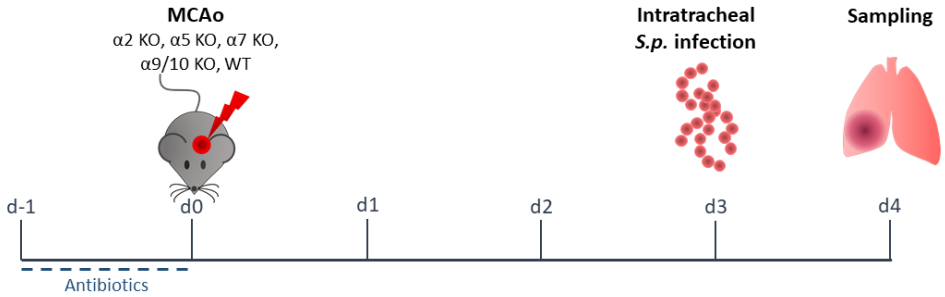

Figure 1: Experimental setup to investigate the impact of different nAChRs on the course of an aspiration-induced pneumococcal pneumonia. d-1/d0: spontaneously developing infections were prevented by antibiotic treatment with marbofloxacin; d0: MCAo, d3: induced pneumococcal infection at the bifurcation of the trachea; d4: analysis of bacterial burden, infarct size, cellular composition of lung and spleen, cytokine secretion in BALF and permeability of the alveolar-capillary barrier. Figure 1 was created by Sandra Jagdmann and is not based on any previously published figure.

3.1.3 α2, α5, α7 and α9/10nAChRs have no impact on pulmonary immune response, splenic leukocyte composition and alveolar-capillary barrier permeability during pneumococcal infection after stroke

Lung and spleen cells were isolated one day after infection and quantified by flow cytometric analysis. The strategy for the analysis of lung leukocytes is presented in **Figure 2**.

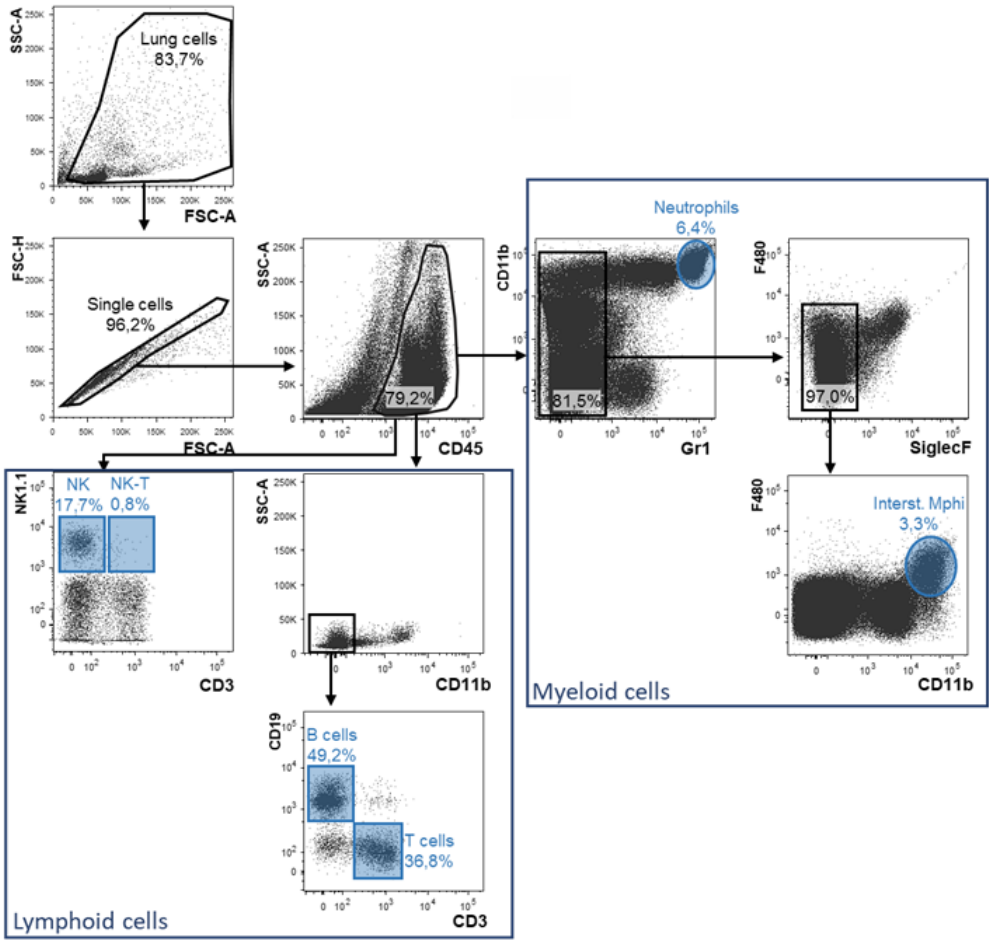

Figure 2: Gating strategy for defining lymphoid and myeloid cells in the lung. Dot plots show the strategy to evaluate neutrophils ($Gr1^{high}$), interstitial macrophages (IMs) ($Gr1^{-}/SiglecF^{-}/CD11b^{high}/F480^{+}$), T cells ($CD11b^{-}/CD3^{+}$), B cells ($CD11b^{-}/CD19^{+}$), NK ($NK1.1^{+}/CD3^{-}$) cells and NKT cells ($NK1.1^{+}/CD3^{+}$). Figure 2 was created by Sandra Jagdmann and is not based on any previously published figure.

We found significantly diminished cell counts of IMs in α7, α9/10 KO MCAo and WT MCAo mice compared to naïve WT littermates, suggesting a contribution to the impaired pathogen clearance after stroke, whereas MCAo had no effect on the cell count of lymphocytes and neutrophils in the lung. Analysis of splenic leukocytes revealed significantly decreased cell counts of neutrophils in α5 KO MCAo mice and WT MCAo mice, significantly diminished numbers of macrophages in α9/10 KO MCAo mice and WT MCAo mice and significantly reduced cell counts of lymphocytes in α5 and α9/10 KO MCAo mice compared to naïve WT mice [52]. But the number of pulmonary and splenic leukocytes did not differ between nAChR KO MCAo mice and WT MCAo littermates (***8.1 Selected publications: Study 1, Figure 3***). Analysis of pro-inflammatory cytokine response in BALF one day after infection revealed increased MIP-1α, KC and TNF-α levels in some MCAo mice compared to naïve mice correlating with bacterial burden in BALF. The anti-inflammatory cytokine IL-10, measured in BALF one day after infection, tended to be increased in MCAo mice compared to naïve mice. However, cytokine levels did not differ between nAChR KO MCAo mice and WT MCAo littermates. Albumin concentrations were measured in BALF as well as in plasma and the ratio (albumin BALF/albumin plasma) calculated to investigate the permeability of the alveolar-capillary barrier. We found no differences between the groups one day after infection (***8.1 Selected publications: Study 1, Figure 4***) [52].

3.2 Study 2: Stroke induces an upregulation of tRFs contributing to the regulation of the cholinergic signaling after stroke

To analyze if stroke induces changes in small regulatory RNA expression, whole blood was collected from 33 male patients two days after stroke onset and 10 age- and sex-matched controls to perform Principal Component Analysis of sequenced small RNAs. Analysis showed a significant increase of tRFs (87%/143) and a significant decline (63%/420) of miRs in stroke patients. Targeting analysis revealed that 131 miRs and 64 tRFs contain complementary motives to 5 cholinergic transcripts, indicating a role in the regulation of the cholinergic signaling after stroke (***8.2 Selected publications: Study 2, Figure 1***). 77 of the upregulated stroke tRFs were found to be expressed in immune cells, from which 10 tRFs contained complementary motives to cholinergic transcripts, suggesting an impact on post-stroke leukocyte immune response (***8.2 Selected publications: Study 2, Figure 3***). To identify, in which immune cells small RNAs might regulate post-stroke cholinergic signaling, long RNA regulatory circuits [57] from different lymphocyte subsets, monocytes and neutrophils were analyzed and showed that CD14+ monocytes were the main cell type expressing the highest amounts of cholinergic transcripts. Stroke induced an upregulation of 204 long RNA transcripts, which were relevant to innate immunity, vascular processes and cholinergic links (***8.2 Selected publications: Study 2, Figure 4***). In addition, we found that active transcription factors (TFs) in monocytes, including TFs regulating cholinergic genes,

were targeted by stroke-induced tRFs, suggesting that stroke-induced tRFs regulate transcriptional state in monocytes after stroke (***8.2 Selected publications: Study 2, Figure 5***). To investigate if stroke-induced tRFs contribute to regulation of the inflammatory response of monocytes, murine RAW 264.7 cells and human monocytes were stimulated with LPS. qRT-PCR revealed that several of the top 6 stroke-induced tRFs (***8.2 Selected publications: Study 2, Figure 2***) were also upregulated upon LPS stimulation in murine, as well as human monocytes. The presence of nicotine resulted in an additional induction and the administration of dexamethasone to a suppression of these tRFs (***8.2 Selected publications: Study 2, Figure 5***). To investigate if the TLR-induced pro-inflammatory cytokine response in monocytes is regulated by the cholinergic signaling, human monocytes were stimulated *ex vivo* with LPS for 6 h, 12 h and 18 h in the presence or absence of the nAChR agonist nicotine and TNF-α levels were measured in supernatant. Unstimulated monocytes served as a control (**Figure 3 A**). We found that nicotine impaired LPS-induced TNF-α secretion, suggesting that TLR-induced TNF-α secretion in monocytes is regulated by cholinergic signals as a part of the cholinergic anti-inflammatory pathway (**Figure 3 B**) [58].

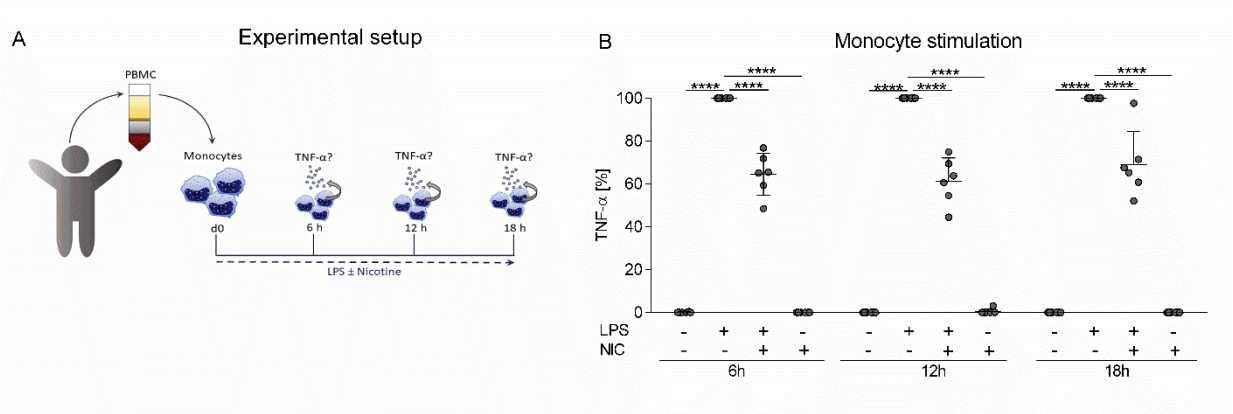

Figure 3: TLR-induced pro-inflammatory cytokine response in human monocytes was regulated by the cholinergic signaling. (**A**) Experimental setup. Figure 3 A was created by Sandra Jagdmann and is not based on any previously published figure. (**B**) The nAChR agonist nicotine significantly impaired TNF-α secretion by LPS stimulated monocytes. Data from three independent experiments are shown as scatter plots ± SD compared to LPS stimulated monocytes as reference group using two-way ANOVA followed by Dunnett´s multiple comparison test. NIC = nicotine. Figure 5B was published in modified form in Winek et al., 2020 [58].

3.3 Study 3: The effect of intratracheal IFN-γ treatment on post-stroke pneumonia

3.3.1 Local pulmonary IFN-γ treatment improved in trend lung cell functionality in stroke mice

Naïve mice were treated i.t. with different doses of IFN-γ to investigate the effect on TNF-α and IFN-γ-induced protein 10 (IP-10) secretion in BALF and plasma, as well as leukocyte recruitment in the lung 12 h after application (**Figure 4 A**). We found that 1 µg IFN-γ was enough to induce IP-10 in BALF and plasma and TNF-α in BALF. However, cellular composition of leukocytes in lung and BALF did not differ between mice treated with 1 µg IFN-γ and solvent (***8.3 Selected publications: Study 3, Figure 1***). In addition, to evaluate the effect of IFN-γ treatment on functionality of pulmonary immune cells, lung

and BAL cells were isolated 12 h after application and stimulated with LPS for 12 h. TNF-α levels tended to be increased in supernatant of lung cells, whereas IL-6 levels showed no differences compared to solvent treated mice. In contrast, IL-6 and TNF-α levels in supernatant of BAL cells were non-significantly decreased compared to solvent treated mice (***8.3 Selected publications: Study 3, Figure 2***). Treatment with 10 µg or 50 µg resulted in an even stronger induction of TNF-α and IP-10 in the BALF, increased lymphocyte and neutrophil recruitment in the lung, as well as an improved functionality of lung cells, but was not suitable since mice showed an intolerance (loss of weight, hunched posture and diminished activity) (***8.3 Selected publications: Study 3, Figure 1-2***). Therefore, for subsequent experiments, an IFN-γ dose of 1 µg was used [59].

To investigate the effect of IFN-γ treatment in the experimental stroke model, mice were treated with IFN-γ or solvent one day after MCAo. Naïve mice served as healthy controls (**Figure 4 B**). Cytokine analysis in BALF 12 h after administration revealed that IFN-γ was capable of inducing TNF-α secretion in naïve mice but not in stroke mice. In order to evaluate pulmonary cytokine response to LPS, lung cells were isolated from IFN-γ or solvent treated stroke or naïve mice 12 h after administration and stimulated *ex vivo* with LPS for 12 h. Cytokine analysis of supernatant showed that IFN-γ treatment resulted in an improved TNF-α response in stroke mice compared to solvent treated stroke mice. However, TNF-α levels were still significantly lower than in naïve mice. In contrast, IL-6 secretion in supernatant of lung cells was improved in IFN-γ treated stroke mice compared to solvent treated stroke mice, as well as to healthy mice. Infarct size, cytokine secretion in plasma and leukocyte recruitment in the lung did not significantly differ between the studied groups (***8.3 Selected publications: Study 3, Figure 3***) [59].

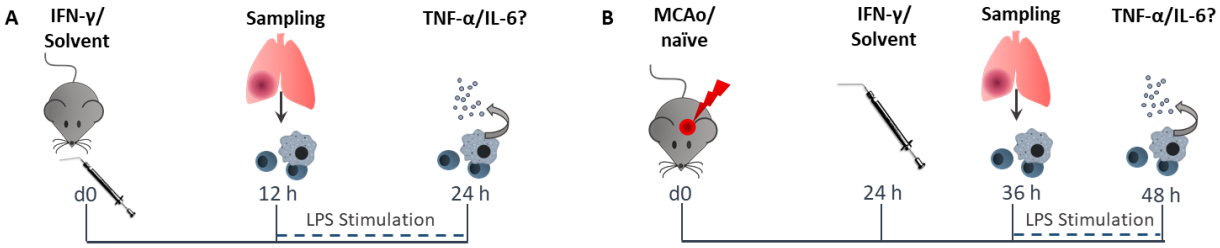

Figure 4: Experimental setup to test the effect of local pulmonary IFN-γ application in naïve and stroke mice. (**A**) d0: i.t. IFN-γ/solvent application in naïve mice, 12 h: Analysis of the lung/spleen/plasma and BALF, as well as *ex vivo* stimulation of BAL/lung cells with LPS for 12 h, 24 h: Measurement of cytokines in supernatant. Figure 4 A was created by Sandra Jagdmann and is not based on any previously published figure. (**B**) d0: MCAo, 24 h: i.t. application of IFN-γ/solvent, 36 h: analysis of infarct size, cytokines in BALF/plasma and leukocyte composition of the lung, as well as *ex vivo* stimulation of lung cells with LPS, 48 h: Measurement of cytokines in supernatant. Figure 4 B was published in modified form in Sandra Jagdmann et al., 2021 [59].

3.3.2 IFN-γ treatment did not prevent spontaneous pulmonary infections after experimental stroke

To test our hypothesis that local pulmonary IFN-γ treatment prevents spontaneously developing infections after stroke, mice were treated i.t. with IFN-γ or solvent one day after MCAo. Two days after administration, mice were examined regarding bacterial burden in the lung, cytokine response in the BALF and plasma, as well as leukocyte numbers in BALF, lung and spleen (**Figure 5**). We found slightly diminished infarct size and bacterial burden in BALF and lung in IFN-γ treated mice compared to solvent treated mice, however the infarct size did not correlate with bacterial burden in the lung. IFN-γ administration had no effect on cytokine levels in BALF and plasma, as well as leukocyte composition in BALF, lung and spleen (***8.3 Selected publications: Study 3, Figure 4***) [59].

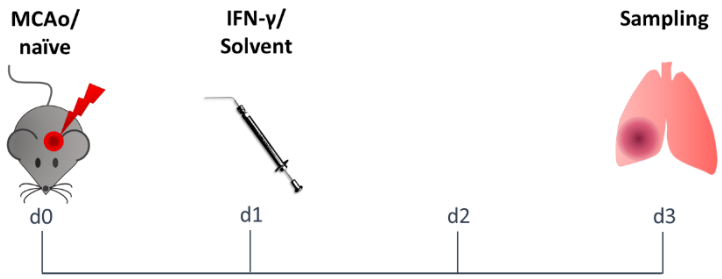

Figure 5: Experimental setup to investigate the effect of i.t. IFN-γ treatment on spontaneous pneumonia after stroke. d0: MCAo, d1: i.t. application of IFN-γ/solvent, d3: analysis of infarct size, bacterial burden in lung/BALF, cytokines in BALF/plasma and leukocyte composition of BALF/lung/spleen. Figure 5 was published in modified form in Sandra Jagdmann et al., 2021 [59].

3.3.3 IFN-γ treatment improved cytokine response and lymphocyte recruitment in the BALF but did not improve the clearance of pneumococcal infection after stroke

Experiments in mice demonstrated that stroke results in diminished clearance of induced pneumococcal pneumonia compared to sham mice [56]. To investigate, whether IFN-γ treatment improves the pathogen clearance of an induced pneumococcal infection after stoke, mice were i.n. infected with 10,000 CFU *S. pneumoniae* PN36 one day after IFN-γ or solvent administration, which was performed three days after MCAo (**Figure 6**). Analysis of bacterial burden revealed that IFN-γ slightly reduced pneumococcal clearance compared to solvent treated mice, whereas infarct size did not differ between the groups. IFN-γ treated mice showed significantly increased IL-6 levels, as well as slightly increased MIP-1α and IP-10 levels in the BALF compared to solvent treated mice. Additionally, IP-10 was found to be significantly increased in plasma from IFN-γ treated mice, whereas pro-inflammatory cytokines, including IFN-γ, showed no differences compared to solvent treated mice. Leukocyte analysis revealed non-significantly reduced number of macrophages in the lung and significantly increased numbers of lymphocytes in spleen and BALF (***8.3 Selected publications: Study 3, Figure 5***) [59].

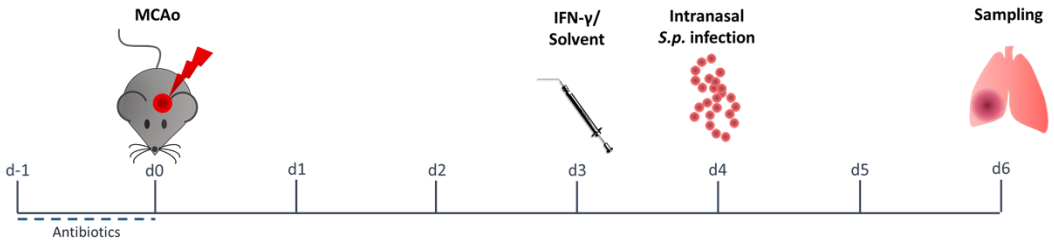

Figure 6: Experimental setup to investigate the effect of i.t. IFN-γ treatment on the course of a pneumococcal pneumonia after experimental stroke. d-1/d0: spontaneously developing infections were prevented by antibiotic treatment with marbofloxacin; d0: MCAo, d3: i.t. application of IFN-γ/solvent, d4: i.n. *S. pneumoniae* PN36 infection, d6: analysis of infarct size, bacterial burden, cytokine secretion in BALF/ plasma, cellular composition of BALF/lung/spleen. Figure 6 was published in modified form in Sandra Jagdmann et al., 2021 [59].

4 DISCUSSION

Pneumonia is the most relevant medical complication after stroke and occurs in up to 33% of all stroke patients. Despite prophylactic antibiotic treatment and other general measures to prevent SAP, the overall frequency of post-stroke pneumonia remained unchanged over the last years [8,51]. Therefore, it is essential to develop new therapeutic approaches on the basis of a better understanding of the underlying mechanisms contributing to SAP. The CNS and the immune system regulate each other in a well-balanced interplay. Stroke results in a disturbance of this homeostasis due to activation of neurohumoral stress pathways and the development of a severe temporary immunosuppression, contributing to the development of SAP. The specific aims of this PhD thesis were on the one hand to investigate mechanisms of the cholinergic system, including nAChRs and small RNAs, contributing to stroke-induced immunosuppression. On the other hand, as a proof-of-concept of an immunomodulatory therapy, an i.t. IFN-γ therapy to reconstitute the pulmonary antibacterial immune response was tested in an experimental mouse model to prevent SAP (**Figure 7**).

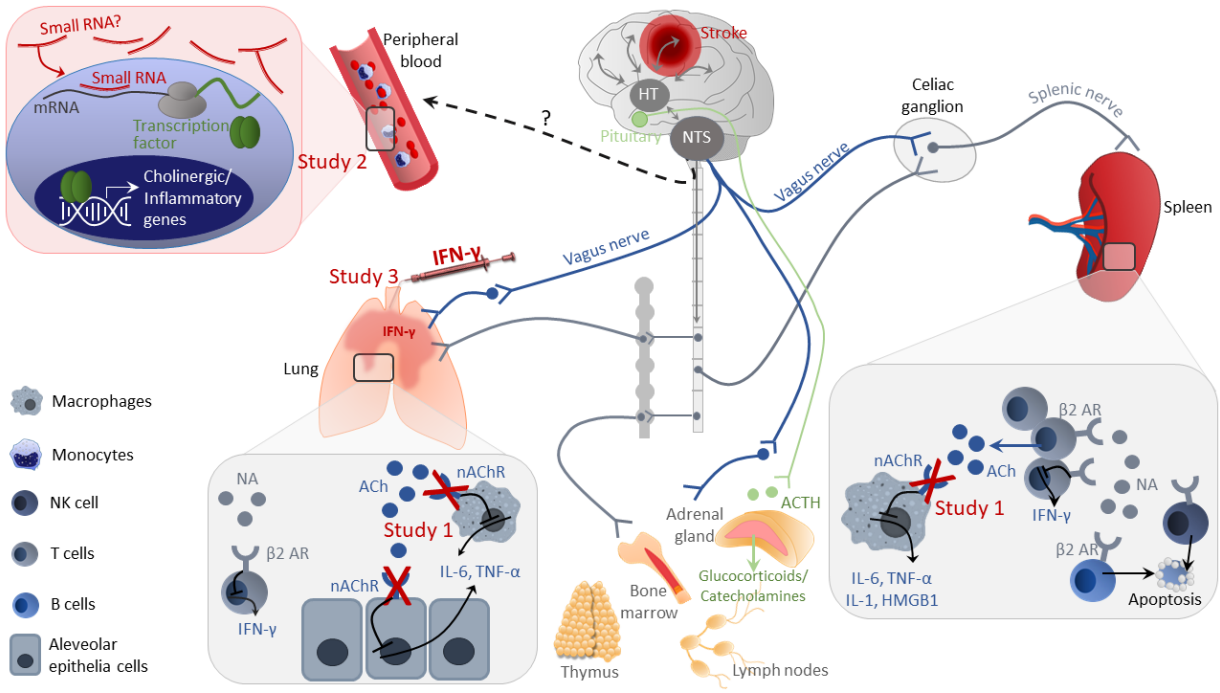

Figure 7: Most important pathophysiological mechanisms resulting in stroke-induced immunosuppression contributing to SAP and the associated research questions of studies 1-3 of this PhD thesis. Stroke leads to an activation of the HPA-axis, the cholinergic signaling and the SNS receiving inputs from the hypothalamus (HT) via the nucleus tractus solitarii (NTS). The release of noradrenaline (NA) and acetylcholine (ACh) in the lung and the lymphatic organs leads to the activation of the β2 adrenergic receptor (β2 AR) and the nicotinic acetylcholine receptor (nAChR), mediating impaired pro-inflammatory cytokine secretion by macrophages and alveolar epithelia cells, an impaired IFN-γ secretion by T cells in the lung, as well as in the spleen and apoptosis of splenic B- and NK cells. In this PhD thesis, the role of the α2, α5, α7, α9/10nAChRs (study 1), as well as small RNAs (study 2) in the cholinergic immunosuppression after stroke and the effect of i.t. IFN-γ treatment on SAP (study 3) was investigated. Figure 7 was created by Sandra Jagdmann and is not based on any previously published figure.

4.1 Study 1: nAChRs did not mediate impaired immune response against *S. pneumoniae* after stroke

Experiments in animals and humans demonstrated that, among others, cholinergic overactivation results in immunosuppression [33,34]. *In vitro* experiments revealed that the cholinergic control of LPS-induced IL-6 secretion by alveolar macrophages (AMs) is partly independent of the α7nAChR [33]. Moreover, we found that besides α7nAChR, α2, α5 and α9/10nAChRs are also expressed in the lung, suggesting a role in the impaired pulmonary immune response after stroke and investigated these receptors in a mouse model of an aspiration-induced pneumococcal pneumonia after stroke to mimic the clinical situation of increased aspiration in stroke patients. Therefore, MCAo mice were i.t. infected with 2000 CFU *S. pneumoniae.* We used the strain D39 serotype 2, whose pathogenesis was very well investigated in the experimental mouse model over the last years [60]. Since i.t. infection was shown to result in a reproducible infection rate, as well as a consistent bacterial load in the lung of infected mice [61], we used this infection technique in study 1. The infection dose of 2000 CFU, applied three days after stroke onset, was already established in our group and resulted in severe pneumococcal pneumonia in MCAo mice one day after infection, whereas naïve mice were capable of clearing bacteria within 24 h.

The recruitment of CD4 lymphocytes, neutrophils and AMs to the lung is essential in the innate immune response against *S. pneumoniae*. Experiments in mice demonstrated that the lack of CD4 lymphocytes or neutrophils results in an impaired clearance of induced pneumococci, whereas depletion of AMs leads to an increased mortality rate [62-64]. Moreover, in animals and humans, it was shown that asplenia is associated with an impaired immune response to pneumococci and an increased mortality rate [65,66], suggesting a pivotal role of the spleen in the immunity to *S. pneumoniae*. Further investigations revealed that especially the antibody response of the B lymphocytes in the marginal zone of the spleen are essential for the clearance of a pneumococcal infections [67]. Therefore, we analyzed if the KO of the α2, α5, α7, α9/10nAChRs has an effect on leukocyte composition in the lung and spleen and thus might improve pneumococcal clearance after stroke. We found no differences in the number of pulmonary and splenic leukocytes between nAChR KO MCAo mice and WT MCAo littermates, suggesting no impact of cholinergic signaling on impaired immune cell recruitment after stroke.

Our group demonstrated that α7nAChR KO mice show significantly diminished bacterial burden in the BALF during the course of a spontaneous SAP [33], mainly caused by Gram-negative bacteria [22]. In contrast, in study 1 we demonstrated that mice lacking nAChRs, including the α7nAChR exhibit no improved bacterial clearance of i.t. induced Gram-positive *S. pneumoniae* after stroke [52]. The mechanism of the pulmonary cholinergic anti-inflammatory pathway is already well described. Inflammation results in the activation of the nervus vagus, stimulating postganglionic cholinergic

neurons that innervate capillary vessels in the inter-alveolar septum, as well as mucous membrane of the bronchi and bronchuli of the lung tissue [68]. ACh is released in the lung and acts on α7nAChRs on immune cells and airway epithelia cells, resulting in impaired pro-inflammatory cytokine secretion. Stimulation of macrophages and DCs with LPS and a nAChR agonist showed diminished TNF-α, IL-1, IL-18, IL-1β, IL-10 and IL-12 secretion compared to LPS stimulated cells [29,69,70]. Interestingly, experiments in humans and animals actually demonstrated that the cytokine response by AMs and DCs to Gram-positive and Gram-negative bacteria varies greatly, which could explain the contradictory data concerning the anti-inflammatory effect, mediated by the α7nAChR: stimulation of porcine AMs with LPS (major component of the outer surface of Gram-negative bacteria) induced significantly increased IL-1β, IL-6, TNF-α and IL-10 levels in a dose-dependent manner. In contrast, only very high doses of lipoteichoic acid (LTA) (component of Gram-positive bacteria) resulted in TNF-α secretion, whereas IL-1β, IL-6 and IL-10 were not inducible [71]. Analysis of human AMs revealed similar results [72]. Investigation of cytokine responses of human DCs demonstrated that Gram-negative bacteria were capable of inducing significantly increased TNF-α, IL-6 and IL-10 levels, whereas Gram-positive bacteria did not induce TNF-α, IL-6 and IL-10 secretion [73]. In accordance with these data, we also found in study 1 that cholinergic blockade does not improve TNF-α secretion in the lung during a Gram-positive pneumococcal pneumonia (serotype 2) after stroke. Therefore, it would be interesting to investigate the role of α2, α5, α7 and α9/10nAChRs in a mouse model of Gram-negative or spontaneous pneumonia after stroke. However, experiments in mice showed that nAChR stimulation impaired clearance of *S. pneumoniae* (serotype 3), suggesting in turn that cholinergic signaling may, after all, contribute to the impaired immune response to pneumococcal infection. Here, cholinergic stimulation did also not influence pro-inflammatory cytokine secretion, suggesting an impaired functionality of leukocytes due to cholinergic signaling [74]. Indeed, it was already demonstrated that cholinergic receptor stimulation results in impaired antimicrobial functions of neutrophils and monocytes, as well as a in a reduction of antimicrobial peptide in epithelia cells, increasing the susceptibility to *S. aureus* and *S. pneumoniae* infections [75,76]. Nevertheless, in study 1, cholinergic blockade did not lead to improved pneumococcal clearance after stroke. An explanation could be that different pneumococcal serotypes were used in the studies eliciting different immune responses. Also possible would be that stroke-induced overactivation of the SNS or the HPA-axis plays a more significant role in the impaired immunity against *S. pneumoniae* D39 and that the cholinergic blockade is not sufficient to reconstitute the immunity to *S. pneumoniae*. Notably, we found significantly diminished numbers of IMs in nAChR KO and WT stroke mice compared to naïve mice supporting this consideration. Since data on IMs are scarce, the role of this leukocyte subpopulation should be further analyzed in SAP. Even though the KO of the α2, α5, α7 and α9/10nAChRs did not result in a clear

improved clearance of *S. pneumoniae* strain D39 serotype 2 after stroke, the regulation of the cholinergic signaling to prevent SAP is still of importance.

4.2 Study 2: Stroke-induced small RNAs regulate inflammation in monocytes

The activation of the cholinergic system can be influenced, among others, through the regulation of cholinergic gene expression. Small RNAs, including miRs and tRFs, were identified as important regulators of gene expression by abolishing transcripts or repressing the translation [77,78]. It was already shown that the small RNA profile changes with different diseases, including cancer, cardiovascular - , inflammatory - and neurodegeneration diseases. Owing to their stability in blood, small RNAs are very suitable as biomarkers [79]. Moreover, target analysis can provide information about the regulated genes and thus also about the underlying pathophysiology of a disease. Investigations of small RNAs in the blood after stroke demonstrated an upregulation of many non-coding RNAs in the acute and subacute phase of stroke, regulating pathophysiological mechanisms, including programmed cell death, inflammation and blood-brain barrier breakdown [80]. However, the role of small RNAs in the cholinergic anti-inflammatory pathway after stroke was not investigated so far. In study 2, we sought tRFs and miRNAs, regulating cholinergic transcripts in blood from stroke patients and found a significant decline of miRs and an increase of tRFs two days after stroke [58]. The stroke-induced tRFs targeted genes, regulating, among others, cholinergic signaling or inflammation in monocytes from stroke patients, including the Signal transducer and activator of transcription 1 (STAT1), transcription factor EC (TFEC) and Z-DNA-binding protein 1 (Zbp1). STAT1 promotes inflammation by inducing chemokine expression and the production of reactive oxygen species [81], whereas TFEC is activated by IL-4, as well as regulates the G-CSF receptor [82] and Zbp was shown to regulate cell death and induce IFN response [83]. These data suggest that stroke-induced tRFs actively contribute to the regulation of inflammation after stroke. Furthermore, we demonstrated that the top 6 upregulated tRFs in stroke patients were also increased in LPS stimulated human monocytes. The presence of the nAChR agonist nicotine resulted in a further increase of these tRFs in LPS stimulated monocytes, indicating that these small RNAs are a characteristic of the cholinergic anti-inflammatory signaling two days after stroke. Further studies, investigating if these 6 upregulated tRFs two days after stroke correlate with an increased infection risk in patients and therefore are suitable for prognosis and diagnosis, are required. Small RNAs could also act as biomarkers to distinguish between a Gram-positive and a Gram-negative SAP. Recent studies could already elaborate miRs profiles in Gram-positive, as well as Gram-negative infections [84]. It is tempting to speculate that even an identification of pathogens might be possible by small RNA analysis and therefore an individually adapted therapy. Additionally, analysis of the small RNA profile in the lung tissue after stroke could also be of critical

importance. It is already known that miRs are pivotal molecular regulators of inflammation in the lung. Pulmonary infections induce, among others, miRs-155, miRs-233 and miRs-302 in the lung, resulting in improved TNF-α secretion, granulocyte activation and the regeneration of alveolar epithelial cells and thus in an enhanced host response and recovery [85,86]. In contrast, *ex vivo* experiments with human macrophages demonstrated that pneumococci-induced miR-146A targets inflammatory genes and prevents overshooting inflammation [87]. Whether or not small RNAs species are involved in the disturbance of the pulmonary defense after stroke is not yet known. Further studies should investigate the small RNA profile in the lung after stroke and identify target genes to elucidate further pathophysiological mechanisms, contributing to the impaired immunity and to find new therapeutic approaches.

4.3 Study 3: Efficacy of local pulmonary IFN-γ treatment on SAP

Increased cholinergic signaling diminishes, among others, the IFN-γ secretion by T cells, whereas the stroke-induced overactivation of the SNS results in apoptosis of IFN-γ producing immune cells in lymphatic organs [22,88]. The reduced IFN-γ levels in blood [22] and the lung [50] are a characteristic of the immunosuppression after stroke and mainly contribute to the diminished antibacterial response [22]. In study 3, we treated stroke mice with IFN-γ to (partially) reconstitute the immune function after stroke and investigated the effect on SAP. Experiments in mice have shown that IFN-γ contributes to neurodegeneration and brain damage after stroke [89,90]. To prevent a worsened neurological outcome, we chose a local pulmonary IFN-γ administration. On the one hand, we tested the efficacy of i.t. IFN-γ in the mouse model of spontaneous post-stroke pneumonia, which simulates the course of SAP in patients and is therefore well suitable to investigate SAP in mice. Up to one-third of patients develop SAP within the first 2-5 days after stroke [5,7,91,92]. In line with these data, study 3 demonstrated that 40% of stroke mice suffer from SAP within three days. Furthermore, microbiological analyses showed that SAP is mainly caused by Gram-negative bacteria, but also to a lesser extent by streptococcus and staphylococcus species in both humans and mice [22,93-95]. Since study 1 demonstrated that different infection mouse models with different bacteria types might result in contradictory results, we investigated the effect of local pulmonary IFN-γ in the aspiration-induced model of post-stroke pneumococcal pneumonia in study 3. Experimental data demonstrated that i.n. and i.t. infection in mice with 2×10^7 CFU of *S. pneumoniae* results in the same bacterial load in the lung 12-24 h after inoculation, suggesting that both infection routes are suitable for the pneumococcal infection and lead to comparable results [96]. Since i.n. infection is easy, non-invasive and most likely mimics the natural route of infection, we used this infection technique in study 3. Experiments in mice showed that especially infection with the strain D39 serotype 2 used in study 1 lead to high-grade

sepsis, whereas a serotype 3 infection causes only pneumonia [97]. These data were in line with our observations. To prevent sepsis in stroke mice and to guarantee the survival for 48 h post infection, we used the *S. pneumoniae* strain PN36 serotype 3 in study 3. In summary, if the individual components, including infection route and bacteria strain are coordinated with each other, the aspiration-induced model of post-stroke pneumococcal pneumonia is also suitable to investigate SAP in mice.

In study 3, we found contradictory results regarding the efficacy of i.t. IFN-γ: IFN-γ treatment tended to diminish the frequency of a mainly Gram-negative spontaneous pneumonia, whereas the course of a Gram-positive pneumococcal pneumonia was tended to worsen by the IFN-γ treatment after stroke. The effect of IFN-γ on a pneumococcal pneumonia was tested with conflicting results: IFN-γ-receptor deficient 129/Sv/Ev mice infected with serotype 3 showed an improved bacterial clearance, whereas IFN-γ deficient C57BL6/J mice infected with serotype 2 revealed a diminished survival rate [98,99]. In study 3, we found a tendency to impaired clearance of *S. pneumoniae* serotype 3 and excessive increased IP-10 levels of up to 4 ng in the BALF in IFN-γ treated stroke mice. Experiments in mice showed that influenza virus infection results in significantly increased IFN-γ levels (up to 7.5 ng/ml) in the BALF, diminishing the pneumococcal clearance serotype 3 by AMs. I.n. inoculation of IFN-γ instead of the influenza virus infection confirmed diminished phagocytosis and significantly increased bacterial burden in BALF compared to PBS treated mice [100]. These data suggest that excessively elevated IFN-γ concentrations in the BALF probably impair the clearance of *S. pneumoniae.* Whether or not the pneumococcal serotype or the infected mouse strain plays a role in the IFN-γ-induced impaired clearance was not investigated, so far. In contrast, spontaneous infections after stroke, mainly caused by Gram-negative bacteria, did not seem to result in such high IFN-γ concentrations in BALF and therefore not to an impaired phagocytosis. Experiments in mice already demonstrated that IFN-γ plays an important role in the clearance of Gram-negative bacteria, including *Klebsiella pneumonia*, *Legionella pneumophila* or *Pseudomonas aeruginosa* [101-104]. Nevertheless, in study 3, IFN-γ treatment did not result in a stable efficacy and the prevention of spontaneous SAP. Stroke induces a loss of lymphocytes in the lung independent of apoptosis. Additionally, the lymphocyte chemoattractant CCL5 was also shown to be reduced in the lung after stroke, which could explain the diminished number of pulmonary lymphocytes [50]. In line with this observation, in study 3, stroke mice showed also significantly diminished numbers of pulmonary lymphocytes compared to naïve mice, suggesting a contribution to the impaired immune function and the development of spontaneous SAP. Therefore, a pulmonary CCL5 administration after stroke might result in an improved lymphocyte recruitment to the site of inflammation, subsequently to a stronger cytokine response and thus would be an interesting therapeutic approach to prevent SAP. Nevertheless, both the IFN-γ and the solvent treated stroke mice showed a lymphopenia in the spleen. This apoptosis-

induced loss of splenic lymphocytes was shown to contribute to the development of SAP [22,105]. Ultimately, the question arises, whether a local pulmonary administration is suitable to prevent SAP, triggered by a systemic immunosuppression. Systemic IFN-γ treatment 24 h after stroke onset was already tested in an experimental mouse model of spontaneous infection and significantly diminished bacterial burden in lung and blood 72 h after stroke. Analysis of the neurological outcome was not performed but is essential to consider a systemic IFN-γ administration for the treatment of SAP in patients [22].

4.4 Limitations

A critical aspect of study 1 is that an i.t. infection avoids the mechanism of mucociliary clearance in the trachea and therefore, a potential impact of stroke on the mucociliary clearance and the effect of the receptor KO would remain unnoticed. Furthermore, investigations of nAChRs in the mouse model of spontaneous SAP and a Gram-negative SAP are essential to completely assess the role of nAChRs in the impaired pulmonary immune response after stroke. Limitations of study 3 are, on the one hand, that a sufficient distribution of the i.t. applied IFN-γ in the whole lung is not ensured and on the other hand, that we tested only a single IFN-γ administration. To investigate the efficacy of i.t. applied IFN-γ we used the mouse model of spontaneous SAP. Since our data suggest that the type of bacteria influences the effect of a therapeutic, the analysis of the bacterial spectrum would have been of critical importance. However, one cannot exclude that both the i.t. IFN-γ treatment and the nAChR KO have an effect on SAP, since sample size caused by current strict animal protection laws, are very small in study 1 and 3. Therefore, small to modest effects between the groups might not be detected due to the insufficient statistical power. Another critical aspect is that in the mouse model of SAP, factors, including the heterogeneity of stroke, comorbidities, the age and gender cannot be considered and therefore the results may not be transferable to humans [106].

4.5 Conclusion

In conclusion, we found that the cholinergic blockade by the KO of α2, α5, α7 and α9/10nAChR did not improve the stroke-perturbed antibacterial defense against *S. pneumoniae*, suggesting that the cholinergic immunosuppression plays a minor role in the defense of pneumococci after stroke. Since the depletion of α7nAChRs showed promising results in the prevention of spontaneous pneumonia after stroke, the inhibition of α2, α5 and α9/10nAChR might also be a potential therapeutic approach to treat infections mainly caused by Gram-negative bacteria. A further possibility to reverse cholinergic immunosuppression would be the manipulation of the cholinergic gene regulation. We found a decline

of miRs and an increase of tRFs in the blood of stroke patients. Stroke-induced tRFs targeted TFs in monocytes, regulating inflammation and the cholinergic system, suggesting a pivotal role of tRFs in the stroke-induced anti-inflammatory pathway. In study 3 we tested an i.t. IFN-γ application to reconstitute pulmonary antibacterial immune response and prevent SAP. Local pulmonary IFN-γ administration was safe, having no effect on infarct maturation and slightly improved lung cell functionality in stroke mice. However, these effects were not sufficient to significantly prevent spontaneous infections or improve the course of an aspiration-induced pneumococcal pneumonia.

4.6 Outlook

This PhD thesis has laid the groundwork for novel therapeutic approaches with the aim to reverse stroke-induced immunosuppression and prevent SAP. Future experiments will find answers to the remaining open aspects and a suitable immunomodulatory therapy to prevent SAP. In subsequent studies further immunostimulatory cytokines should be tested, including G-CSF and IL-12 but also TLR-ligands should be considered for the prevention of SAP. The TLR-ligands MALP-2 and CpG have already been successfully tested as immunostimulators to reverse immunosuppression after influenza infection [107] or by myeloid-derived suppressor cells [108] in a mouse model. Therefore, the investigation of MALP-2 or CpG for the prevention of a SAP would also be interesting. In study 3 was shown that IFN-γ treatment results in a pronounced cytokine response but has no impact on the impaired leukocyte recruitment after stroke. Therefore, the administration of a single immunostimulator seemed to be insufficient to completely reconstitute the pulmonary immune response. Here, a combination of immunostimulators to prevent SAP would be a further therapeutic approach. Data on a combined immunostimulation are scarce, but the treatment of an abdominal mucormycosis due to a trauma-induced immunosuppression with IFN-γ combined with nivolumab (an antagonist of PD-1, inhibiting T-cell proliferation and cytokine production) showed promising results [109]. Besides the administration of immunostimulators, the manipulation of small RNA profiles could also be a new therapeutic approach to reverse immunosuppression. On the one hand, the administration of stroke-induced tRFs targets would be possible to prevent the inhibition of the gene expression of inflammatory genes, including STAT1 or Zbp1. On the other hand, the administration of small RNAs inhibiting cholinergic or adrenergic signaling after stroke could also be of critical importance. MiRs were already identified inhibiting gene expression of the β2 adrenergic receptor [110] or the nAChR [111] and therefore could possibly also used as a therapy for the prevention of SAP.

5 REFERENCES

1. Sacco Ralph, L.; Kasner Scott, E.; Broderick Joseph, P.; Caplan Louis, R.; Connors, J.J.; Culebras, A.; Elkind Mitchell, S.V.; George Mary, G.; Hamdan Allen, D.; Higashida Randall, T.; Hoh Brian, L.; Janis, L.S.; Kase Carlos, S.; Kleindorfer Dawn, O.; Lee, J.-M.; Moseley Michael, E.; Peterson Eric, D.; Turan Tanya, N.; Valderrama Amy, L.; Vinters Harry, V. An Updated Definition of Stroke for the 21st Century. *Stroke* **2013**, *44*, 2064-2089, doi:10.1161/STR.0b013e318296aeca.

2. Avan, A.; Digaleh, H.; Di Napoli, M.; Stranges, S.; Behrouz, R.; Shojaeianbabaei, G.; Amiri, A.; Tabrizi, R.; Mokhber, N.; Spence, J.D.; Azarpazhooh, M.R. Socioeconomic status and stroke incidence, prevalence, mortality, and worldwide burden: an ecological analysis from the Global Burden of Disease Study 2017. *BMC Medicine* **2019**, *17*, 191, doi:10.1186/s12916-019-1397-3.

3. Wolfe Charles, D.A.; Tilling, K.; Beech, R.; Rudd Anthony, G. Variations in Case Fatality and Dependency From Stroke in Western and Central Europe. *Stroke* **1999**, *30*, 350-356, doi:10.1161/01.STR.30.2.350.

4. Kolominsky-Rabas Peter, L.; Heuschmann Peter, U.; Marschall, D.; Emmert, M.; Baltzer, N.; Neundörfer, B.; Schöffski, O.; Krobot Karl, J. Lifetime Cost of Ischemic Stroke in Germany: Results and National Projections From a Population-Based Stroke Registry. *Stroke* **2006**, *37*, 1179-1183, doi:10.1161/01.STR.0000217450.21310.90.

5. Kumar, S.; Selim, M.H.; Caplan, L.R. Medical complications after stroke. *The Lancet Neurology* **2010**, *9*, 105-118, doi:https://doi.org/10.1016/S1474-4422(09)70266-2.

6. Langhorne, P.; Stott, D.J.; Robertson, L.; MacDonald, J.; Jones, L.; McAlpine, C.; Dick, F.; Taylor, G.S.; Murray, G. Medical complications after stroke: a multicenter study. *Stroke* **2000**, *31*, 1223-1229.

7. Meisel, C.; Schwab, J.M.; Prass, K.; Meisel, A.; Dirnagl, U. Central nervous system injury-induced immune deficiency syndrome. *Nat Rev Neurosci* **2005**, *6*, 775-786, doi:10.1038/nrn1765.

8. Emsley, H.C.A.; Hopkins, S.J. Acute ischaemic stroke and infection: recent and emerging concepts. *The Lancet Neurology* **2008**, *7*, 341-353, doi:https://doi.org/10.1016/S1474-4422(08)70061-9.

9. Johnston, K.C.; Li, J.Y.; Lyden, P.D.; Hanson, S.K.; Feasby, T.E.; Adams, R.J.; Faught, R.E., Jr.; Haley, E.C., Jr. Medical and neurological complications of ischemic stroke: experience from the RANTTAS trial. RANTTAS Investigators. *Stroke* **1998**, *29*, 447-453.

10. Perry, L.; Love, C.P. Screening for dysphagia and aspiration in acute stroke: a systematic review. *Dysphagia* **2001**, *16*, 7-18.

11. Martino, R.; Foley, N.; Bhogal, S.; Diamant, N.; Speechley, M.; Teasell, R. Dysphagia After Stroke. *Stroke* **2005**, *36*, 2756-2763, doi:10.1161/01.STR.0000190056.76543.eb.

12. Smithard, D.G.; O'Neill, P.A.; Park, C.; Morris, J.; Wyatt, R.; England, R.; Martin, D.F. Complications and Outcome After Acute Stroke. *Stroke* **1996**, *27*, 1200-1204, doi:10.1161/01.STR.27.7.1200.

13. Armstrong, J.R.; Mosher, B.D. Aspiration pneumonia after stroke: intervention and prevention. *The Neurohospitalist* **2011**, *1*, 85-93, doi:10.1177/1941875210395775.

14. McCullough, G.H.; Rosenbek, J.C.; Wertz, R.T.; McCoy, S.; Mann, G.; McCullough, K. Utility of Clinical Swallowing Examination Measures for Detecting Aspiration Post-Stroke. *Journal of Speech, Language, and Hearing Research* **2005**, *48*, 1280-1293, doi:10.1044/1092-4388(2005/089).

15. Liesz, A.; Dalpke, A.; Mracsko, E.; Antoine, D.J.; Roth, S.; Zhou, W.; Yang, H.; Na, S.-Y.; Akhisaroglu, M.; Fleming, T.; Eigenbrod, T.; Nawroth, P.P.; Tracey, K.J.; Veltkamp, R. DAMP signaling is a key pathway inducing immune modulation after brain injury. *J Neurosci* **2015**, *35*, 583-598, doi:10.1523/JNEUROSCI.2439-14.2015.

16. Barugh, A.J.; Gray, P.; Shenkin, S.D.; MacLullich, A.M.J.; Mead, G.E. Cortisol levels and the severity and outcomes of acute stroke: a systematic review. *J Neurol* **2014**, *261*, 533-545, doi:10.1007/s00415-013-7231-5.

17. Olsson, T.; Marklund, N.; Gustafson, Y.; Näsman, B. Abnormalities at different levels of the hypothalamic-pituitary-adrenocortical axis early after stroke. *Stroke* **1992**, *23*, 1573-1576, doi:10.1161/01.STR.23.11.1573.

18. Fassbender, K.; Schmidt, R.; Mössner, R.; Daffertshofer, M.; Hennerici, M. Pattern of activation of the hypothalamic-pituitary-adrenal axis in acute stroke. Relation to acute confusional state, extent of brain damage, and clinical outcome. *Stroke* **1994**, *25*, 1105-1108, doi:10.1161/01.STR.25.6.1105.

19. Buckley, T.M.; Schatzberg, A.F. On the interactions of the hypothalamic-pituitary-adrenal (HPA) axis and sleep: normal HPA axis activity and circadian rhythm, exemplary sleep disorders. *J Clin Endocrinol Metab* **2005**, *90*, 3106-3114, doi:10.1210/jc.2004-1056.

20. Huang, Y.-y.; Li, X.; Li, X.; Sheng, Y.-y.; Zhuang, P.-w.; Zhang, Y.-j. Neuroimmune crosstalk in central nervous system injury-induced infection and pharmacological intervention. *Brain Research Bulletin* **2019**, *153*, 232-238, doi:https://doi.org/10.1016/j.brainresbull.2019.09.003.

21. El Husseini, N.; Laskowitz, D.T. The role of neuroendocrine pathways in prognosis after stroke. *Expert Rev Neurother* **2014**, *14*, 217-232, doi:10.1586/14737175.2014.877841.

22. Prass, K.; Meisel, C.; Höflich, C.; Braun, J.; Halle, E.; Wolf, T.; Ruscher, K.; Victorov, I.V.; Priller, J.; Dirnagl, U.; Volk, H.-D.; Meisel, A. Stroke-induced Immunodeficiency Promotes Spontaneous Bacterial Infections and Is Mediated by Sympathetic Activation Reversal by Poststroke T Helper Cell Type 1–like Immunostimulation. *J Exp Med* **2003**, *198*, 725, doi:10.1084/jem.20021098.

23. Bankenahally, R.; Krovvidi, H. Autonomic nervous system: anatomy, physiology, and relevance in anaesthesia and critical care medicine. *BJA Education* **2016**, *16*, 381-387, doi:10.1093/bjaed/mkw011.

24. Bellinger, D.L.; Millar, B.A.; Perez, S.; Carter, J.; Wood, C.; ThyagaRajan, S.; Molinaro, C.; Lubahn, C.; Lorton, D. Sympathetic modulation of immunity: relevance to disease. *Cell Immunol* **2008**, *252*, 27-56, doi:10.1016/j.cellimm.2007.09.005.

25. Breit, S.; Kupferberg, A.; Rogler, G.; Hasler, G. Vagus Nerve as Modulator of the Brain–Gut Axis in Psychiatric and Inflammatory Disorders. *Frontiers in Psychiatry* **2018**, *9*, doi:10.3389/fpsyt.2018.00044.

26. Pavlov, V.A.; Wang, H.; Czura, C.J.; Friedman, S.G.; Tracey, K.J. The cholinergic anti-inflammatory pathway: a missing link in neuroimmunomodulation. *Molecular medicine (Cambridge, Mass.)* **2003**, *9*, 125-134.

27. Fujii, T.; Mashimo, M.; Moriwaki, Y.; Misawa, H.; Ono, S.; Horiguchi, K.; Kawashima, K. Physiological functions of the cholinergic system in immune cells. *Journal of Pharmacological Sciences* **2017**, *134*, 1-21, doi:https://doi.org/10.1016/j.jphs.2017.05.002.

28. Kummer, W.; Lips, K.S.; Pfeil, U. The epithelial cholinergic system of the airways. *Histochemistry and Cell Biology* **2008**, *130*, 219, doi:10.1007/s00418-008-0455-2.

29. Tracey, K.J. The inflammatory reflex. *Nature* **2002**, *420*, 853-859, doi:10.1038/nature01321.

30. Shaked, I.; Meerson, A.; Wolf, Y.; Avni, R.; Greenberg, D.; Gilboa-Geffen, A.; Soreq, H. MicroRNA-132 Potentiates Cholinergic Anti-Inflammatory Signaling by Targeting Acetylcholinesterase. *Immunity* **2009**, *31*, 965-973, doi:https://doi.org/10.1016/j.immuni.2009.09.019.

31. Sun, Y.; Li, Q.; Gui, H.; Xu, D.-P.; Yang, Y.-L.; Su, D.-F.; Liu, X. MicroRNA-124 mediates the cholinergic anti-inflammatory action through inhibiting the production of pro-inflammatory cytokines. *Cell Research* **2013**, *23*, 1270-1283, doi:10.1038/cr.2013.116.

32. Huston, J.M.; Ochani, M.; Rosas-Ballina, M.; Liao, H.; Ochani, K.; Pavlov, V.A.; Gallowitsch-Puerta, M.; Ashok, M.; Czura, C.J.; Foxwell, B.; Tracey, K.J.; Ulloa, L. Splenectomy inactivates the cholinergic antiinflammatory pathway during lethal endotoxemia and polymicrobial sepsis. *Journal of Experimental Medicine* **2006**, *203*, 1623-1628, doi:10.1084/jem.20052362.

33. Engel, O.; Akyuz, L.; da Costa Goncalves, A.C.; Winek, K.; Dames, C.; Thielke, M.; Herold, S.; Bottcher, C.; Priller, J.; Volk, H.D.; Dirnagl, U.; Meisel, C.; Meisel, A. Cholinergic Pathway Suppresses Pulmonary Innate Immunity Facilitating Pneumonia After Stroke. *Stroke* **2015**, *46*, 3232-3240, doi:10.1161/STROKEAHA.115.008989.

34. Yuan, M.; Han, B.; Xia, Y.; Liu, Y.; Wang, C.; Zhang, C. Augmentation of peripheral lymphocyte-derived cholinergic activity in patients with acute ischemic stroke. *BMC Neurology* **2019**, *19*, 236, doi:10.1186/s12883-019-1481-5.

35. Gahring, L.; Rogers, S. Neuronal Nicotinic Acetylcholine Receptor Expression and Function on Nonneuronal Cells. *Drug Addiction: From Basic Research to Therapy* **2008**, 10.1007/978-0-387-76678-2_10, 149-166, doi:10.1007/978-0-387-76678-2_10.

36. Kawashima, K.; Fujii, T.; Moriwaki, Y.; Misawa, H. Critical roles of acetylcholine and the muscarinic and nicotinic acetylcholine receptors in the regulation of immune function. *Life Sci* **2012**, *91*, 1027-1032, doi:10.1016/j.lfs.2012.05.006.

37. Beckmann, J.; Lips, K.S. The Non-Neuronal Cholinergic System in Health and Disease. *Pharmacology* **2013**, *92*, 286-302, doi:10.1159/000355835.

38. Wang, H.; Liao, H.; Ochani, M.; Justiniani, M.; Lin, X.; Yang, L.; Al-Abed, Y.; Wang, H.; Metz, C.; Miller, E.J.; Tracey, K.J.; Ulloa, L. Cholinergic agonists inhibit HMGB1 release and improve survival in experimental sepsis. *Nat Med* **2004**, *10*, 1216-1221, doi:10.1038/nm1124.

39. Han, Z.; Shen, F.; He, Y.; Degos, V.; Camus, M.; Maze, M.; Young, W.L.; Su, H. Activation of α-7 nicotinic acetylcholine receptor reduces ischemic stroke injury through reduction of pro-inflammatory macrophages and oxidative stress. *PLoS One* **2014**, *9*, e105711, doi:10.1371/journal.pone.0105711.

40. Zou, D.; Luo, M.; Han, Z.; Zhan, L.; Zhu, W.; Kang, S.; Bao, C.; Li, Z.; Nelson, J.; Zhang, R.; Su, H. Activation of Alpha-7 Nicotinic Acetylcholine Receptor Reduces Brain Edema in Mice with

Ischemic Stroke and Bone Fracture. *Mol Neurobiol* **2017**, *54*, 8278-8286, doi:10.1007/s12035-016-0310-8.

41. Teramoto, S. Novel preventive and therapeutic strategy for post-stroke pneumonia. *Expert Review of Neurotherapeutics* **2009**, *9*, 1187-1200, doi:10.1586/ern.09.72.

42. Schwarz, S. Prophylactic Antibiotic Therapy for Preventing Poststroke Infection. *Neurotherapeutics* **2016**, *13*, 783-790, doi:10.1007/s13311-016-0466-y.

43. Westendorp, W.F.; Vermeij, J.-D.; Zock, E.; Hooijenga, I.J.; Kruyt, N.D.; Bosboom, H.J.L.W.; Kwa, V.I.H.; Weisfelt, M.; Remmers, M.J.M.; ten Houten, R.; Schreuder, A.H.C.M.; Vermeer, S.E.; van Dijk, E.J.; Dippel, D.W.J.; Dijkgraaf, M.G.W.; Spanjaard, L.; Vermeulen, M.; van der Poll, T.; Prins, J.M.; Vermeij, F.H.; Roos, Y.B.W.E.M.; Kleyweg, R.P.; Kerkhoff, H.; Brouwer, M.C.; Zwinderman, A.H.; van de Beek, D.; Nederkoorn, P.J. The Preventive Antibiotics in Stroke Study (PASS): a pragmatic randomised open-label masked endpoint clinical trial. *The Lancet* **2015**, *385*, 1519-1526, doi:10.1016/S0140-6736(14)62456-9.

44. Kalra, L.; Irshad, S.; Hodsoll, J.; Simpson, M.; Gulliford, M.; Smithard, D.; Patel, A.; Rebollo-Mesa, I. Prophylactic antibiotics after acute stroke for reducing pneumonia in patients with dysphagia (STROKE-INF): a prospective, cluster-randomised, open-label, masked endpoint, controlled clinical trial. *The Lancet* **2015**, *386*, 1835-1844, doi:https://doi.org/10.1016/S0140-6736(15)00126-9.

45. Döcke, W.D.; Randow, F.; Syrbe, U.; Krausch, D.; Asadullah, K.; Reinke, P.; Volk, H.D.; Kox, W. Monocyte deactivation in septic patients: restoration by IFN-gamma treatment. *Nat Med* **1997**, *3*, 678-681, doi:10.1038/nm0697-678.

46. Meisel, C.; Schefold, J.C.; Pschowski, R.; Baumann, T.; Hetzger, K.; Gregor, J.; Weber-Carstens, S.; Hasper, D.; Keh, D.; Zuckermann, H.; Reinke, P.; Volk, H.D. Granulocyte-macrophage colony-stimulating factor to reverse sepsis-associated immunosuppression: a double-blind, randomized, placebo-controlled multicenter trial. *Am J Respir Crit Care Med* **2009**, *180*, 640-648, doi:10.1164/rccm.200903-0363OC.

47. Spies, C.; Luetz, A.; Lachmann, G.; Renius, M.; von Haefen, C.; Wernecke, K.-D.; Bahra, M.; Schiemann, A.; Paupers, M.; Meisel, C. Influence of Granulocyte-Macrophage Colony-Stimulating Factor or Influenza Vaccination on HLA-DR, Infection and Delirium Days in Immunosuppressed Surgical Patients: Double Blind, Randomised Controlled Trial. *PLoS One* **2015**, *10*, e0144003-e0144003, doi:10.1371/journal.pone.0144003.

48. Standiford, T.J.; Deng, J.C. Immunomodulation for the prevention and treatment of lung infections. *Semin Respir Crit Care Med* **2004**, *25*, 95-108, doi:10.1055/s-2004-822309.

49. Dames, C.; Winek, K.; Beckers, Y.; Engel, O.; Meisel, A.; Meisel, C. Immunomodulatory treatment with systemic GM-CSF augments pulmonary immune responses and improves neurological outcome after experimental stroke. *Journal of Neuroimmunology* **2018**, *321*, 144-149, doi:https://doi.org/10.1016/j.jneuroim.2018.03.005.

50. Farris, B.Y.; Monaghan, K.L.; Zheng, W.; Amend, C.D.; Hu, H.; Ammer, A.G.; Coad, J.E.; Ren, X.; Wan, E.C.K. Ischemic stroke alters immune cell niche and chemokine profile in mice independent of spontaneous bacterial infection. *Immunity, Inflammation and Disease* **2019**, *7*, 326-341, doi:10.1002/iid3.277.

51. Meisel, A.; Smith, C.J. Preventive antibiotics for stroke-associated pneumonia. *Nature Reviews Neurology* **2015**, *11*, 672-673, doi:10.1038/nrneurol.2015.220.

52. Jagdmann, S.; Dames, C.; Berchtold, D.; Winek, K.; Weitbrecht, L.; Meisel, A.; Meisel, C. Impact of Key Nicotinic AChR Subunits on Post-Stroke Pneumococcal Pneumonia. *Vaccines (Basel)* **2020**, *8*, doi:10.3390/vaccines8020253.

53. Engel, O.; Kolodziej, S.; Dirnagl, U.; Prinz, V. Modeling stroke in mice - middle cerebral artery occlusion with the filament model. *J Vis Exp* **2011**, 10.3791/2423, doi:10.3791/2423.

54. Dames, C.; Akyüz, L.; Reppe, K.; Tabeling, C.; Dietert, K.; Kershaw, O.; Gruber, A.D.; Meisel, C.; Meisel, A.; Witzenrath, M.; Engel, O. Miniaturized bronchoscopy enables unilateral investigation, application, and sampling in mice. *Am J Respir Cell Mol Biol* **2014**, *51*, 730-737, doi:10.1165/rcmb.2014-0052ma.

55. Sun, F.; Xiao, G.; Qu, Z. Murine Bronchoalveolar Lavage. *Bio Protoc* **2017**, *7*, e2287, doi:10.21769/BioProtoc.2287.

56. Prass, K.; Braun Johann, S.; Dirnagl, U.; Meisel, C.; Meisel, A. Stroke Propagates Bacterial Aspiration to Pneumonia in a Model of Cerebral Ischemia. *Stroke* **2006**, *37*, 2607-2612, doi:10.1161/01.STR.0000240409.68739.2b.

57. Marbach, D.; Lamparter, D.; Quon, G.; Kellis, M.; Kutalik, Z.; Bergmann, S. Tissue-specific regulatory circuits reveal variable modular perturbations across complex diseases. *Nature Methods* **2016**, *13*, 366-370, doi:10.1038/nmeth.3799.

58. Winek, K.; Lobentanzer, S.; Nadorp, B.; Dubnov, S.; Dames, C.; Jagdmann, S.; Moshitzky, G.; Hotter, B.; Meisel, C.; Greenberg, D.S.; Shifman, S.; Klein, J.; Shenhar-Tsarfaty, S.; Meisel, A.; Soreq, H. Transfer RNA fragments replace microRNA regulators of the cholinergic poststroke immune blockade. *Proceedings of the National Academy of Sciences* **2020**, 10.1073/pnas.2013542117, 202013542, doi:10.1073/pnas.2013542117.

59. Jagdmann, S.; Berchtold, D.; Gutbier, B.; Witzenrath, M.; Meisel, A.; Meisel, C.; Dames, C. Efficacy and safety of intratracheal IFN-γ treatment to reverse stroke-induced susceptibility to pulmonary bacterial infections. *Journal of Neuroimmunology* **2021**, https://doi.org/10.1016/j.jneuroim.2021.577568, 577568, doi:https://doi.org/10.1016/j.jneuroim.2021.577568.

60. Chiavolini, D.; Pozzi, G.; Ricci, S. Animal models of Streptococcus pneumoniae disease. *Clin Microbiol Rev* **2008**, *21*, 666-685, doi:10.1128/CMR.00012-08.

61. Rubins, J.B.; Charboneau, D.; Paton, J.C.; Mitchell, T.J.; Andrew, P.W.; Janoff, E.N. Dual function of pneumolysin in the early pathogenesis of murine pneumococcal pneumonia. *The Journal of clinical investigation* **1995**, *95*, 142-150, doi:10.1172/JCI117631.

62. Kadioglu, A.; Coward, W.; Colston, M.J.; Hewitt, C.R.A.; Andrew, P.W. CD4-T-Lymphocyte Interactions with Pneumolysin and Pneumococci Suggest a Crucial Protective Role in the Host Response to Pneumococcal Infection. *Infection and Immunity* **2004**, *72*, 2689, doi:10.1128/IAI.72.5.2689-2697.2004.

63. José, R.J.; Williams, A.E.; Mercer, P.F.; Sulikowski, M.G.; Brown, J.S.; Chambers, R.C. Regulation of neutrophilic inflammation by proteinase-activated receptor 1 during bacterial pulmonary infection. *Journal of immunology (Baltimore, Md. : 1950)* **2015**, *194*, 6024-6034, doi:10.4049/jimmunol.1500124.

64. Knapp, S.; Leemans, J.C.; Florquin, S.; Branger, J.; Maris, N.A.; Pater, J.; van Rooijen, N.; van der Poll, T. Alveolar macrophages have a protective antiinflammatory role during murine

pneumococcal pneumonia. *Am J Respir Crit Care Med* **2003**, *167*, 171-179, doi:10.1164/rccm.200207-698OC.

65. Holdsworth, R.J.; Irving, A.D.; Cuschieri, A. Postsplenectomy sepsis and its mortality rate: actual versus perceived risks. *Br J Surg* **1991**, *78*, 1031-1038, doi:10.1002/bjs.1800780904.

66. Brown, E.J.; Hosea, S.W.; Frank, M.M. The role of the spleen in experimental pneumococcal bacteremia. *J Clin Invest* **1981**, *67*, 975-982, doi:10.1172/jci110148.

67. Birjandi, S.; Witte, P. Why are the elderly so susceptible to pneumonia? *Expert Review of Respiratory Medicine* **2011**, *5*, 593-595, doi:10.1586/ers.11.50.

68. Wojtarowicz, A.; Podlasz, P.; Czaja, K. Adrenergic and cholinergic innervation of pulmonary tissue in the pig. *Folia Morphol (Warsz)* **2003**, *62*, 215-218.

69. Yamada, M.; Ichinose, M. The cholinergic anti-inflammatory pathway: an innovative treatment strategy for respiratory diseases and their comorbidities. *Current Opinion in Pharmacology* **2018**, *40*, 18-25, doi:https://doi.org/10.1016/j.coph.2017.12.003.

70. Nouri-Shirazi, M.; Guinet, E. Evidence for the immunosuppressive role of nicotine on human dendritic cell functions. *Immunology* **2003**, *109*, 365-373, doi:10.1046/j.1365-2567.2003.01655.x.

71. Islam, M.A.; Pröll, M.; Hölker, M.; Tholen, E.; Tesfaye, D.; Looft, C.; Schellander, K.; Cinar, M.U. Alveolar macrophage phagocytic activity is enhanced with LPS priming, and combined stimulation of LPS and lipoteichoic acid synergistically induce pro-inflammatory cytokines in pigs. *Innate Immun* **2013**, *19*, 631-643, doi:10.1177/1753425913477166.

72. Hoogerwerf, J.J.; Vos, A.F.d.; Bresser, P.; Zee, J.S.v.d.; Pater, J.M.; Boer, A.d.; Tanck, M.; Lundell, D.L.; Her-Jenh, C.; Draing, C.; Aulock, S.v.; Poll, T.v.d. Lung Inflammation Induced by Lipoteichoic Acid or Lipopolysaccharide in Humans. *American Journal of Respiratory and Critical Care Medicine* **2008**, *178*, 34-41, doi:10.1164/rccm.200708-1261OC.

73. Karlsson, H.; Larsson, P.; Wold, A.E.; Rudin, A. Pattern of cytokine responses to gram-positive and gram-negative commensal bacteria is profoundly changed when monocytes differentiate into dendritic cells. *Infection and immunity* **2004**, *72*, 2671-2678, doi:10.1128/iai.72.5.2671-2678.2004.

74. Giebelen, I.A.J.; Leendertse, M.; Florquin, S.; van der Poll, T. Stimulation of acetylcholine receptors impairs host defence during pneumococcal pneumonia. *European Respiratory Journal* **2009**, *33*, 375, doi:10.1183/09031936.00103408.

75. Pabst, M.J.; Pabst, K.M.; Collier, J.A.; Coleman, T.C.; Lemons-Prince, M.L.; Godat, M.S.; Waring, M.B.; Babu, J.P. Inhibition of Neutrophil and Monocyte Defensive Functions by Nicotine. *Journal of Periodontology* **1995**, *66*, 1047-1055, doi:https://doi.org/10.1902/jop.1995.66.12.1047.

76. Radek, K.A.; Elias, P.M.; Taupenot, L.; Mahata, S.K.; O'Connor, D.T.; Gallo, R.L. Neuroendocrine Nicotinic Receptor Activation Increases Susceptibility to Bacterial Infections by Suppressing Antimicrobial Peptide Production. *Cell Host & Microbe* **2010**, *7*, 277-289, doi:https://doi.org/10.1016/j.chom.2010.03.009.

77. Ardekani, A.M.; Naeini, M.M. The Role of MicroRNAs in Human Diseases. *Avicenna J Med Biotechnol* **2010**, *2*, 161-179.

78. Keam, S.P.; Hutvagner, G. tRNA-Derived Fragments (tRFs): Emerging New Roles for an Ancient RNA in the Regulation of Gene Expression. *Life (Basel)* **2015**, *5*, 1638-1651, doi:10.3390/life5041638.

79. Zhang, C. Novel functions for small RNA molecules. *Curr Opin Mol Ther* **2009**, *11*, 641-651.

80. Tiedt, S.; Dichgans, M. Role of Non-Coding RNAs in Stroke. *Stroke* **2018**, *49*, 3098-3106, doi:doi:10.1161/STROKEAHA.118.021010.

81. Kaplan, M.H. STAT signaling in inflammation. *JAKSTAT* **2013**, *2*, e24198-e24198, doi:10.4161/jkst.24198.

82. Rehli, M.; Sulzbacher, S.; Pape, S.; Ravasi, T.; Wells, C.A.; Heinz, S.; Söllner, L.; El Chartouni, C.; Krause, S.W.; Steingrimsson, E.; Hume, D.A.; Andreesen, R. Transcription Factor Tfec Contributes to the IL-4-Inducible Expression of a Small Group of Genes in Mouse Macrophages Including the Granulocyte Colony-Stimulating Factor Receptor. *The Journal of Immunology* **2005**, *174*, 7111, doi:10.4049/jimmunol.174.11.7111.

83. Kuriakose, T.; Kanneganti, T.-D. ZBP1: Innate Sensor Regulating Cell Death and Inflammation. *Trends in Immunology* **2018**, *39*, 123-134, doi:https://doi.org/10.1016/j.it.2017.11.002.

84. Eulalio, A.; Schulte, L.; Vogel, J. The mammalian microRNA response to bacterial infections. *RNA Biol* **2012**, *9*, 742-750, doi:10.4161/rna.20018.

85. Rupani, H.; Sanchez-Elsner, T.; Howarth, P. MicroRNAs and respiratory diseases. *Eur Respir J* **2013**, *41*, 695-705, doi:10.1183/09031936.00212011.

86. Wang, Y.; Li, Y.; Zhang, P.; Baker, S.T.; Wolfson, M.R.; Weiser, J.N.; Tian, Y.; Shen, H. Regenerative therapy based on miRNA-302 mimics for enhancing host recovery from pneumonia caused by <em>Streptococcus pneumoniae</em&gt. *Proceedings of the National Academy of Sciences* **2019**, *116*, 8493, doi:10.1073/pnas.1818522116.

87. Griss, K.; Bertrams, W.; Sittka-Stark, A.; Seidel, K.; Stielow, C.; Hippenstiel, S.; Suttorp, N.; Eberhardt, M.; Wilhelm, J.; Vera, J.; Schmeck, B. MicroRNAs Constitute a Negative Feedback Loop in Streptococcus pneumoniae–Induced Macrophage Activation. *The Journal of Infectious Diseases* **2016**, *214*, 288-299, doi:10.1093/infdis/jiw109.

88. Nizri, E.; Irony-Tur-Sinai, M.; Lory, O.; Orr-Urtreger, A.; Lavi, E.; Brenner, T. Activation of the Cholinergic Anti-Inflammatory System by Nicotine Attenuates Neuroinflammation via Suppression of Th1 and Th17 Responses. *The Journal of Immunology* **2009**, *183*, 6681, doi:10.4049/jimmunol.0902212.

89. Lambertsen, K.L.; Gregersen, R.; Meldgaard, M.; Clausen, B.H.; Heibøl, E.K.; Ladeby, R.; Knudsen, J.; Frandsen, A.; Owens, T.; Finsen, B. A Role for Interferon-Gamma in Focal Cerebral Ischemia in Mice. *Journal of Neuropathology & Experimental Neurology* **2004**, *63*, 942-955, doi:10.1093/jnen/63.9.942.

90. Seifert, H.A.; Collier, L.A.; Chapman, C.B.; Benkovic, S.A.; Willing, A.E.; Pennypacker, K.R. Pro-inflammatory interferon gamma signaling is directly associated with stroke induced neurodegeneration. *J Neuroimmune Pharmacol* **2014**, *9*, 679-689, doi:10.1007/s11481-014-9560-2.

91. Kishore, A.K.; Jeans, A.R.; Garau, J.; Bustamante, A.; Kalra, L.; Langhorne, P.; Chamorro, A.; Urra, X.; Katan, M.; Napoli, M.D.; Westendorp, W.; Nederkoorn, P.J.; van de Beek, D.; Roffe, C.;

Woodhead, M.; Montaner, J.; Meisel, A.; Smith, C.J. Antibiotic treatment for pneumonia complicating stroke: Recommendations from the pneumonia in stroke consensus (PISCES) group. *Eur Stroke J* **2019**, *4*, 318-328, doi:10.1177/2396987319851335.

92. Sellars, C.; Bowie, L.; Bagg, J.; Sweeney, M.P.; Miller, H.; Tilston, J.; Langhorne, P.; Stott David, J. Risk Factors for Chest Infection in Acute Stroke. *Stroke* **2007**, *38*, 2284-2291, doi:10.1161/STROKEAHA.106.478156.

93. Kishore Amit, K.; Vail, A.; Jeans Adam, R.; Chamorro, A.; Di Napoli, M.; Kalra, L.; Langhorne, P.; Roffe, C.; Westendorp, W.; Nederkoorn Paul, J.; Garau, J.; van de Beek, D.; Montaner, J.; Woodhead, M.; Meisel, A.; Smith Craig, J.; null, n. Microbiological Etiologies of Pneumonia Complicating Stroke. *Stroke* **2018**, *49*, 1602-1609, doi:10.1161/STROKEAHA.117.020250.

94. Meisel, C.; Prass, K.; Braun, J.; Victorov, I.; Wolf, T.; Megow, D.; Halle, E.; Volk, H.-D.; Dirnagl, U.; Meisel, A. Preventive Antibacterial Treatment Improves the General Medical and Neurological Outcome in a Mouse Model of Stroke. *Stroke* **2004**, *35*, 2-6, doi:doi:10.1161/01.STR.0000109041.89959.4C.

95. Liesz, A.; Hagmann, S.; Zschoche, C.; Adamek, J.; Zhou, W.; Sun, L.; Hug, A.; Zorn, M.; Dalpke, A.; Nawroth, P.; Veltkamp, R. The Spectrum of Systemic Immune Alterations After Murine Focal Ischemia. *Stroke* **2009**, *40*, 2849-2858, doi:doi:10.1161/STROKEAHA.109.549618.

96. Jeong, D.-G.; Jeong, E.-S.; Seo, J.-H.; Heo, S.-H.; Choi, Y.-K. Difference in Resistance to Streptococcus pneumoniae Infection in Mice. *Lab Anim Res* **2011**, *27*, 91-98, doi:10.5625/lar.2011.27.2.91.

97. Orihuela, C.J.; Gao, G.; McGee, M.; Yu, J.; Francis, K.P.; Tuomanen, E. Organ-specific models of Streptococcus pneumoniae Disease. *Scandinavian Journal of Infectious Diseases* **2003**, *35*, 647-652, doi:10.1080/00365540310015854.

98. Rubins, J.B.; Pomeroy, C. Role of gamma interferon in the pathogenesis of bacteremic pneumococcal pneumonia. *Infection and immunity* **1997**, *65*, 2975-2977.

99. Rijneveld, A.W.; Lauw, F.N.; Schultz, M.J.; Florquin, S.; Te Velde, A.A.; Speelman, P.; Van Deventer, S.J.; Van Der Poll, T. The role of interferon-gamma in murine pneumococcal pneumonia. *J Infect Dis* **2002**, *185*, 91-97, doi:10.1086/338122.

100. Sun, K.; Metzger, D.W. Inhibition of pulmonary antibacterial defense by interferon-γ during recovery from influenza infection. *Nature Medicine* **2008**, *14*, 558-564, doi:10.1038/nm1765.

101. Moore, T.A.; Perry, M.L.; Getsoian, A.G.; Newstead, M.W.; Standiford, T.J. Divergent Role of Gamma Interferon in a Murine Model of Pulmonary versus Systemic Klebsiella pneumoniae Infection. *Infection and Immunity* **2002**, *70*, 6310, doi:10.1128/IAI.70.11.6310-6318.2002.

102. Yoshida, K.; Matsumoto, T.; Tateda, K.; Uchida, K.; Tsujimoto, S.; Iwakura, Y.; Yamaguchi, K. Protection against pulmonary infection with Klebsiella pneumoniae in mice by interferon-gamma through activation of phagocytic cells and stimulation of production of other cytokines. *J Med Microbiol* **2001**, *50*, 959-964, doi:10.1099/0022-1317-50-11-959.

103. Shinozawa, Y.; Matsumoto, T.; Uchida, K.; Tsujimoto, S.; Iwakura, Y.; Yamaguchi, K. Role of interferon-gamma in inflammatory responses in murine respiratory infection with Legionella pneumophila. *J Med Microbiol* **2002**, *51*, 225-230, doi:10.1099/0022-1317-51-3-225.

104. Lei, D.; Lancaster, J.R., Jr.; Joshi, M.S.; Nelson, S.; Stoltz, D.; Bagby, G.J.; Odom, G.; Shellito, J.E.; Kolls, J.K. Activation of alveolar macrophages and lung host defenses using transfer of the interferon-gamma gene. *Am J Physiol* **1997**, *272*, L852-859, doi:10.1152/ajplung.1997.272.5.L852.

105. McCulloch, L.; Smith, C.J.; McColl, B.W. Adrenergic-mediated loss of splenic marginal zone B cells contributes to infection susceptibility after stroke. *Nature Communications* **2017**, *8*, 15051, doi:10.1038/ncomms15051.

106. Mergenthaler, P.; Meisel, A. Do stroke models model stroke? *Dis Model Mech* **2012**, *5*, 718-725, doi:10.1242/dmm.010033.

107. Reppe, K.; Radünzel, P.; Dietert, K.; Tschernig, T.; Wolff, T.; Hammerschmidt, S.; Gruber, A.D.; Suttorp, N.; Witzenrath, M. Pulmonary immunostimulation with MALP-2 in influenza virus-infected mice increases survival after pneumococcal superinfection. *Infect Immun* **2015**, *83*, 4617-4629, doi:10.1128/iai.00948-15.

108. Zoglmeier, C.; Bauer, H.; Noerenberg, D.; Wedekind, G.; Bittner, P.; Sandholzer, N.; Rapp, M.; Anz, D.; Endres, S.; Bourquin, C. CpG blocks immunosuppression by myeloid-derived suppressor cells in tumor-bearing mice. *Clin Cancer Res* **2011**, *17*, 1765-1775, doi:10.1158/1078-0432.Ccr-10-2672.

109. Grimaldi, D.; Pradier, O.; Hotchkiss, R.S.; Vincent, J.-L. Nivolumab plus interferon-γ in the treatment of intractable mucormycosis. *The Lancet Infectious Diseases* **2017**, *17*, 18, doi:https://doi.org/10.1016/S1473-3099(16)30541-2.

110. Yu, B.; Yao, L.; Liu, C.; Tang, L.; Xing, T. Upregulation of microRNA-16 alters the response to inhaled β-agonists in patients with asthma though modulating expression of ADRB2. *Mol Med Rep* **2019**, *19*, 4027-4034, doi:10.3892/mmr.2019.10097.

111. Hogan, E.M.; Casserly, A.P.; Scofield, M.D.; Mou, Z.; Zhao-Shea, R.; Johnson, C.W.; Tapper, A.R.; Gardner, P.D. miRNAome analysis of the mammalian neuronal nicotinic acetylcholine receptor gene family. *RNA* **2014**, *20*, 1890-1899, doi:10.1261/rna.034066.112.

6 STATUTORY DECLARATION

“I, Sandra Jagdmann, by personally signing this document in lieu of an oath, hereby affirm that I prepared the submitted dissertation on the topic „ Paralysis of pulmonary immunity after stroke by neurohumoral mechanisms / Paralyse der pulmonalen Immunität durch neurohumorale Mechanismen nach Schlaganfall”, independently and without the support of third parties, and that I used no other sources and aids than those stated.

All parts, which are based on the publications or presentations of other authors, either in letter or in spirit, are specified as such in accordance with the citing guidelines. The sections on methodology (in particular regarding practical work, laboratory regulations, statistical processing) and results (in particular regarding figures, charts and tables) are exclusively my responsibility.

Furthermore, I declare that I have correctly marked all of the data, the analyses, and the conclusions generated from data obtained in collaboration with other persons, and that I have correctly marked my own contribution and the contributions of other persons (cf. declaration of contribution). I have correctly marked all texts or parts of texts that were generated in collaboration with other persons.

My contributions to any publications to this dissertation correspond to those stated in the below joint declaration made together with the supervisor. All publications created within the scope of the dissertation comply with the guidelines of the ICMJE (International Committee of Medical Journal Editors; www.icmje.org) on authorship. In addition, I declare that I shall comply with the regulations of Charité – Universitätsmedizin Berlin on ensuring good scientific practice.

I declare that I have not yet submitted this dissertation in identical or similar form to another Faculty.

The significance of this statutory declaration and the consequences of a false statutory declaration under criminal law (Sections 156, 161 of the German Criminal Code) are known to me.”

_____	_____
Date	Sandra Jagdmann

7 DECLARATION OF CONTRIBUTION TO THE PUBLICATIONS

Sandra Jagdmann contributed the following to the below listed publications:

Publication 1: **Jagdmann, S**.; Dames, C.; Berchtold, D.; Winek, K.; Weitbrecht, L.; Meisel, A.; Meisel, C. Impact of Key Nicotinic AChR Subunits on Post-Stroke Pneumococcal Pneumonia. Vaccines (Basel) 2020.

Streptococcal cultivation tests; genotyping of the different mice strains; organization of animal breeding; planning and exertion of experiments (monitoring of animals, antibiotic treatment, MCAo and induced infection together with Dr. Claudia Dames; isolation of lung cells and splenocytes partly supported by Dr. Katarzyna Winek, Susanne Metzkow, Daniel Berchtold or Dr. Claudia Dames; microbiological analysis, FACS analyses; analysis of cytokines in BALF and albumin in BALF as well as in plasma; infarct analyses together with Sabine Kolodziej; qRT-PCR together with Claudia Muselmann-Genschow). Sandra Jagdmann also performed: Data analysis; data presentation in figures, which was discussed with all co-authors; interpretation of the data together with co-authors; statistical analyses; writing of the entire initial version of the manuscript, which was proofread and optimized by all co-authors, but primarily by Dr. Christian Meisel and Prof. Dr. Andreas Meisel; submission of the manuscript; optimization of the manuscript together with Dr. Christian Meisel and Prof. Dr. Andreas Meisel based on the comments during the review process. All figures (1-4) were created based on the experiments, data analysis and statistical analysis performed by Sandra Jagdmann. The idea and conception of the study was done by Dr. Christian Meisel, Prof. Dr. Andreas Meisel and Dr. Claudia Dames.

Publication 2: Winek, K.; Lobentanzer, S.; Nadorp, B.; Dubnov, S.; Dames, C.; **Jagdmann, S.**; Moshitzky, G.; Hotter, B.; Meisel, C.; Greenberg, D.S., Shifman, S.; Klein, J.; Shenhar-Tsarfaty, S.; Meisel, A.; Soreq, H. Transfer RNA fragments replace microRNA regulators of the cholinergic poststroke immune blockade. Proceedings of the National Academy of Sciences 2020.

Establishment of RNA isolation of human monocytes, isolation and stimulation of human monocytes as well as collection of supernatants and cells together with Dr. Claudia Dames, TNF-α ELISA, data analysis, statistical analyses, participation in writing the manuscript ("Isolation and Ex Vivo Stimulation of Human Monocytes"), proofreading of the manuscript. Figure S8 was created on the basis of the experiments, data analysis and statistical analysis performed by Sandra Jagdmann.

Dr. Katarzyna Winek analyzed RNA-sequencing data together with Gilli Moshitzky and Sebastian Lobentanzer, wrote the manuscript together with Sebastian Lobentanzer and performed cell culture tests as well as qRT-PCR measurements together with Serafima Dubnov. Prof. Dr. Andreas Meisel, Dr. Christian Meisel and Dr. Benjamin Hotter collected the stroke cohort, the blood samples and performed immunological measurements. Sebastian Lobentanzer conducted bioinformatic

analyses. Dr. Bettina Nadorp and Dr. Shani Shenhar-Tsarfatyh processed the blood samples and prepared the sequencing data. Dr. David Greenberg, Sagiv Shifmang and Prof. Dr. Jochen Klein interpreted the data. Prof. Dr. Andreas Meisel and Prof. Dr. Hermona Soreq coguided the project, planned the experiments, interpreted the data and contributed to the manuscript writing.

Publication 3: Jagdmann, S.; Berchtold, D.; Gutbier, B.; Witzenrath, M.; Meisel, A.; Meisel, C.; Dames, C. Efficacy and safety of intratracheal IFN-γ treatment to reverse stroke-induced susceptibility to pulmonary bacterial infections. Journal of Neuroimmunology 2021.

Planning and exertion of the experiments (3.2. Efficacy and safety of IFN-γ treatment after experimental stroke; 3.3. Impact of IFN-γ treatment on spontaneously developing infections after experimental stroke; 3.4. IFN-γ treatment in a model of induced pneumococcal pneumonia after experimental stroke) together with Dr. Claudia Dames (monitoring of the animals, MCAo, IFN-γ treatment, induced infection with *S. pneumoniae* PN36 was supported by Birgitt Gutbier and Prof. Dr. Martin Witzenrath, antibiotic treatment, microbiological analysis, analysis of cytokines in BALF and plasma, analysis of leukocytes, infarct analysis together with Sabine Kolodziej, stimulation of BALF and lung cells; sample collection and processing was supported by Daniel Berchtold and Susanne Metzkow). Sandra Jagdmann also performed: Data analysis; interpretation of the data together with co-authors; statistical analysis; data presentation in figures; writing of the entire initial version of the manuscript, which was proofread and optimized by all co-authors, but primarily by Dr. Christian Meisel, Prof. Dr. Andreas Meisel and Dr. Claudia Dames; submission of the manuscript; optimization of the manuscript mainly together with Dr. Christian Meisel, Prof. Dr. Andreas Meisel and Dr. Claudia Dames based on the comments during the review process. Figure 1-2 and supplement figure 1-2 were created based on the data analysis and statistical analysis performed by Sandra Jagdmann, whereas Dr. Claudia Dames performed the experiment (3.1. IFN-γ dose escalation in naïve mice). Figure 3-5 were created on the basis of the experiments, data analysis and statistical analysis done by Sandra Jagdmann. The idea and conception was done by Dr. Claudia Dames, Dr. Christian Meisel and Prof. Dr. Andreas Meisel.

In addition, Sandra Jagdmann was responsible for the laboratory animals in studies 1 and 3 as deputy project leader in accordance with the animal protection law, in particular for animal welfare and compliance with the relevant legal requirements.

_____

Sandra Jagdmann

8 SELECTED PUBLICATIONS

8.1 Study 1

vaccines

MDPI

Article

Impact of Key Nicotinic AChR Subunits on Post-Stroke Pneumococcal Pneumonia

Sandra Jagdmann [1], Claudia Dames [1,2], Daniel Berchtold [2], Katarzyna Winek [2], Luis Weitbrecht [2], Andreas Meisel [2,3,4,5,*] and Christian Meisel [1,6]

1 Institute for Medical Immunology, Charité-Universitätsmedizin Berlin, Corporate Member of Freie Universität Berlin, Humboldt-Universität zu Berlin, Berlin Institute of Health, 13353 Berlin, Germany; Sandra.jagdmann@charite.de (S.J.); Claudia.dames@charite.de (C.D.); chr.meisel@charite.de (C.M.)
2 Department of Experimental Neurology, Charité-Universitätsmedizin Berlin, Corporate Member of Freie Universität Berlin, Humboldt-Universität zu Berlin, Berlin Institute of Health, 10117 Berlin, Germany; daniel.berchtold@charite.de (D.B.); Katarzyna.winek@alumni.charite.de or katarzyna.winek@mail.huji.ac.il (K.W.); Luis.weitbrecht@charite.de (L.W.)
3 Center for Stroke Research Berlin, Charité-Universitätsmedizin Berlin, Corporate Member of Freie Universität Berlin, Humboldt-Universität zu Berlin, and Berlin Institute of Health, 10117 Berlin, Germany
4 Neurocure Clinical Research Center, Charité-Universitätsmedizin Berlin, Corporate Member of Freie Universität Berlin, Humboldt-Universität zu Berlin, and Berlin Institute of Health, 10117 Berlin, Germany
5 Department of Neurology, Charité-Universitätsmedizin Berlin, Corporate Member of Freie Universität Berlin, Humboldt-Universität zu Berlin, and Berlin Institute of Health, 10117 Berlin, Germany
6 Labor Berlin, Charité-Universitätsmedizin Berlin Vivantes, 10117 Berlin, Germany
* Correspondence: Andreas.meisel@charite.de; Tel.: +49-(0)-3045-056-0026

Received: 30 April 2020; Accepted: 25 May 2020; Published: 28 May 2020

check for updates

Abstract: Pneumonia is the most frequent severe medical complication after stroke. An overactivation of the cholinergic signaling after stroke contributes to immunosuppression and the development of spontaneous pneumonia caused by Gram-negative pathogens. The α7 nicotinic acetylcholine receptor (α7nAChR) has already been identified as an important mediator of the anti-inflammatory pathway after stroke. However, whether the α2, α5 and α9/10 nAChR expressed in the lung also play a role in suppression of pulmonary innate immunity after stroke is unknown. In the present study, we investigate the impact of various nAChRs on aspiration-induced pneumonia after stroke. Therefore, α2, α5, α7 and α9/10 nAChR knockout (KO) mice and wild type (WT) littermates were infected with *Streptococcus pneumoniae* (*S. pneumoniae*) three days after middle cerebral artery occlusion (MCAo). One day after infection pathogen clearance, cellularity in lung and spleen, cytokine secretion in bronchoalveolar lavage (BAL) and alveolar-capillary barrier were investigated. Here, we found that deficiency of various nAChRs does not contribute to an enhanced clearance of a Gram-positive pathogen causing post-stroke pneumonia in mice. In conclusion, these findings suggest that a single nAChR is not sufficient to mediate the impaired pulmonary defense against *S. pneumoniae* after experimental stroke.

Keywords: MCAo; immunosuppression; nicotinic acetylcholine receptor; aspiration-induced pneumonia; *Streptococcus pneumoniae*

1. Introduction

Stroke is a leading cause of death worldwide. The outcome depends on the occurrence of complications. Up to 95% of stroke patients experience medical complications in the first three months after stroke. Among these, infection is one of the most frequent, severe complications [1–4]. Long-lasting immunosuppression due to overactivation of neurohumoral stress pathways, besides other factors

such as neurological deficits leading to dysphagia and aspiration, contribute to the high incidence of pneumonia in stroke patients [5–7]. We have previously shown in an experimental mouse model, that excessive cholinergic signaling induced by stroke results in impaired innate immune responses in the lung [8]. In this cholinergic anti-inflammatory pathway, acetylcholine (ACh) released by vagal efferents and by non-neuronal cells was shown to impair antibacterial responses in the lung via the α7 nAChR expressed on alveolar epithelial cells (AECs) and macrophages (MΦ), contributing to an increased susceptibility to spontaneous Gram-negative bacterial pneumonia [8–12]. Nicotine as well as the α7 nAChR-specific agonist PNU282987 diminished LPS-induced IL-6 secretion in AECs isolated from WT but not α7 nAChR KO mice in a dose-dependent manner. In contrast, nicotine and PNU282987 dose-dependently reduced LPS-induced IL-6 secretion in MΦ from WT as well as α7 nAChR KO mice. Thus, nicotine suppressed the TLR-induced pro-inflammatory cytokine secretion in the absence of α7 nAChR, suggesting that suppression of pulmonary immune responses after stroke by the cholinergic anti-inflammatory pathway may in part be independent from the α7 nAChR [8]. nAChRs are homomeric or heteromeric combinations of α2-10 and β3-4 subunits. Beyond the α7 nAChR subunit, mRNA expression of α2 nAChR, α5 nAChR, α6 nAChR, α9 nAChR and α10 nAChR was detected in immune cells including mononuclear leukocytes, dendritic cells (DCs), MΦ and T-cells supporting our hypothesis that not only α7 nAChRs are involved in the regulation of immune response after stroke [12–14].

Clinical studies have shown that impaired swallowing, aspiration and stroke-induced immunosuppression contribute to the increased incidence of bacterial pneumonia after stroke [7,15]. Microbiological analysis identified especially Gram-negative bacteria such as *Pseudomonas aeruginosa*, *Klebsiella pneumoniae*, *Enterobacter*, *Escherichia coli* and *Acinetobacter* in blood and lung of patients. However, also Gram-positive bacteria such as *S. pneumoniae*, the leading cause of community-acquired pneumonia, are relevant pathogens causing post-stroke pneumonia [16–18]. We have previously shown in an experimental mouse model, that nasal infection with 200 colony-forming units (CFU) of *S. pneumoniae* resulted in severe pulmonary infection after stroke, whereas sham operated mice were able to clear bacteria [19]. β-adrenoreceptor blockade by propranolol treatment significantly reduced bacterial burden in the lung suggesting sympathetic hyperactivity contributes to impaired pulmonary defense after experimental stroke [19–21].

In the present study, we aimed to investigate the role of various nAChRs expressed in the lung in the impaired antibacterial responses after stroke in an aspiration-induced model of post-stroke pneumococcal pneumonia.

2. Materials and Methods

2.1. Animals and Housing

Experiments were executed in accordance with the European directive on the protection of animals used for scientific purposes and further applicable legislation, and approved on 31 March 2016 by the relevant authority, Landesamt für Gesundheit und Soziales (LAGeSo), Berlin, Germany (project identification code: G0244/15). Male α2 nAChR KO (MMRRC_030508-UCD B6.129 × 1-Chrna2$^{tm1\ Jbou}$/Mmucd; University of California Davis Mutant Mouse Regional Resource Center (MMRRC)) [22], α5 nAChR KO (MMRRC_000421-UNC B6.129S7-Chrna5$^{tm1\ Mdb}$/MmNc; University of North Carolina MMRRC) [23], α7 nAChR KO (JAX #003232B6.129 S7-Chrna7$^{tm1\ Bay}$/J; The Jackson Laboratory, Bar Harbor) [24], α9/10 nAChR KO (JAX #005696 CBACaJ;129 S-Chrna9$^{tm1\ Bedv}$/J; The Jackson Laboratory, Bar Harbor and MMRRC_030509-UCD 129 S4-Chrna10$^{tm1\ Bedv}$/Mmcd; University of California Davis MMRRC) [25,26] mice and corresponding WT littermates were used for infection experiments. Standard-genotyping using STR-marker and C57BL/6 substrain-specific mutation analysis confirmed that α2 nAChR KO, α5 nAChR KO and α7 nAChR KO strains carry an autosomal C57BL/6JCrl background (GVG genetic monitoring). α9/10 nAChR KO strain was backcrossed for 8 generations to C57BL/6JCrl. Since all mouse strains carry the same genetic

background, mixed WT littermates from all strains were used as control groups (WT MCAo and WT naïve). C57BL/6J mice (The Jackson Laboratory, Bar Harbor, ME, USA) were used for nAChR expression analysis in lung and brain. All animals were housed with identical conditions in cages with chip bedding, mouse tunnel and mouse igloo on a 12 h light/dark cycle with ad libitum access to standard food and water. Experiments were performed with 12–20 weeks old mice.

2.2. Experimental Model of Stroke

The surgical procedure of MCAo was performed according to the standard operating procedures of the Department of Experimental Neurology, Charité-Universitätsmedizin Berlin [27]. Under general isoflurane anesthesia, a silicon-coated filament (7019PK5Re, Doccol Corp. Redlands, CA, USA) was introduced into the left common carotid artery and advanced to the origin of the middle cerebral artery (MCA) for 60 min. Infarct volume and success of MCAo was verified by hematoxylin staining from fresh-frozen brains. Animals without infarcts were excluded from the study.

2.3. Antibiotic Treatment

Spontaneously developing infection after MCAo was prevented by intraperitoneal (i.p.) injection of marbofloxacin (5 g/kg BW, Vétoquinol GmbH, Ravensburg, Germany) one day before and on the day of MCAo.

2.4. Bronchoscopy-Guided Application of S. Pneumoniae Three Days after MCAo

S. pneumoniae (D39 capsular type 2 *S. pneumoniae*, Rockefeller University, New York, NY, USA) was grown as described elsewhere [19] and diluted in PBS to 2000 CFU/50 µL. In previous experiments, an optimal dose of bacterial load of 200 CFU for intranasal infection in 129S6SvEv mice was established [19]. Since the C57BL/6J mouse strain used in this study is less susceptible to bacterial infection including *S. pneumoniae* D39 as compared to 129S6SvEv mice [28,29], we established 2000 CFU for infection in previous experiments when developing a miniaturized bronchoscopy protocol in mice [30]. Therefore, we used 2000 CFU for all experiments in this study. The same batch of bacteria from Rockefeller University was used for all experiments.

Under anesthesia with midazolam (5.0 mg/kg BW, Roche Pharma AG, Grenzach-Whylen, Germany) and medetomidin (0.5 mg/kg BW, Orion Corporation, Espoo, Finland) the bronchoscope (Polydiagnost, Pfaffenhofen, Germany) was inserted under visual control into the trachea and advanced to the bifurcation. Subsequently, 50 µL of defined pneumococcal suspension was applied in the main bronchi. Afterward, anesthesia was antagonized subcutaneous (s.c.) with flumazenil (0.5 mg/kg BW, Inresa, Freiburg, Germany) and atipamezol (5 mg/kg BW, Orion Corporation, Espoo, Finland) injection [30].

2.5. Microbiological Investigation

Bronchoalveolar lavage (BAL) was performed as described elsewhere [31]. Lungs were removed and homogenized in 500 µL PBS. BAL fluid, blood and lung tissue homogenate were serially diluted, plated on Columbia-Agar plates (BD Bioscience, Heidelberg, Germany), incubated at 37 °C for 18 h and bacterial colonies were counted to calculate the CFUs per ml tissue/liquid.

2.6. Flow Cytometry

Isolation of lung cells and splenocytes was performed as described elsewhere [8]. Cell phenotyping was performed on LSRII flow cytometer using FACS Diva software (BD Bioscience, Heidelberg, Germany) and Flowjo software 9.6.6 (Tree Star Inc, San Carlos, CA, USA) with the following anti-mouse monoclonal antibodies: CD45 Peridinin-Chlorophyll-protein (PerCP), CD11b Allophycocyanin-cyanine dye 7 (APC-Cy7), NK1.1 phycoerythrin (PE), CD19 Fluorescein (FITC), CD3 APC, CD4 Alexa Fluor 700 (A700), CD8 Pacific-Blue (PB), Gr1PE, CD11bPE-Cy7, F480 APC, Siglec F APC-Cy7, CD11 c PB (Biolegend, San Diego, CA, USA).

2.7. Analysis of Cytokines in BAL and Albumin in BAL and Plasma

Macrophage inflammatory protein-1α (MIP-1α), IL-10, keratinocyte chemoattractant (KC) and tumor necrosis factor α (TNFα) concentration in BAL were measured by using a commercially available Milliplex Map Kit (Merk Millipore, Darmstadt, Germany). Albumin level in BAL and plasma were quantified by an enzyme-linked immunosorbent assay (ELISA) (Bethyl Laboratories Inc., Montgomery, AL, USA).

2.8. Quantitative Reverse Transcriptase Polymerase Chain Reaction (qRT-PCR)

RNA from naïve lung and brain was extracted in Trizol according to the manufacturer's protocol (Roth, Karlsruhe, Germany). All samples were subsequently incubated with DNase (Promega, Fichtburg, MA, USA) followed by purification with Phenol-Chloroform. cDNA synthesis was performed using ProtoScript® II Reverse Transcriptase (New England Biolabs, Ipswich, UK) and the expression of nAChRs was quantified using a LightCycler 480 (Roche, Mannheim, Germany) and the LightCycler-FastStart-DNA-Master-SYBR-Green-I-Kit (Roche, Mannheim, Germany) according to the manufacturer's guidelines. β-actin was used as "housekeeping gene" for normalization. The following primers were used: mChrnaalpha2 (F: TGGATGGGCTGCAGAGAGACAGG, R: GGTCCTCGGCATGGGTGTGC), mChrnaalpha5 (F: ATCAACATCCACCACCGCTC, R: CTTCAACAACCTCGCGGACG), mChrnaalpha7 (F: TCCGTGCCCTTGATAGCACA, R: TCTCCCGGCCTCTTCATGCG), mChrnaalpha9 (F: CGGACGCGGTGCTGAACGTC, R: AGACTCGTCATCGGCCTTGTTGT), mChrnaalpha10 (F: ACCCTCTGGCTGTGGTAGCG, R: GCACTTGGTTCCGTTCATCCATA). The amplification of Chrna 2, Chrna 7, Chrna 9, Chrna 10 and β-actin was performed at 95 °C (5 s), 66 °C (10 s) and 72 °C (15 s) for 45 cycles. Chrna 5 was amplified with the following conditions: 95 °C (5 s), 60 °C (10 s) and 72 °C (15 s) for 45 cycles. Melting curve analysis was performed to exclude the measurement of non-specific products. PCR products were sequenced to verify primer specificity.

2.9. Statistics

Statistical analysis was performed using Prism 6.0 Software (GraphPad, San Diego, CA, USA). Nonparametric one-way analysis of variance (ANOVA) with Dunn's multiple comparison test was used to compare the mean rank of each group with WT naïve group as a control group.

3. Results

3.1. α2, α5, α9 and α10 nAChR Subunits are Expressed in Lung and Brain of Naïve Mice

We previously demonstrated expression of α7 nAChR in MΦ and AECs [8]. To investigate which additional nAChR subunits are expressed in lungs and brain, α2, α5, α9 and α10 nAChR mRNA expression in whole organ tissue isolated from naïve mice was quantified by qRT-PCR and compared to α7 nAChR mRNA expression. All subunits were found to be expressed in both lung and brain, however with higher levels in brain compared to lung except for the α10 subunit (Figure 1). These data suggest that other nicotinic receptors in addition to α7 nAChR may be involved in cholinergic suppression of pulmonary immune response after stroke.

3.2. Role of Various nAChRs in an Aspiration-Induced Post-Stroke Pneumococcal Pneumonia

To investigate the impact of various nAChRs on the clearance of aspiration-induced pneumococcal pneumonia after experimental stroke, a pneumococcal suspension was applied at the tracheal bifurcation from α2, α5, α7, α9/10 KO mice and WT littermates three days after MCAo. Infected naïve WT mice served as controls. Bacterial burden in the lung, BAL and blood was determined one day after infection. Whereas naïve WT mice were able to clear bacteria, MCAo treated mice showed increased bacterial burden in lung and BAL one day after infection (Figure 2A,B), although the effect in BAL

was not significant compared to naïve WT mice. In contrast to naïve WT mice and stroked α7 KO mice, several MCAo-treated α2, α5, α9/10 KO mice and WT littermates suffered from bacteremia after bacterial challenge, whereby α9/10 KO mice exhibited significantly increased bacterial burden in blood compared to naïve WT mice (Figure 2C). However, bacterial burden in lung, BAL and blood was not significantly different between all nAChR KO and WT MCAo groups using WT MCAo mice as the reference group (Figure 2A,C). The infarct size was determined by histological staining and did not differ significantly between WT mice and nAChR KO mice (Figure 2D).

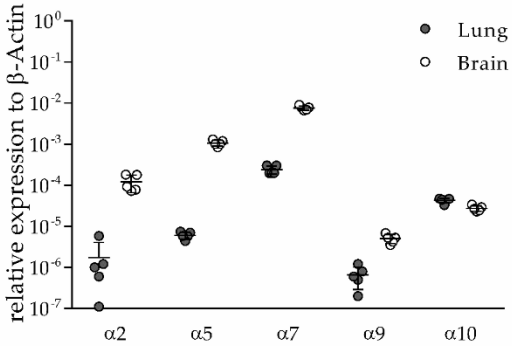

Figure 1. Expression of nAChR subunits in lung and brain tissue. α2, α5, α7, α9 and α10 nAChR subunits are expressed in lung and brain tissue of naïve wild type (WT) mice suggesting a possible role in anti-inflammatory cholinergic signaling after stroke. RNA was isolated from lung and brain tissue, and expression levels were determined by qRT-PCR. Target gene expression was normalized to β-actin as the housekeeping gene. Values are given as mean ± SD (n = 5).

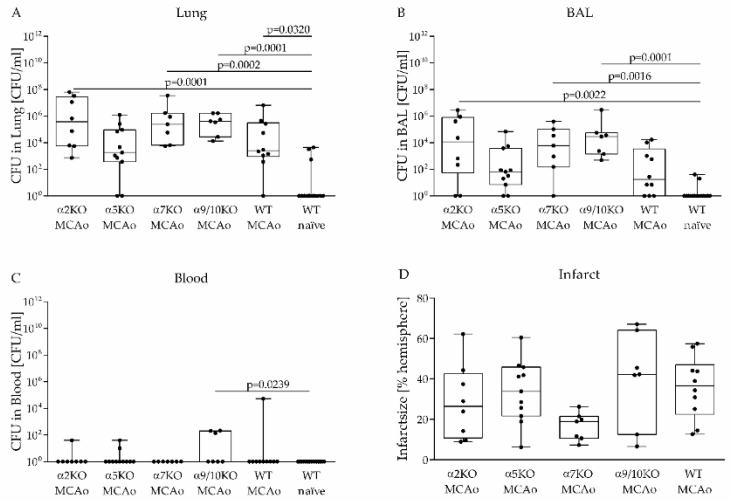

Figure 2. The susceptibility to aspiration-induced pneumococcal pneumonia after experimental stroke is not altered in nAChR knockout (KO) mice. (**A**–**C**) Untreated WT mice (naïve) or WT and nAChR KO

mice subjected to MCAo surgery were infected with *S. pneumoniae* three days after MCAo. Microbiological analysis of lung, bronchoalveolar lavage (BAL) and blood was performed one day after infection. Deficiency of α2, α5, α7 and α9/10 nAChRs had no effect on bacterial burden in lung, BAL and blood after experimental stroke. (**D**) nAChRs does not have an impact on infarct size assessed four days after MCAo by histological staining. Data from 6 independent experiments are shown (n = 7–15 per group) as box plots compared to WT naïve mice as a reference group for bacterial analysis and compared to WT MCAo mice as the reference group for infarct analysis using the Kruskal–Wallis test followed by Dunn´s test for multiple comparisons.

3.3. α2, α5, α7, α9/10 nAChRs Have No Effect on Immune Cell Recruitment after Stroke

To investigate the underlying mechanisms of impaired clearance of induced pneumococcal lung infection after stroke and the impact of nAChRs on immune cell recruitment, cellularity in the lung and spleen was determined by flow cytometry one day after infection, which was induced on day three after stroke onset. The number of pulmonary interstitial macrophages (IM) was significantly reduced in α7, α9/10 KO mice and WT littermates and non-significantly reduced in α2 and α5 KO mice compared to naïve WT mice one day after infection. In contrast, MCAo surgery had no effect on the number of neutrophils and lymphocytes in the lung (Figure 3A,C,E). Investigation of cellularity in the spleen revealed a significant decrease in the number of macrophages in α9/10 KO and WT MCAo mice, neutrophils in α5 KO and WT MCAo mice and lymphocytes in α5 KO and α9/10 KO mice compared to infected naïve WT mice (Figure 3B,D,F). The Kruskal–Wallis test using WT MCAo mice as the reference group showed that cell counts of leukocytes in lung and spleen were similar in α2 KO, α5 KO, α7 KO, α9/10 KO and MCAo treated WT mice one day after infection.

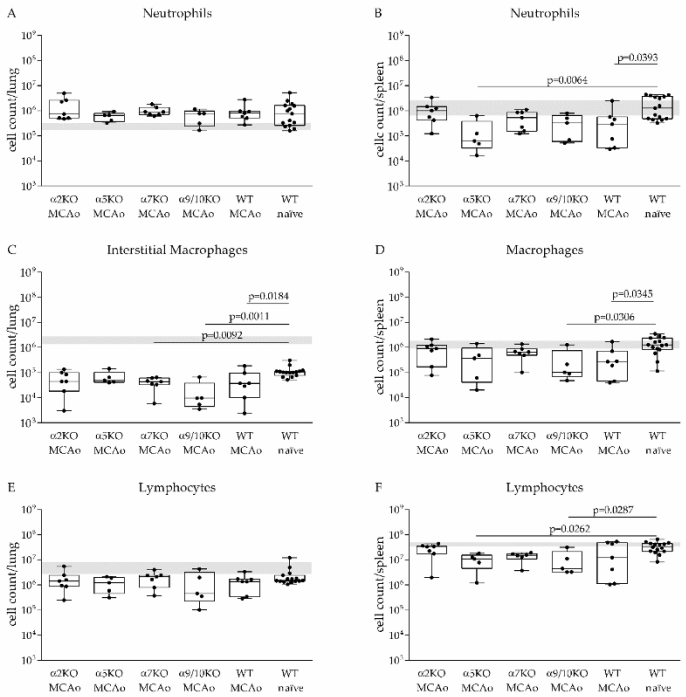

Figure 3. Impact of *S. pneumoniae* infection on cellularity in the lung and spleen of WT and nAChR KO mice. Lung and spleen cells were isolated and quantified by flow cytometry one day after infection with

S. pneumoniae. WT mice without MCAo surgery show significantly increased numbers of interstitial macrophages (IMs) (CD45/Gr1−/SiglecF−/CD11 b^{high}/F480) in the lung (**C**) and increased number of neutrophils (CD45+/CD11 b^{high}/Gr1^{high}), macrophages (CD45+/Gr1−/CD11 b+/CD11c−) and lymphocytes (B cells: CD45+/CD11 b−/CD19+; T cells: CD45+/CD11 b−/CD3+; NK cells: CD45+/NK1.1+/CD3−; NKT cells: CD45+/NK1.1+/CD3+) in the spleen (**B**,**D**,**F**) compared to MCAo mice. No differences between MCAo mice and naïve WT mice in the number of pulmonary lymphocytes and neutrophils were found (**A**,**E**). Cellularity of the lung and spleen does not differ between WT MCAo mice and nAChR KO MCAo mice. The grey area represents numbers of leukocyte subsets in healthy mice (median with IQR). Data from 6 independent experiments are shown (n = 5–15 per group) as box plots compared to naïve WT mice as a reference group using the Kruskal–Wallis test followed by Dunn´s test for multiple comparison.

3.4. Effect of α2, α5, α7, α9/10 nAChRs on Alveolar-Capillary Barrier and Cytokine Secretion in BAL after Stroke

To investigate the inflammatory response during pneumococcal pneumonia after stroke, MIP-1α, IL-10, KC and TNFα concentrations in BAL were measured one day after infection. Cytokine levels tended to be lower in naïve WT mice compared to MCAo mice. MIP-1α, KC, IL-10 and TNFα concentrations were only increased in some mice and did not differ significantly between groups. (Figure 4A–D). Regression analysis between cytokine concentrations and CFU in BAL showed positive correlation between MIP-1α, KC and TNFα level and bacterial burden in BAL (KC: r = 0.5186, p = 0.0004; MIP-1α: r = 0.3391, p = 0.028; TNFα: r = 0.4492, p = 0.0028) (Figure 4E).

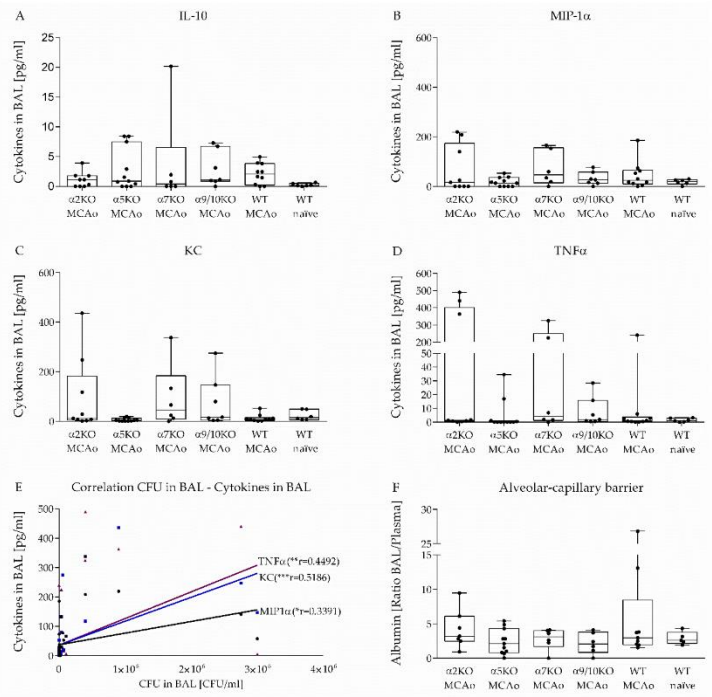

Figure 4. nAChR deficiency has no impact on the alveolar-capillary barrier or cytokine response in lung during *S. pneumoniae* infection after experimental stroke. MIP-1α, IL-10, KC and TNFα concentrations

in BAL were measured one day after infection as described in Material and Methods. MIP-1α, IL-10, KC and TNFα level did not differ between groups (**A**–**D**). Positive correlation between MIP-1α, KC and TNFα concentrations and bacterial burden in BAL was found (Pearson Correlation, two tailed) (**E**). To investigate the effect of α2, α5, α7 and α9/10 nAChRs on the permeability of the alveolar-capillary barrier after MCAo, albumin concentrations in BAL and plasma were measured and the ratio of BAL albumin and plasma albumin was calculated. Albumin ratio is increased in several mice but does not differ between nAChR KO mice and WT mice (**F**). Data from 6 independent experiments are shown (n = 5–11 per group) as box plots compared to naïve WT mice as a reference group using the Kruskal–Wallis test followed by Dunn´s test for multiple comparison.

To investigate changes in permeability of the alveolar-capillary barrier in the model of aspiration-induced post-stroke pneumonia, we measured albumin concentrations in BAL and plasma one day after infection. Since the plasma albumin concentrations fluctuate, the ratio of BAL albumin and plasma albumin was calculated. It has been shown that albumin ratio in healthy mice is up to three [32]. Here, we found that albumin ratio one day after pneumococcal infection was only increased in some mice and did not differ significantly between the study groups (Figure 4F).

4. Discussion

The main finding of the present study is that the depletion of single α nAChR subunits has no effect on the course of an aspiration-induced pneumococcal pneumonia after stroke. Experimental stroke results in severe pneumococcal pneumonia after induced aspiration of *S. pneumoniae* three days after stroke onset, which was harmless for naïve mice. α2 KO, α5 KO, α7 KO, α9/10 KO mice do not show significant differences in the clearance of pathogens, recruitment of immune cells in the lung or pro-inflammatory cytokine secretion compared to WT littermates following stroke.

Pneumonia is the most frequent complication of acute stroke and increases acute and long-term mortality. Besides old age, diabetes mellitus and dysphagia, immunosuppression is recognized as an important contributor for the development of spontaneous infection after stroke. Findings in animals and patients have shown that this impaired peripheral cellular immune response after central nervous system (CNS) injury is a result of activation of the hypothalamic-pituitary-adrenal (HPA) axis, the sympathetic nervous system (SNS) and the cholinergic signaling [5,6,33–37].

Overactivation of the cholinergic signaling in response to infection or inflammation-induced tissue damage is also called 'the cholinergic anti-inflammatory pathway' and is described as a protective mechanism that controls the inflammatory response [11]. Peripheral inflammation is sensed by vagal afferent fibers, which leads to an activation of vagal efferent fibers resulting in ACh release in the reticuloendothelial system and interacts with various muscarinic receptors (mAChRs) and nAChRs [10,11]. ACh is not only synthesized as a classical neurotransmitter by parasympathetic nerve fibers but also by non-neuronal cells including airway epithelia cells [38]. This excessive ACh release by non-neuronal and neuronal cells following nervus vagus activation suppresses via nAChRs endotoxin-inducible pro-inflammatory cytokine production, such as TNFα, IL-1β, IL-6 and IL-18 [39].

Until now, five mAChRs subtypes (M1–M5) were found expressed by neuronal and non-neuronal cells including epithelial cells, fibroblasts, smooth muscle cells, macrophages, lymphocytes, mast cells and neutrophils. Non-neuronal mAChRs were shown to mediate inflammation and tissue remodeling in the airways [40]. In the CNS, mAChRs have been associated with the cholinergic anti-inflammatory pathway. An anti-inflammatory and anti-oxidant effect in the hippocampus of rats was demonstrated by stimulation of mAChRs with the agonist oxotremorine [41]. Furthermore, adrenocorticotropin treatment of rats diminished hemorrhagic shock by activation of the cholinergic anti-inflammatory pathway via mAChRs in the CNS [42]. Stimulation of the central localized M1 and M2 receptors resulted in a decrease of TNFα level in blood in an endotoxemia model. Interestingly, a blockade of peripheral mAChRs did not enhance TNFα secretion [43]. These data indicate that stimulation of the mAChRs in the CNS elicits—through cholinergic and potentially other neurotransmitter systems—an anti-inflammatory response in the periphery, whereas anti-inflammatory cholinergic

effects in the periphery do not appear to be mediated by mAChRs. Thus, the immunomodulatory effects of cholinergic signaling via mAChRs differ considerably from nAChRs such as α7, which directly exert anti-inflammatory responses in the periphery. Nonetheless, whether central mAChRs play a role in mediating stroke-induced immunosuppression remains to be elucidated.

nAChRs are composed of different combinations of α (α2–α10) and β subunits (β2–β4) and found both in the nervous system and in non-neuronal cells. Structural analysis has shown that α10 subunits form functional channels, when they are co-expressed with α9 and that α9 and α7 subunits are able to form homomeric receptors [44]. So far, especially the α7 nAChR was identified as an important mediator of the cholinergic anti-inflammatory pathway. Previous studies have reported that electrical stimulation of the vagus nerve inhibits the macrophage TNFα release from WT mice but not from α7 nAChR KO mice [9]. Furthermore, it was shown that stimulation of nAChRs with nicotine is associated with decreased neutrophils migration by inhibition of adhesion molecule expression both on the endothelial surface and neutrophils, whereas deficiency of α7 leads to a faster recruitment of neutrophils and decreased bacterial burden after i.p. infection with *Escherichia coli* [45,46]. In addition, α7 nAChR has been demonstrated to play an important role in the development of spontaneous infection after experimental stroke. Depletion of the α7 nAChR by using KO mice reduced bacterial burden in BAL significantly compared to WT littermates [8]. However, the role of nAChRs including the α7 nAChR in pulmonary infections caused by Gram-positive bacteria such as *S. pneumoniae* after stroke had not been investigated, so far.

Expression analysis has shown that α5, α7, α9 and α10 are the most frequently expressed subunits in non-neuronal cells including immune cells [12,13,44]. Besides the anti-inflammatory effect of ACh on macrophages, a cholinergic immunosuppressive effect on human DCs was observed. mRNAs encoding the α2, α5, α6, α7, α10 nAChRs and β2 were found in DC isolated from C57BL/6 J mice suggesting that these subunits mediate anti-inflammatory signaling of DC [47,48]. While the α7 and α9 subunits form either homomeric or, in case of α9 together with the α10 subunit, heteromeric nAChR receptors, respectively, the α2 and α5 subunit co-assembles with other alpha (α3–5) and beta subunits (β2, β4) to different heteromeric receptors [44]. Findings that the α3β2 and α3β4 receptors can also be functional without the α5 subunit suggested that depletion of α5 has no impact on physiological processes and diseases [49]. Nevertheless, α5 KO mice showed reduced hyperalgesia and allodynic responses to carrageenan and complete Freund´s adjuvant (CFA) injections and reduced sensitivity to nicotine-induced seizures and hypolocomotion [23,50,51]. Furthermore, it was shown that the α5 subunit influences the affinity and sensitivity of agonists and antagonists. A 50-fold increased acetylcholine sensitivity was detected if the α5 subunit incorporated with α3β2 [49,52]. Depletion of the α2 subunit resulted in major changes in immune-adipose communication including compromised adaptation to chronic cold challenge, dysregulation of whole-body metabolism and exacerbates diet-induced obesity [53]. In this study, we found expression of α2, α5, α7, α9 and α10 subunits in lungs of naïve mice and suspected that depletion of these subunits may modify the immunomodulatory effects of cholinergic signaling after stroke.

In our experimental stroke model, we have previously shown that signs of immunosuppression in blood, spleen and thymus started as early as 12 h after MCAo with a maximum at day three. Already after five to seven days, lymphocyte numbers and pro-inflammatory cytokines in blood started to recover. Correspondingly, spontaneous bacterial infections in mice were observed between days three and five after experimental stroke [54]. This is in accordance with the clinical observation that the risk to develop infections in stroke patients is highest within two to five days after stroke onset [55]. Therefore, in a translational approach we choose to infect MCAo mice before day five, in the phase of maximum immunosuppression. This time window has been used in aspiration-induced post-stroke pneumonia models using a low number of *S. pneumoniae* capable of inducing severe pneumonia with high bacterial burden in lung of MCAo but not sham animals [19]. Moreover, bacterial burden in lung was lower at day two compared to day one after inoculation [56]. Since naïve mice require usually 24 h

to clear induced infection, we used this time point to assess immune parameters and bacterial burden after inoculation of *S. pneumoniae*.

In the present study, we have demonstrated that induced aspiration with *S. pneumoniae* by applying a bacterial suspension at the tracheal bifurcation leads to severe pneumonia after experimental stroke but remains harmless in naïve mice. Microbiological analysis demonstrated significantly lower bacterial burden in WT naive mice compared to stroked animals (Figure 2A). Analysis of the lung showed that out of 15 WT naive mice, 12 mice were able to completely clear inoculated bacteria within 24 h compared to only 3 out of 43 stroked mice (Figure 2A). Microbiological analysis of BAL obtained from the same animals showed similar results (Figure 2B). Moreover, all naive mice remained symptomless in contrast to the MCAo mice suggesting near complete bacterial clearance. This finding corroborates previous findings that stroke impairs the antibacterial defense [7,8,19–21,34,54]. *S. pneumoniae* infection in healthy mice leads to neutrophil recruitment in BAL starting 12 h after infection. A reduction of neutrophil numbers was observed 60 h after infection due to cell death [57,58]. Investigation of the lung showed up to 10^6 neutrophils/mL 24 h after infection, whereas 10^4 neutrophils/mL were reported in the lung of uninfected mice [59]. In the present study, we could also observe increased numbers of neutrophils in the lung (up to 10^6 neutrophils/lung) of naïve WT mice and MCAo mice. We found no differences between stroke and naive mice in terms of neutrophil numbers in the lung at day one after infection. One explanation could be a faster kinetic of neutrophil recruitment in naïve animals with already decreasing numbers of neutrophils in the lung one day after bacterial inoculation due to clearance of bacteria. Therefore, a diminished neutrophil recruitment after MCAo would not have been detected with our experimental design. Nevertheless, since we also not observed differences in lung neutrophil counts between WT and nAChR KO mice after stroke, the nAChR subunit status does not seem to have a major impact on neutrophil recruitment into the lung due to *S. pneumoniae* infection after stroke.

Stroke has been demonstrated to induce a long-lasting lymphopenia in blood and spleen starting very early after stroke onset, which is a hallmark of stroke-induced immune depression [54]. In addition, investigations of the lung immunity after stroke have shown a significant reduction of CD4+, CD8+ and B cells 24 h and 72 h after MCAo [60]. Here, we did not observe a significant difference in lung lymphocyte counts between naïve WT and MCAo mice. Investigation of the spleen showed a significant reduction of lymphocyte numbers only in MCAo treated α5 and α9/10 nAChR KO mice compared to naïve WT mice, whereas MCAo treated α2, α7 nAChR KO mice and WT littermates showed no differences compared to naïve WT mice. Notably, we found that infected WT naïve mice also showed diminished lymphocyte counts in the lung compared to normal lymphocyte numbers in untreated WT mice. Clinical data from patients with pneumococcal infections have shown that the acute phase of infection was associated with a diminished number of lymphocytes in blood. Further analysis demonstrated increased apoptosis among lymphocytes [61]. This is in line with experimental data showing increased lymphocyte apoptosis in a mouse model of pneumococcal pneumonia [62]. In addition, *S. pneumoniae* D39 strain has been shown to mediate activation-dependent death in human lymphocytes [63]. Nevertheless, it was reported that the number of CD4+ cells reached normal levels in blood one week after infections suggesting trafficking of CD4+ cells instead of inflow of de novo-generated cells after apoptosis-induced lymphopenia. Therefore, it was assumed that the reduced number of lymphocytes in blood is also caused by migration of lymphocytes to the site of inflammation [61]. This was supported by experiment findings in mice showing that pneumococcal infection increased the number of lymphocytes in BAL compared to uninfected mice [64]. These data suggest that in the present study naïve WT mice developed lymphopenia in spleen and lung due to pneumococcal infection, and consequently, the number of lymphocytes differs only marginally between MCAo mice and naïve WT mice.

Besides alveolar macrophages, a smaller subset of interstitial macrophages (IMs) is found in the lung. While generally IMs are believed to have homeostatic and immunomodulatory functions, these cells may also play an important role in host pathogen defense. Experiments in mice have shown

that pulmonary infection induces accumulation of IMs in the lung. In addition, depletion of IMs results in increased bacterial burden after infection suggesting that these cells are essential for controlling pathogens in the lung [65]. Here, we observed a diminished number of IMs in MCAo mice compared to naïve WT mice. These data suggest that the decreased number of IMs in the lung in MCAo mice may contribute to impaired clearance of *S. pneumoniae*.

It is well known that several pneumococcal factors such as opaque variants might disrupt epithelial barriers resulting in a transition of bacteria from the mucosal surface to the bloodstream [66]. Findings in animals and patients have demonstrated that alveolar-capillary barrier disruption leads to increased albumin concentrations in BAL and is associated with neutrophil recruitment into the lung [67–69]. Experiments in mice have shown that infection with a lethal dose of *S. pneumoniae* D39 leads to increased albumin level in BAL due to the disruption of the alveolar barrier [70,71]. In healthy mice, the BAL/plasma albumin ratio is 1–3 [32]. Here, we found an increased albumin ratio in several mice, but no differences between groups of various nAChR KO mice, WT littermates and naïve WT mice. Possibly the low impact of pneumococcal infection on the permeability of the alveolar-capillary barrier can be explained by the use of a low infection dose in our model compared to the lethal infection dose in the acute pneumococcal pneumonia mouse model. Neutrophils have been demonstrated to mediate increased epithelial permeability in the lung during pulmonary infection [71,72]. Since nAChR depletion has no effect on neutrophil recruitment into the lung during pneumococcal infection, nAChRs also do not influence the alveolar-capillary barrier 24 h after infection.

In addition, we have investigated the level of pro-inflammatory cytokines in BAL fluid. WT mice without MCAo surgery were able to clear the induced infection within 24 h and did not show elevated levels of pro-inflammatory cytokines in BAL fluid. In contrast, persistent bacterial infection in MCAo mice leads to continuous cytokine secretion, which correlated with bacterial burden in BAL fluid. Experiments in mice have shown that MIP-1α, KC and TNFα level in BAL fluid dramatically increase in the acute phase of pneumococcal pneumonia. [57,59]. In the present study, we could observe that only several MCAo mice were able to induce the pro-inflammatory cytokine response in BAL during the acute phase of pneumococcal infection after stroke. Previous studies have shown that TNFα, KC and MIP-1α secretion is regulated by the cholinergic anti-inflammatory pathway [39,73,74]. These data indicate that stroke impairs pro-inflammatory cytokine secretion during pneumococcal infection contributing to impaired pathogen clearance.

Nevertheless, we found no significant differences between nAChR KO mice and WT mice concerning bacterial burden, cellularity of the lung and spleen, permeability of the alveolar-capillary barrier and cytokine secretion in BAL fluid. These results suggest that various nAChRs including the α7 nAChR do not play a role in increased susceptibility to pneumococcal lung infection after stroke. The apparent discrepancy between earlier studies [8,9,45,46] and the current study concerning the anti-inflammatory effect mediated by the α7 nAChR may be caused by the usage of different types of bacteria in these models. So far, the protective effect of α7 nAChR was solely detected in conjunction with Gram-negative infections. In a mouse model of spontaneous infections after stroke, it was shown that >95% of bacteria cultures from peripheral blood and lung were *E. coli* and depletion of α7 nAChR resulted in diminished bacterial burden in BAL [8,54]. Experiments in mice have shown that the α7 nAChR also mediates impaired immunity in an induced infection with Gram-negative *Pseudomonas aeruginosa* after stroke. α7 nAChR depletion attenuated the effect of stroke on lung injury due to *P. aeruginosa* infection. In contrast, blockade of β-adrenergic receptors by propranolol increased lung injury [75]. Interestingly, propranolol treatment of MCAo mice prevented pulmonary infection with Gram-positive bacteria, such as *S. pneumoniae* [19] and *Listeria monocytogenes* [76]. Many studies investigated the cholinergic anti-inflammatory pathway in the context of uncontrolled inflammatory host response such as sepsis. Findings in animals have demonstrated that stimulation of the cholinergic anti-inflammatory pathway reduced inflammation and mortality in sepsis-induced lung injury due to pulmonary *E. coli* infection and enhanced survival in oral *Salmonella typhimurium* infection [77,78]. Interestingly, nonselective stimulation of nAChRs had no effect on lung inflammation in induced

pneumococcal pneumonia with bacteremia [79]. These data suggest that cholinergic activation due to CNS injury may preferentially impair immunity against Gram-negative bacteria. However, further comparative studies including infection models with Gram-negative bacteria and other Gram-positive bacterial strains after stroke are required to further elucidate the immunomodulatory role in cholinergic signaling during infections with different types of bacteria.

5. Conclusions

In summary, our findings show that stroke results in impaired pulmonary immunity against *S. pneumoniae* resulting in reduced bacterial clearance and prolonged infection. Blocking of cholinergic signaling by depletion of various nAChRs subunits does not enhance antibacterial immune response suggesting that cholinergic pathways, at least not mediated by α2 nAChR, α5 nAChR, α7 nAChR, α9/10 nAChR subunits, does not play a role in impaired immunity against *S. pneumonia* after stroke. In this respect, it would be interesting to study the impact of non-α7 nAChRs on spontaneous infections or induced-aspiration infections with Gram-negative bacteria, such as *Pseudomonas aeruginosa*, *Klebsiella pneumoniae*, *Enterobacter*, *Escherichia Coli* after stroke.

Author Contributions: Conceptualization, C.M., A.M. and C.D.; methodology, S.J., C.D., D.B. and K.W.; formal analysis, S.J.; investigation, S.J.; writing—original draft preparation, S.J.; writing—review and editing, C.M, A.M., S.J. and C.D.; visualization, D.B., L.W., C.D., K.W., A.M. and C.M.; supervision, C.M. and A.M.; project administration, C.M. and A.M.; funding acquisition, C.M. and A.M. All authors have read and agreed to the published version of the manuscript.

Funding: This research was funded by the German Research Foundation (SFB-TR84), Einstein Foundation and Leducq Foundation.

Acknowledgments: We thank Sabine Kolodziej, Claudia Muselmann-Genschow and Susanne Metzkow for excellent technical assistance, Désirée Kunkel for support with flow cytometry. We acknowledge support from the German Research Foundation (DFG) and the Open Access Publication Funds of Charité-Universitätsmedizin Berlin.

Conflicts of Interest: The authors have declared that no conflict of interest exists.

References

1. Davenport, R.J.; Dennis, M.S.; Wellwood, I.; Warlow, C.P. Complications after acute stroke. *Stroke* **1996**, *27*, 415–420. [CrossRef] [PubMed]
2. Johnston, K.C.; Li, J.Y.; Lyden, P.D.; Hanson, S.K.; Feasby, T.E.; Adams, R.J.; Faught, R.E., Jr.; Haley, E.C., Jr. Medical and neurological complications of ischemic stroke: Experience from the RANTTAS trial. RANTTAS Investigators. *Stroke* **1998**, *29*, 447–453. [CrossRef] [PubMed]
3. Langhorne, P.; Stott, D.J.; Robertson, L.; MacDonald, J.; Jones, L.; McAlpine, C.; Dick, F.; Taylor, G.S.; Murray, G. Medical complications after stroke: A multicenter study. *Stroke* **2000**, *31*, 1223–1229. [CrossRef] [PubMed]
4. Weimar, C.; Roth, M.P.; Zillessen, G.; Glahn, J.; Wimmer, M.L.; Busse, O.; Haberl, R.L.; Diener, H.C.; German Stroke Data Bank Collaborators O. Complications following acute ischemic stroke. *Eur. Neurol.* **2002**, *48*, 133–140. [CrossRef]
5. Meisel, C.; Schwab, J.M.; Prass, K.; Meisel, A.; Dirnagl, U. Central nervous system injury-induced immune deficiency syndrome. *Nat. Rev. Neurosci.* **2005**, *6*, 775–786. [CrossRef]
6. Sellars, C.; Bowie, L.; Bagg, J.; Sweeney, M.P.; Miller, H.; Tilston, J.; Langhorne, P.; Stott David, J. Risk Factors for Chest Infection in Acute Stroke. *Stroke* **2007**, *38*, 2284–2291. [CrossRef]
7. Hoffmann, S.; Harms, H.; Ulm, L.; Nabavi, D.G.; Mackert, B.-M.; Schmehl, I.; Jungehulsing, G.J.; Montaner, J.; Bustamante, A.; Hermans, M.; et al. Stroke-induced immunodepression and dysphagia independently predict stroke-associated pneumonia—The PREDICT study. *J. Cereb. Blood Flow Metab.* **2017**, *37*, 3671–3682. [CrossRef]
8. Engel, O.; Akyuz, L.; da Costa Goncalves, A.C.; Winek, K.; Dames, C.; Thielke, M.; Herold, S.; Bottcher, C.; Priller, J.; Volk, H.D.; et al. Cholinergic Pathway Suppresses Pulmonary Innate Immunity Facilitating Pneumonia after Stroke. *Stroke* **2015**, *46*, 3232–3240. [CrossRef]

9. Wang, H.; Yu, M.; Ochani, M.; Amella, C.A.; Tanovic, M.; Susarla, S.; Li, J.H.; Wang, H.; Yang, H.; Ulloa, L.; et al. Nicotinic acetylcholine receptor α7 subunit is an essential regulator of inflammation. *Nature* **2003**, *421*, 384–388. [CrossRef]
10. Pavlov, V.A.; Wang, H.; Czura, C.J.; Friedman, S.G.; Tracey, K.J. The cholinergic anti-inflammatory pathway: A missing link in neuroimmunomodulation. *Mol. Med.* **2003**, *9*, 125–134. [CrossRef]
11. Tracey, K.J. The inflammatory reflex. *Nature* **2002**, *420*, 853–859. [CrossRef] [PubMed]
12. Fujii, T.; Mashimo, M.; Moriwaki, Y.; Misawa, H.; Ono, S.; Horiguchi, K.; Kawashima, K. Physiological functions of the cholinergic system in immune cells. *J. Pharmacol. Sci.* **2017**, *134*, 1–21. [CrossRef] [PubMed]
13. Qian, J.; Galitovskiy, V.; Chernyavsky, A.I.; Marchenko, S.; Grando, S.A. Plasticity of the murine spleen T-cell cholinergic receptors and their role in in vitro differentiation of naïve CD4 T cells toward the Th1, Th2 and Th17 lineages. *Genes Immun.* **2011**, *12*, 222–230. [CrossRef] [PubMed]
14. Papke, R.L.; Lindstrom, J.M. Nicotinic acetylcholine receptors: Conventional and unconventional ligands and signaling. *Neuropharmacology* **2020**, *168*, 108021. [CrossRef] [PubMed]
15. Perry, L.; Love, C.P. Screening for dysphagia and aspiration in acute stroke: A systematic review. *Dysphagia* **2001**, *16*, 7–18. [CrossRef]
16. Kollef, M.H.; Shorr, A.; Tabak, Y.P.; Gupta, V.; Liu, L.Z.; Johannes, R.S. Epidemiology and outcomes of health-care-associated pneumonia: Results from a large US database of culture-positive pneumonia. *Chest* **2005**, *128*, 3854–3862. [CrossRef]
17. Trouillet, J.L.; Chastre, J.; Vuagnat, A.; Joly-Guillou, M.L.; Combaux, D.; Dombret, M.C.; Gibert, C. Ventilator-associated pneumonia caused by potentially drug-resistant bacteria. *Am. J. Respir. Crit. Care Med.* **1998**, *157*, 531–539. [CrossRef]
18. Kishore Amit, K.; Vail, A.; Jeans Adam, R.; Chamorro, A.; Di Napoli, M.; Kalra, L.; Langhorne, P.; Roffe, C.; Westendorp, W.; Nederkoorn Paul, J.; et al. Microbiological Etiologies of Pneumonia Complicating Stroke. *Stroke* **2018**, *49*, 1602–1609. [CrossRef]
19. Prass, K.; Braun Johann, S.; Dirnagl, U.; Meisel, C.; Meisel, A. Stroke Propagates Bacterial Aspiration to Pneumonia in a Model of Cerebral Ischemia. *Stroke* **2006**, *37*, 2607–2612. [CrossRef]
20. McCulloch, L.; Smith, C.J.; McColl, B.W. Adrenergic-mediated loss of splenic marginal zone B cells contributes to infection susceptibility after stroke. *Nat. Commun.* **2017**, *8*, 15051. [CrossRef]
21. Wong, C.H.; Jenne, C.N.; Lee, W.Y.; Léger, C.; Kubes, P. Functional innervation of hepatic iNKT cells is immunosuppressive following stroke. *Science* **2011**, *334*, 101–105. [CrossRef] [PubMed]
22. Lotfipour, S.; Byun, J.S.; Leach, P.; Fowler, C.D.; Murphy, N.P.; Kenny, P.J.; Gould, T.J.; Boulter, J. Targeted deletion of the mouse α2 nicotinic acetylcholine receptor subunit gene (Chrna2) potentiates nicotine-modulated behaviors. *J. Neurosci.* **2013**, *33*, 7728–7741. [CrossRef]
23. Salas, R.; Orr-Urtreger, A.; Broide, R.S.; Beaudet, A.; Paylor, R.; De Biasi, M. The Nicotinic Acetylcholine Receptor Subunit α5 Mediates Short-Term Effects of Nicotine in Vivo. *Mol. Pharmacol.* **2003**, *63*, 1059. [CrossRef]
24. Orr-Urtreger, A.; Göldner, F.M.; Saeki, M.; Lorenzo, I.; Goldberg, L.; De Biasi, M.; Dani, J.A.; Patrick, J.W.; Beaudet, A.L. Mice Deficient in the α7 Neuronal Nicotinic Acetylcholine Receptor Lack α-Bungarotoxin Binding Sites and Hippocampal Fast Nicotinic Currents. *J. Neurosci.* **1997**, *17*, 9165. [CrossRef] [PubMed]
25. Vetter, D.E.; Katz, E.; Maison, S.F.; Taranda, J.; Turcan, S.; Ballestero, J.; Liberman, M.C.; Elgoyhen, A.B.; Boulter, J. The α10 nicotinic acetylcholine receptor subunit is required for normal synaptic function and integrity of the olivocochlear system. *Proc. Natl. Acad. Sci. USA* **2007**, *104*, 20594. [CrossRef] [PubMed]
26. Vetter, D.E.; Liberman, M.C.; Mann, J.; Barhanin, J.; Boulter, J.; Brown, M.C.; Saffiote-Kolman, J.; Heinemann, S.F.; Elgoyhen, A.B. Role of α9 Nicotinic ACh Receptor Subunits in the Development and Function of Cochlear Efferent Innervation. *Neuron* **1999**, *23*, 93–103. [CrossRef]
27. Engel, O.; Kolodziej, S.; Dirnagl, U.; Prinz, V. Modeling stroke in mice-middle cerebral artery occlusion with the filament model. *J. Vis. Exp.* **2011**. [CrossRef]
28. Jeong, D.-G.; Jeong, E.-S.; Seo, J.-H.; Heo, S.-H.; Choi, Y.-K. Difference in Resistance to Streptococcus pneumoniae Infection in Mice. *Lab. Anim. Res.* **2011**, *27*, 91–98. [CrossRef]
29. Schulte-Herbrüggen, O.; Klehmet, J.; Quarcoo, D.; Meisel, C.; Meisel, A. Mouse strains differ in their susceptibility to poststroke infections. *Neuroimmunomodulation* **2006**, *13*, 13–18. [CrossRef]

30. Dames, C.; Akyüz, L.; Reppe, K.; Tabeling, C.; Dietert, K.; Kershaw, O.; Gruber, A.D.; Meisel, C.; Meisel, A.; Witzenrath, M.; et al. Miniaturized bronchoscopy enables unilateral investigation, application, and sampling in mice. *Am. J. Respir. Cell Mol. Biol.* **2014**, *51*, 730–737. [CrossRef]
31. Sun, F.; Xiao, G.; Qu, Z. Murine Bronchoalveolar Lavage. *Bio-protocol* **2017**, *7*, e2287. [CrossRef] [PubMed]
32. Müller-Redetzky, H.C.; Felten, M.; Hellwig, K.; Wienhold, S.-M.; Naujoks, J.; Opitz, B.; Kershaw, O.; Gruber, A.D.; Suttorp, N.; Witzenrath, M. Increasing the inspiratory time and I:E ratio during mechanical ventilation aggravates ventilator-induced lung injury in mice. *Crit. Care* **2015**, *19*, 23. [CrossRef] [PubMed]
33. Huang, Y.-Y.; Li, X.; Li, X.; Sheng, Y.-Y.; Zhuang, P.-W.; Zhang, Y.-J. Neuroimmune crosstalk in central nervous system injury-induced infection and pharmacological intervention. *Brain Res. Bull.* **2019**, *153*, 232–238. [CrossRef] [PubMed]
34. Shi, K.; Wood, K.; Shi, F.-D.; Wang, X.; Liu, Q. Stroke-induced immunosuppression and poststroke infection. *Stroke Vasc. Neurol.* **2018**, *3*, 34. [CrossRef]
35. El Husseini, N.; Laskowitz, D.T. The role of neuroendocrine pathways in prognosis after stroke. *Expert Rev. Neur.* **2014**, *14*, 217–232. [CrossRef]
36. Dirnagl, U.; Klehmet, J.; Braun Johann, S.; Harms, H.; Meisel, C.; Ziemssen, T.; Prass, K.; Meisel, A. Stroke-Induced Immunodepression. *Stroke* **2007**, *38*, 770–773. [CrossRef]
37. Chamorro, Á.; Meisel, A.; Planas, A.M.; Urra, X.; van de Beek, D.; Veltkamp, R. The immunology of acute stroke. *Nat. Rev. Neurol.* **2012**, *8*, 401. [CrossRef]
38. Kummer, W.; Lips, K.S.; Pfeil, U. The epithelial cholinergic system of the airways. *Histochem. Cell Biol.* **2008**, *130*, 219. [CrossRef]
39. Borovikova, L.V.; Ivanova, S.; Zhang, M.; Yang, H.; Botchkina, G.I.; Watkins, L.R.; Wang, H.; Abumrad, N.; Eaton, J.W.; Tracey, K.J. Vagus nerve stimulation attenuates the systemic inflammatory response to endotoxin. *Nature* **2000**, *405*, 458–462. [CrossRef]
40. Koarai, A.; Ichinose, M. Possible involvement of acetylcholine-mediated inflammation in airway diseases. *Allergol. Int.* **2018**, *67*, 460–466. [CrossRef]
41. Frinchi, M.; Nuzzo, D.; Scaduto, P.; Di Carlo, M.; Massenti, M.F.; Belluardo, N.; Mudò, G. Anti-inflammatory and antioxidant effects of muscarinic acetylcholine receptor (mAChR) activation in the rat hippocampus. *Sci. Rep.* **2019**, *9*, 14233. [CrossRef] [PubMed]
42. Guarini, S.; Cainazzo, M.M.; Giuliani, D.; Mioni, C.; Altavilla, D.; Marini, H.; Bigiani, A.; Ghiaroni, V.; Passaniti, M.; Leone, S.; et al. Adrenocorticotropin reverses hemorrhagic shock in anesthetized rats through the rapid activation of a vagal anti-inflammatory pathway. *Cardiovasc. Res.* **2004**, *63*, 357–365. [CrossRef] [PubMed]
43. Pavlov, V.A.; Ochani, M.; Gallowitsch-Puerta, M.; Ochani, K.; Huston, J.M.; Czura, C.J.; Al-Abed, Y.; Tracey, K.J. Central muscarinic cholinergic regulation of the systemic inflammatory response during endotoxemia. *Proc. Natl. Acad. Sci. USA* **2006**, *103*, 5219–5223. [CrossRef] [PubMed]
44. Zoli, M.; Pucci, S.; Vilella, A.; Gotti, C. Neuronal and Extraneuronal Nicotinic Acetylcholine Receptors. *Curr. Neuropharmacol.* **2018**, *16*, 338–349. [CrossRef] [PubMed]
45. Giebelen, I.A.J.; Le Moine, A.; van den Pangaart, P.S.; Sadis, C.; Goldman, M.; Florquin, S.; van der Poll, T. Deficiency of α7 Cholinergic Receptors Facilitates Bacterial Clearance in Escherichia coli Peritonitis. *J. Infect. Dis.* **2008**, *198*, 750–757. [CrossRef]
46. Speer, P.; Zhang, Y.; Gu, Y.; Lucas, M.J.; Wang, Y. Effects of nicotine on intercellular adhesion molecule expression in endothelial cells and integrin expression in neutrophils in vitro. *Am. J. Obstet. Gynecol.* **2002**, *186*, 551–556. [CrossRef]
47. Kawashima, K.; Yoshikawa, K.; Fujii, Y.X.; Moriwaki, Y.; Misawa, H. Expression and function of genes encoding cholinergic components in murine immune cells. *Life Sci.* **2007**, *80*, 2314–2319. [CrossRef]
48. Nouri-Shirazi, M.; Guinet, E. Evidence for the immunosuppressive role of nicotine on human dendritic cell functions. *Immunology* **2003**, *109*, 365–373. [CrossRef]
49. Wang, F.; Gerzanich, V.; Wells, G.B.; Anand, R.; Peng, X.; Keyser, K.; Lindstrom, J. Assembly of human neuronal nicotinic receptor alpha5 subunits with alpha3, beta2, and beta4 subunits. *J. Biol. Chem.* **1996**, *271*, 17656–17665. [CrossRef]
50. Kedmi, M.; Beaudet, A.L.; Orr-Urtreger, A. Mice lacking neuronal nicotinic acetylcholine receptor beta4-subunit and mice lacking both alpha5- and beta4-subunits are highly resistant to nicotine-induced seizures. *Physiol. Genom.* **2004**, *17*, 221–229. [CrossRef]

51. Bagdas, D.; AlSharari, S.D.; Freitas, K.; Tracy, M.; Damaj, M.I. The role of alpha5 nicotinic acetylcholine receptors in mouse models of chronic inflammatory and neuropathic pain. *Biochem. Pharmacol.* **2015**, *97*, 590–600. [CrossRef] [PubMed]
52. Wang, N.; Orr-Urtreger, A.; Chapman, J.; Rabinowitz, R.; Nachman, R.; Korczyn, A.D. Autonomic function in mice lacking alpha5 neuronal nicotinic acetylcholine receptor subunit. *J. Physiol.* **2002**, *542*, 347–354. [CrossRef] [PubMed]
53. Jun, H.; Yu, H.; Gong, J.; Jiang, J.; Qiao, X.; Perkey, E.; Kim, D.-i.; Emont, M.P.; Zestos, A.G.; Cho, J.-S.; et al. An immune-beige adipocyte communication via nicotinic acetylcholine receptor signaling. *Nat. Med.* **2018**, *24*, 814–822. [CrossRef] [PubMed]
54. Prass, K.; Meisel, C.; Höflich, C.; Braun, J.; Halle, E.; Wolf, T.; Ruscher, K.; Victorov, I.V.; Priller, J.; Dirnagl, U.; et al. Stroke-induced Immunodeficiency Promotes Spontaneous Bacterial Infections and Is Mediated by Sympathetic Activation Reversal by Poststroke T Helper Cell Type 1–like Immunostimulation. *J. Exp. Med.* **2003**, *198*, 725. [CrossRef] [PubMed]
55. Kishore, A.K.; Jeans, A.R.; Garau, J.; Bustamante, A.; Kalra, L.; Langhorne, P.; Chamorro, A.; Urra, X.; Katan, M.; Napoli, M.D.; et al. Antibiotic treatment for pneumonia complicating stroke: Recommendations from the pneumonia in stroke consensus (PISCES) group. *Eur. Stroke J.* **2019**, *4*, 318–328. [CrossRef] [PubMed]
56. Mracsko, E.; Stegemann-Koniszewski, S.; Na, S.Y.; Dalpke, A.; Bruder, D.; Lasitschka, F.; Veltkamp, R. A Mouse Model of Post-Stroke Pneumonia Induced by Intra-Tracheal Inoculation with Streptococcus pneumoniae. *Cerebrovasc. Dis.* **2017**, *43*, 99–109. [CrossRef] [PubMed]
57. Fillion, I.; Ouellet, N.; Simard, M.; Bergeron, Y.; Sato, S.; Bergeron, M.G. Role of chemokines and formyl peptides in pneumococcal pneumonia-induced monocyte/macrophage recruitment. *J. Immunol.* **2001**, *166*, 7353–7361. [CrossRef]
58. Haste, L.; Hulland, K.; Bolton, S.; Yesilkaya, H.; McKechnie, K.; Andrew, P.W. Development and Characterization of a Long-Term Murine Model of Streptococcus pneumoniae Infection of the Lower Airways. *Infect. Immun.* **2014**, *82*, 3289. [CrossRef]
59. Peñaloza, H.F.; Nieto, P.A.; Muñoz-Durango, N.; Salazar-Echegarai, F.J.; Torres, J.; Parga, M.J.; Alvarez-Lobos, M.; Riedel, C.A.; Kalergis, A.M.; Bueno, S.M. Interleukin-10 plays a key role in the modulation of neutrophils recruitment and lung inflammation during infection by Streptococcus pneumoniae. *Immunology* **2015**, *146*, 100–112. [CrossRef]
60. Farris, B.Y.; Monaghan, K.L.; Zheng, W.; Amend, C.D.; Hu, H.; Ammer, A.G.; Coad, J.E.; Ren, X.; Wan, E.C.K. Ischemic stroke alters immune cell niche and chemokine profile in mice independent of spontaneous bacterial infection. *Immun. Inflamm. Dis.* **2019**, *7*, 326–341. [CrossRef]
61. Kemp, K.; Bruunsgaard, H.; Skinhøj, P.; Klarlund Pedersen, B. Pneumococcal infections in humans are associated with increased apoptosis and trafficking of type 1 cytokine-producing T cells. *Infect. Immun.* **2002**, *70*, 5019–5025. [CrossRef] [PubMed]
62. Schreiber, T.; Swanson, P.E.; Chang, K.C.; Davis, C.C.; Dunne, W.M.; Karl, I.E.; Reinhart, K.; Hotchkiss, R.S. Both gram-negative and gram-positive experimental pneumonia induce profound lymphocyte but not respiratory epithelial cell apoptosis. *Shock* **2006**, *26*. [CrossRef] [PubMed]
63. Grayson, K.M.; Blevins, L.K.; Oliver, M.B.; Ornelles, D.A.; Swords, W.E.; Alexander-Miller, M.A. Activation-dependent modulation of Streptococcus pneumoniae-mediated death in human lymphocytes. *Pathog. Dis.* **2017**, *75*. [CrossRef] [PubMed]
64. McKenzie, C.W.; Klonoski, J.M.; Maier, T.; Trujillo, G.; Vitiello, P.F.; Huber, V.C.; Lee, L. Enhanced response to pulmonary Streptococcus pneumoniae infection is associated with primary ciliary dyskinesia in mice lacking Pcdp1 and Spef2. *Cilia* **2013**, *2*, 18. [CrossRef] [PubMed]
65. Huang, L.; Nazarova, E.V.; Tan, S.; Liu, Y.; Russell, D.G. Growth of Mycobacterium tuberculosis in vivo segregates with host macrophage metabolism and ontogeny. *J. Exp. Med.* **2018**, *215*, 1135–1152. [CrossRef] [PubMed]
66. Kadioglu, A.; Weiser, J.N.; Paton, J.C.; Andrew, P.W. The role of Streptococcus pneumoniae virulence factors in host respiratory colonization and disease. *Nat. Rev. Microbiol.* **2008**, *6*, 288. [CrossRef]
67. Chignard, M.; Balloy, V. Neutrophil recruitment and increased permeability during acute lung injury induced by lipopolysaccharide. *Am. J. Physiol. Lung Cell. Mol. Physiol.* **2000**, *279*, L1083–L1090. [CrossRef]

68. O'Grady, N.P.; Preas, H.L.; Pugin, J.; Fiuza, C.; Tropea, M.; Reda, D.; Banks, S.M.; Suffredini, A.F. Local Inflammatory Responses following Bronchial Endotoxin Instillation in Humans. *Am. J. Respir. Crit. Care Med.* **2001**, *163*, 1591–1598. [CrossRef]
69. Speyer, C.L.; Neff, T.A.; Warner, R.L.; Guo, R.-F.; Sarma, J.V.; Riedemann, N.C.; Murphy, M.E.; Murphy, H.S.; Ward, P.A. Regulatory effects of iNOS on acute lung inflammatory responses in mice. *Am. J. Pathol.* **2003**, *163*, 2319–2328. [CrossRef]
70. Williams, A.E.; José, R.J.; Brown, J.S.; Chambers, R.C. Enhanced inflammation in aged mice following infection with Streptococcus pneumoniae is associated with decreased IL-10 and augmented chemokine production. *Am. J. Physiol. Lung. Cell. Mol. Physiol.* **2015**, *308*, L539–L549. [CrossRef]
71. José, R.J.; Williams, A.E.; Mercer, P.F.; Sulikowski, M.G.; Brown, J.S.; Chambers, R.C. Regulation of neutrophilic inflammation by proteinase-activated receptor 1 during bacterial pulmonary infection. *J. Immunol.* **2015**, *194*, 6024–6034. [CrossRef] [PubMed]
72. Kantrow, S.P.; Shen, Z.; Jagneaux, T.; Zhang, P.; Nelson, S. Neutrophil-mediated lung permeability and host defense proteins. *Am. J. Physiol. Lung Cell. Mol. Physiol.* **2009**, *297*, L738–L745. [CrossRef] [PubMed]
73. Li, S.; Zhou, B.; Liu, B.; Zhou, Y.; Zhang, H.; Li, T.; Zuo, X. Activation of the cholinergic anti-inflammatory system by nicotine attenuates arthritis via suppression of macrophage migration. *Mol. Med. Rep.* **2016**, *14*, 5057–5064. [CrossRef] [PubMed]
74. Sadis, C.; Teske, G.; Stokman, G.; Kubjak, C.; Claessen, N.; Moore, F.; Loi, P.; Diallo, B.; Barvais, L.; Goldman, M.; et al. Nicotine protects kidney from renal ischemia/reperfusion injury through the cholinergic anti-inflammatory pathway. *PLoS ONE* **2007**, *2*, e469. [CrossRef] [PubMed]
75. Lafargue, M.; Xu, L.; Carlès, M.; Serve, E.; Anjum, N.; Iles, K.E.; Xiong, X.; Giffard, R.; Pittet, J.-F. Stroke-induced activation of the α7 nicotinic receptor increases Pseudomonas aeruginosa lung injury. *FASEB J.* **2012**, *26*, 2919–2929. [CrossRef] [PubMed]
76. Liu, Q.; Jin, W.-N.; Liu, Y.; Shi, K.; Sun, H.; Zhang, F.; Zhang, C.; Gonzales, R.J.; Sheth, K.N.; La Cava, A.; et al. Brain Ischemia Suppresses Immunity in the Periphery and Brain via Different Neurogenic Innervations. *Immunity* **2017**, *46*, 474–487. [CrossRef]
77. Fernandez-Cabezudo, M.J.; Lorke, D.E.; Azimullah, S.; Mechkarska, M.; Hasan, M.Y.; Petroianu, G.A.; al-Ramadi, B.K. Cholinergic stimulation of the immune system protects against lethal infection by Salmonella enterica serovar Typhimurium. *Immunology* **2010**, *130*, 388–398. [CrossRef]
78. Su, X.; Matthay, M.A.; Malik, A.B. Requisite role of the cholinergic alpha7 nicotinic acetylcholine receptor pathway in suppressing Gram-negative sepsis-induced acute lung inflammatory injury. *J. Immunol.* **2010**, *184*, 401–410. [CrossRef]
79. Giebelen, I.A.J.; Leendertse, M.; Florquin, S.; van der Poll, T. Stimulation of acetylcholine receptors impairs host defence during pneumococcal pneumonia. *Eur. Respir. J.* **2009**, *33*, 375. [CrossRef]

8.2 Study 2

Transfer RNA fragments replace microRNA regulators of the cholinergic poststroke immune blockade

Katarzyna Winek[a,b,1], Sebastian Lobentanzer[c,1], Bettina Nadorp[a,d], Serafima Dubnov[a,b], Claudia Dames[e], Sandra Jagdmann[e], Gilli Moshitzky[a,b], Benjamin Hotter[f], Christian Meisel[e], David S. Greenberg[b], Sagiv Shifman[g], Jochen Klein[c], Shani Shenhar-Tsarfaty[h], Andreas Meisel[f], and Hermona Soreq[a,b,2]

[a]The Edmond & Lily Safra Center for Brain Sciences, The Hebrew University of Jerusalem, 9190401 Jerusalem, Israel; [b]The Alexander Silberman Institute of Life Sciences, The Hebrew University of Jerusalem, 9190401 Jerusalem, Israel; [c]Department of Pharmacology, College of Pharmacy, Goethe University, 60438 Frankfurt am Main, Germany; [d]The Grass Center for Bioengineering, Benin School of Computer Science and Engineering, The Hebrew University of Jerusalem, 9190401 Jerusalem, Israel; [e]The Institute for Medical Immunology, Charité-Universitätsmedizin Berlin, 10117 Berlin, Germany; [f]NeuroCure Clinical Research, Center for Stroke Research Berlin, Department of Neurology, Charité-Universitätsmedizin Berlin, 10117 Berlin, Germany; [g]Department of Genetics, The Hebrew University of Jerusalem, 9190401 Jerusalem, Israel; and [h]Department of Internal Medicine "C," "D," and "E," Tel Aviv Sourasky Medical Center and Sackler Faculty of Medicine, Tel Aviv University, 6997801 Tel Aviv, Israel

Edited by Lawrence Steinman, Stanford University School of Medicine, Stanford, CA, and approved October 23, 2020 (received for review July 2, 2020)

Stroke is a leading cause of death and disability. Recovery depends on a delicate balance between inflammatory responses and immune suppression, tipping the scale between brain protection and susceptibility to infection. Peripheral cholinergic blockade of immune reactions fine-tunes this immune response, but its molecular regulators are unknown. Here, we report a regulatory shift in small RNA types in patient blood sequenced 2 d after ischemic stroke, comprising massive decreases of microRNA levels and concomitant increases of transfer RNA fragments (tRFs) targeting cholinergic transcripts. Electrophoresis-based size-selection followed by qRT-PCR validated the top six up-regulated tRFs in a separate cohort of stroke patients, and independent datasets of small and long RNA sequencing pinpointed immune cell subsets pivotal to these responses, implicating CD14$^+$ monocytes in the cholinergic inflammatory reflex. In-depth small RNA targeting analyses revealed the most-perturbed pathways following stroke and implied a structural dichotomy between microRNA and tRF target sets. Furthermore, lipopolysaccharide stimulation of murine RAW 264.7 cells and human CD14$^+$ monocytes up-regulated the top six stroke-perturbed tRFs, and overexpression of stroke-inducible tRF-22-WE8SPOX52 using a single-stranded RNA mimic induced down-regulation of immune regulator Z-DNA binding protein 1. In summary, we identified a "changing of the guards" between small RNA types that may systemically affect homeostasis in poststroke immune responses, and pinpointed multiple affected pathways, which opens new venues for establishing therapeutics and biomarkers at the protein and RNA level.

acetylcholine | immunology | ischemic stroke | microRNA | transfer RNA fragment

Stroke is a global burden of growing dimensions, accounting for ∼5.5 million deaths annually, and leaving most of the surviving patients permanently disabled (1). The immune system is one of the main players in the pathophysiology of stroke. Brain injury dampens immune functions in the periphery, which limits the inflammatory response and infiltration of immune cells into the CNS and may pose a neuroprotective mechanism in stroke patients. However, this systemic immunosuppression simultaneously increases the risk of infectious complications (2), for example, by inducing lymphocyte apoptosis and decreasing the production of proinflammatory cytokines such as lymphocytic IFN-γ and monocytic TNF-α (3). Therefore, poststroke recovery largely depends on a delicate balance between inflammation, which exacerbates the severity of symptoms, and the poststroke suppression of immune functions, which increases the susceptibility to infections (3). This involves incompletely understood molecular regulators of cholinergic and sympathetic signaling and the hypothalamus–pituitary–adrenal gland axis (HPA). Among other processes, brain injury leads to activation of the vagus nerve, which mediates antiinflammatory signaling through the cholinergic efferent fibers and the noradrenergic splenic nerve (4). Binding of acetylcholine (ACh) to the nicotinic α7 receptors on monocytes/macrophages decreases the production of proinflammatory cytokines (4, 5) in a manner susceptible to suppression by microRNA (miR) regulators of cholinergic signaling, such as miR-132 (6). We hypothesized that this and other small RNA fine-tuners of innate immune responses, including miRs and the recently rediscovered transfer RNA (tRNA) fragments (tRFs), may contribute to regulation of poststroke processes.

Both miRs and tRFs may control entire biological pathways, such that their balanced orchestration could modulate brain-induced systemic immune functioning. miRs are small noncoding RNAs whose expression requires transcription yet can be rapidly induced, enabling degradation and translational suppression of target genes

Significance

Ischemic stroke triggers peripheral immunosuppression, increasing the susceptibility to poststroke pneumonia that is linked with poor survival. The poststroke brain initiates intensive communication with the immune system, and acetylcholine contributes to these messages; but the responsible molecules are yet unknown. We discovered a "changing of the guards," where microRNA levels decreased but small transfer RNA fragments increased in poststroke blood. This molecular switch may rebalance acetylcholine signaling in CD14$^+$ monocytes by regulating their gene expression and modulating poststroke immunity. Our observations point to transfer RNA fragments as molecular regulators of poststroke immune responses that may be potential therapeutic targets.

Author contributions: K.W. and S.L. analyzed and interpreted RNA-sequencing data and wrote the paper; S.L. conducted bioinformatic analyses; B.N. and S.S-T. processed the blood samples and prepared the sequencing data; K.W. and S.D. established tRF size selection protocols and performed the qRT-PCR measurements; K.W. performed the cell culture tests; G.M. contributed to the sequencing analyses; B.H., C.M., and A.M. collected the stroke cohort, the blood samples, and performed immunological measurements; C.D. and S.J. performed experiments with human monocytes and immunological measurements; D.S.G., S.S., and J.K. interpreted the data; A.M. and H.S. coguided the project, planned the experiments, interpreted the data, and contributed to the manuscript writing; and all co-authors read and commented on the manuscript contents.

The authors declare no competing interest.

This article is a PNAS Direct Submission.

[1]K.W. and S.L. contributed equally to this work.

[2]To whom correspondence may be addressed. Email: hermona.soreq@mail.huji.ac.il.

This article contains supporting information online at https://www.pnas.org/lookup/suppl/doi:10.1073/pnas.2013542117/-/DCSupplemental.

First published December 7, 2020.

carrying a complementary motif. One miR may suppress the expression of many targets involved in the same biological pathway, and many miRs may cotarget the same transcripts, enabling cooperative suppression. Hence, miR regulators of ACh signaling may regulate the role of ACh in both cognitive function and systemic inflammation (6, 7).

Recent reports highlight tRNA as another major source of small-noncoding RNA (8), including tRNA halves (tiRNAs) and smaller tRNA fragments, tRFs. tiRNAs are created by angiogenin cleavage at the anticodon loop (9), raising the possibility that the poststroke angiogenin increase might change their levels (10). Among other functions (11, 12), smaller fragments derived from the 3′- or 5′-end of tRNA (3′-tRF/5′-tRF) or internal tRNA parts (i-tRF) may incorporate into Argonaute (Ago) protein complexes and act like miRs to suppress their targets (13). Differential expression of tRFs was reported under hypoxia, oxidative stress, ischemic reperfusion (9, 14), and in epilepsy (15), which are all involved in ischemic stroke complications. tRFs may be generated via enzymatic degradation of tRNA, independent of de novo transcription, which implies that tRF levels may be modulated more rapidly than miR levels. However, whether brain–body communication and immune suppression after ischemic stroke in human patients involves blood tRF changes has not yet been studied.

Taking into consideration that the cholinergic system is one of the controllers of immune functions, we investigated changes in the levels of miR- and tRF-regulators, with a specific focus on those that may control the ACh-mediated suppression of poststroke immune functions. We performed small and long RNA sequencing (RNA-seq) of whole-blood samples collected from ischemic stroke patients 2 d after stroke onset, mined RNA-seq datasets of blood cell transcripts, and sought potential links between perturbed miRs and tRFs, poststroke immune responses, and the cholinergic antiinflammatory pathway.

Results

Stroke-Perturbed Small RNAs Display a Cholinergic-Associated Shift from miRs to tRFs. To seek poststroke small RNA regulators of body–brain communication, we first performed small RNA-seq of whole-blood samples collected on day 2 after ischemic stroke from 33 male patients of the PREDICT cohort (484 participants) (16) and 10 age- and sex-matched controls (Fig. 1*A*; see demographic data in Dataset S1). Principal component analysis (PCA) of the differentially expressed (DE) small RNAs completely segregated the stroke and control groups (Fig. 1*B*). The respective direction of change among the two small RNA classes involved a statistically significant decline in miRs and a parallel increase in tRFs, indicating a "changing of the guards" from miRs to tRFs. Specifically, 87% of the 143 DE tRFs were up-regulated, whereas 63% of the 420 DE miRs were down-regulated (Benjamini–Hochberg corrected $P < 0.05$) (Fig. 1 *C* and *D*). Of the 143 DE tRFs, 87 were 3′-tRFs and 30 of those (all up-regulated) were derived from alanine binding tRNA (*SI Appendix*, Fig. S1), indicating nonarbitrary fragment generation.

Notably, the 420 DE miRs included several miRs known to be perturbed in stroke: hsa-miR-532-5p ($\log_2$ fold-change [log2FC] = −2.27, P = 1.81e-33) (17), hsa-miR-148a-3p (log2FC = −2.30, P = 9.61e-19), and hsa-let-7i-3p (log2FC = −1.07, P = 4.31e-04) (18). To test the potential involvement of miRs and tRFs in regulating the cholinergic antiinflammatory pathway after stroke, we performed targeting analysis of DE miRs and tRFs toward cholinergic transcripts (*SI Appendix*, *Expanded Methods*; for a complete list of cholinergic genes, see Dataset S2) via an in-house integrative database (*miRNeo*) (19) containing comprehensive transcription factor (TF)- and miR-targeting data, complemented by de novo prediction of tRF-targeting using TargetScan (20). A restrictive approach identified 131 miRs and 64 tRFs containing complementary motifs to at least five cholinergic-associated transcripts each (further termed "Cholino-miRs" and "Cholino-tRFs") (Fig. 1 *C* and *D* and *SI Appendix*, Fig. S2; for full lists see Datasets S3 and S4). Permutation targeting analysis showed an enrichment of cholinergic targets for both DE miRs (100,000 permutations, P = 0.0036) and DE tRFs (100,000 permutations, P = 2e-05). Further indicating nonrandom generation of these fragments, the tRFs identified in our dataset clustered into oligonucleotide families with high sequence homology via t-distributed stochastic neighbor embedding (t-SNE) (Fig. 1*E*), including families known to associate with Ago and suppress growth and proliferation via posttranscriptional down-regulation in lymphocytes (e.g., tRF-22-WE8SPOX52 from tRNAGly) (21)

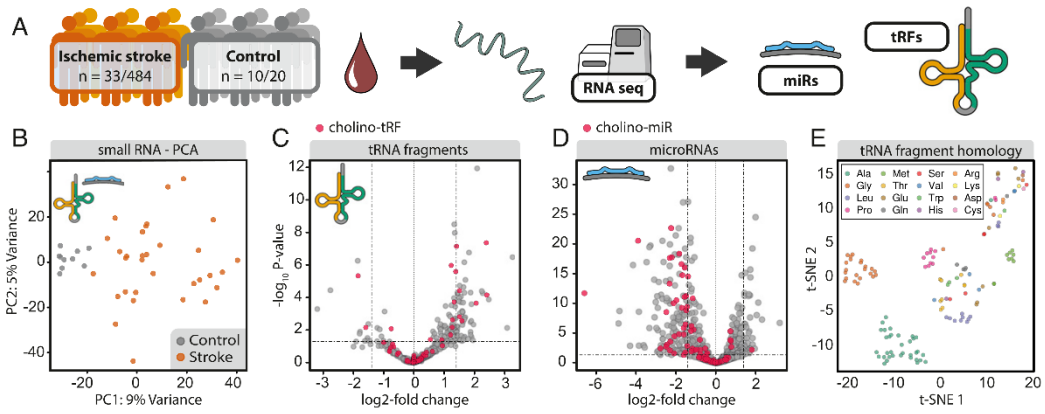

Fig. 1. Poststroke differential expression of small RNA species and tRF homology clustering. (*A*) Whole-blood total RNA samples were collected on day 2 poststroke from patients of the PREDICT cohort (NCT01079728) (16) and age-matched controls. (*B*) PCA of DE tRFs/miRs in patients' blood separated stroke and control samples. (*C*) Volcano plot of DE tRFs from stroke patients and controls (horizontal line at adjusted P = 0.05) showing up-regulation of most DE tRFs. (*D*) Volcano plot of DE miRs shows predominant down-regulation in stroke patients compared with controls (horizontal line at adjusted P = 0.05). Red dots in *C* and *D* reflect Cholino-tRFs and Cholino-miRs, respectively. (*E*) t-SNE visualization of tRF homology based on pairwise alignment scores of sequences of all detected tRFs shows grouped tRFs of several specific amino acid origins.

and metastatic cancer cells (tRF-18-HR0VX6D2 from tRNA-Leu) (22). This supported our prediction that the concomitant elevation of tRF levels and decline of miR levels in poststroke blood could contribute to the poststroke changes in cholinergic signaling pathways.

To further challenge our findings, we validated the expression levels of prominently DE tRFs identified by RNA-seq in a separate cohort of PREDICT patients (16). Standard qPCR techniques cannot distinguish between the full-length tRNA molecules and their 3′-tRF cleavage products. Therefore, to experimentally validate tRF changes (Fig. 2*A*), we implemented an electrophoresis size selection-based strategy followed by cDNA synthesis from the selected small RNAs and qRT-PCR (maximum 25 nt) (Fig. 2*B*). This procedure validated the top six up-regulated tRFs identified in RNA-seq data (tRF-22-WEKSPM852, tRF-18-8R6546D2, tRF-18-HR0VX6D2, tRF-18-8R6Q46D2, tRF-22-8EKSP1852, and tRF-22-WE8SPOX52, according to count-change) (Fig. 2 *B* and *C* and *SI Appendix, Expanded Methods*) and demonstrated significant increases accompanied by higher variability in the blood levels of these tRFs in poststroke patients compared to controls.

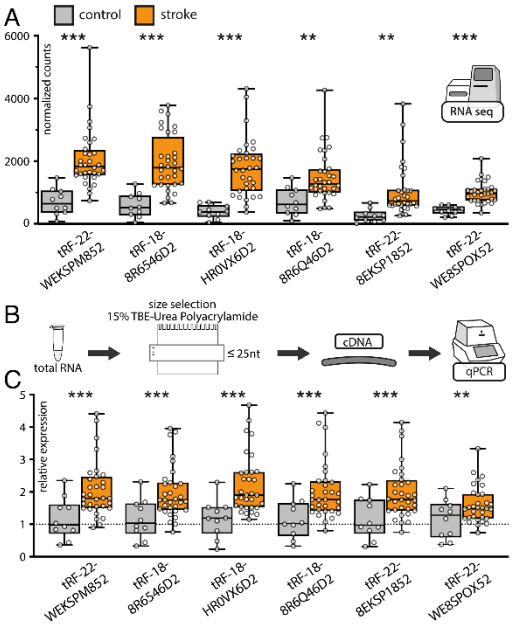

Fig. 2. qRT-PCR validation of the top six up-regulated tRFs in PREDICT stroke patients following size selection for small RNA. (*A*) RNA-seq counts normalized to the size of the library [using DESeq2 (23)] of the top six up-regulated tRFs (from left to right). Asterisks indicate adjusted *P* values of Wald test via DESeq2, $^{**}P < 0.01$, $^{***}P < 0.001$; shown are box-plots with whiskers minimum to maximum. (*B*) Size-selection workflow for validations in a separate subgroup of PREDICT stroke patients ($n = 32$) using the same control group ($n = 10$). (*C*) qRT-PCR validations using normalized expression (hsa-miR-30d-5p, hsa-let7d-5p, hsa-miR-106b-3p, and hsa-miR-3615 served as housekeeping transcripts) (*SI Appendix, Expanded Methods*), relative to the control group (line at mean normalized expression for the control group = 1) confirmed up-regulation of top six DE tRFs identified in RNA-seq, one-way ANOVA, $^{**}P < 0.01$, $^{***}P < 0.001$, box-plots with whiskers minimum to maximum.

Stroke-Perturbed Whole-Blood tRFs Are Biased toward Cellular Blood Compartments. To clarify the distribution of stroke-perturbed tRFs among the immunologically relevant blood cell types, we mined an RNA-seq dataset comprising sorted cell populations collected from healthy volunteers: $CD4^+$ T helper cells, $CD8^+$ T cytotoxic cells, $CD56^+$ NK cells, $CD19^+$ B cells, $CD14^+$ monocytes, $CD15^+$ neutrophils, $CD235a^+$ erythrocytes, serum, exosomes, and whole blood (450 samples in total) (24) (Fig. 3*A*). Predicting that log-normal distribution of the counts in different samples would point toward biological significance, we categorized all tRFs found in this dataset into present/absent in a specific blood compartment (without introducing a limit for counts) (*Materials and Methods* and Fig. 3*B*). Two main clusters of specific blood compartments could be identified based on their specific tRF profile: 1) monocytes, B-, T-, and NK cells; 2) neutrophils, whole blood, serum, exosomes, and erythrocytes (*SI Appendix*, Fig. S3). Furthermore, we distinguished eight tRF subclusters, based on the presence/absence of specific tRFs in blood compartments (Fig. 3*C*), with cluster four comprising molecules expressed specifically in monocytes, B-, T-, and NK cells, and cluster seven consisting of tRFs expressed only in monocytes.

Based on this methodology, we conducted a census of small RNA species found intra- vs. extracellularly: We detected 1,624 distinct intracellular tRFs but only 93 extracellular tRFs; 149 in whole blood, but 1,417 in $CD14^+$ monocytes alone. Similarly, we detected 559 distinct intracellular miRs but 145 extracellular miRs, 475 in monocytes alone, and 331 in whole blood. Using the presence/absence measure for analyzing the poststroke DE tRFs (Fig. 3*D* and *SI Appendix*, Fig. S4 for the top 20 stroke DE tRFs), we detected 77 DE tRFs from the PREDICT dataset as expressed in immune cells (Fig. 3*E*; for a detailed list of tRFs and affiliated clusters, see Dataset S5), including 10 Cholino-tRFs. Notably, tRFs previously shown to function posttranscriptionally in a miR-like manner [e.g., tRF-22-WE8SPOX52 from tRNAGly (21) and tRF-18-HR0VX6D2 from tRNALeu, alias hsa-miR-1280 (22)] segregated into whole blood, monocyte, T-, B-, and NK-cell compartments rather than into erythrocyte, serum, or exosome compartments. Thus, the poststroke-modified tRFs may be functionally involved in regulating the leukocytic poststroke response.

$CD14^+$ Monocytes Show Highest Cholinergic-Related Transcriptional Repertoire. The enrichment of DE Cholino-miRs and Cholino-tRFs identified in the PREDICT dataset and the contribution of the cholinergic antiinflammatory pathway to peripheral immunosuppression called for pinpointing the immune compartments in which these small RNAs might affect poststroke immune suppression. Analysis of long RNA regulatory circuits (25) specific to blood-borne leukocytes (Fig. 4*A*) identified $CD14^+$ monocytes as the main cell type expressing cholinergic core and receptor genes (Fig. 4*B* and Dataset S2). To confirm the relevance of this effect, we performed long RNA-seq in blood samples from 20 stroke patients from the PREDICT study and 4 controls. This showed 204 up-regulated and 490 down-regulated long RNA transcripts. Gene ontology (GO) enrichment analyses of the most implicated genes yielded highly specific terms relevant to innate immunity, vascular processes, and cholinergic links (Fig. 4*C*; for a list of all significant terms, see *SI Appendix*, Table S1). More specifically, terms linked to innate immune processes in poststroke blood involved responses to lipopolysaccharide (LPS) mediated by interferons and other cytokines (Fig. 4*C*, *Left*); vascular processes comprised platelet activation and degranulation, control of cell–cell adhesion, and regulation of angiogenesis (Fig. 4*C*, *Right*). Intriguingly, differentially regulated genes also showed involvement in response to organophosphorus agents, which are known acetylcholinesterase (AChE) inhibitors, supporting a cholinergic participation.

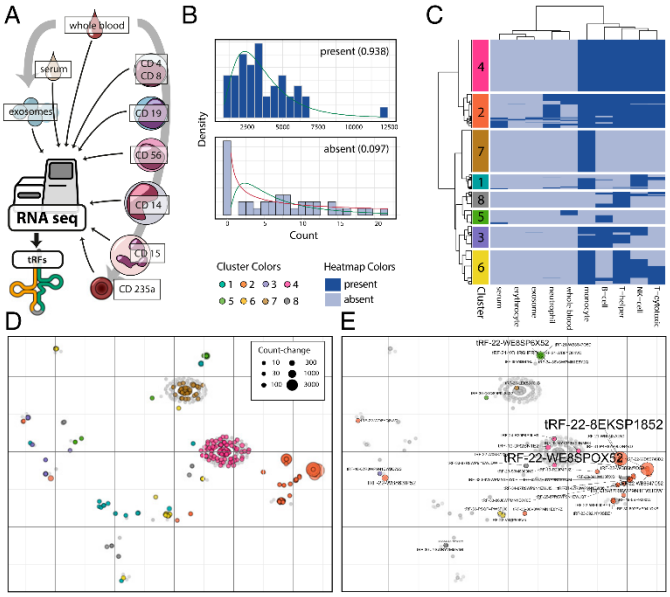

Fig. 3. Immune cell tRF expression clustering and cell type-specific analysis. (*A*) Analysis of RNA-seq datasets from T lymphocytes (CD4$^+$ T helper cells and CD8$^+$ T cytotoxic cells), B lymphocytes (CD19$^+$), NK cells (CD56$^+$), monocytes (CD14$^+$), neutrophils (CD15$^+$), erythrocytes (CD235a$^+$), serum, exosomes, and whole blood (24) yielded a blood tRF profile. (*B*) Definition of presence/absence of small RNAs in these blood compartments via statistical assertion of log-normal count distribution (values between 0 and 1, closer to 1: present). (*C*) Detailed analysis of identified tRFs found eight subclusters based on cell types expressing specific molecules. (*D*) t-SNE of all found tRFs represented by gray dots, DE tRFs identified in the PREDICT study are marked with cluster-specific color. (*E*) t-SNE of all tRFs found, Cholino-tRFs identified in the PREDICT study are marked with cluster-specific color.

Stroke Leads to Perturbation of miRNA Regulatory Networks. Notably, miRs up-regulated after stroke both appear in smaller numbers compared to down-regulated miRs and possess significantly fewer gene targets per individual miR [via *miRNeo*, mean (up vs. down) 463 vs. 804, median 266 vs. 717, one-way ANOVA $P = 2.1e\text{-}07$, $F(1, 352) = 28.06$]. To unravel target genes of these two miR populations, we performed gene target enrichment via permutation inside *miRNeo* (10,000 permutations). Significantly enriched gene targets (permutation $P < 0.05$) were subjected to GO analyses and visualized in a t-SNE projection, yielding 13 clusters of related terms, indicating most-affected pathways (Fig. 5*A* and *SI Appendix*, Fig. S5). Within each cluster, we determined the most relevant genes via hypergeometric enrichment (Fisher's exact test). Ranking of the clusters by the absolute number of enriched genes (Benjamini–Hochberg adjusted $P < 0.05$) revealed the putative biological processes that were most influenced by the miR perturbation following ischemic stroke in our patients (Fig. 5*B*).

The significantly derepressed cluster no. 6 (84 enriched genes) pointed toward perturbation of pathways involved in responses to hypoxia (GO:0036293, $P = 0.008$) and drugs (GO:0042493, $P = 0.035$), including antibiotics (GO:0071236, $P = 0.013$), glucocorticoids (GO:0051384, $P = 0.007$), and the cholinesterase-blocking organophosphorus agents (GO:0046683, $P = 0.019$), which reinforced the notion of cholinergic participation. Cross-check of enriched genes via DAVID (26) confirmed a role of cluster no. 6 in hypoxia (GO:0071456, $P = 8.3e\text{-}13$), drug response (GO:0042493, 5.4e-10), and the cholinergic synapse (Kyoto Encyclopedia of Genes and Genomes pathway 04725, $P = 0.006$). Cluster no. 8 (with second-most 58 enriched genes) highlighted perturbed transmembrane ion conductivity, particularly in regulation of cardiac muscle cell action (GO:0098901, $P = 0.044$) and negative regulation of blood circulation (GO:1903523, $P = 0.016$). DAVID analysis confirmed involvement in "regulation of cardiac muscle contraction by the release of sequestered calcium ion" (GO:0010881, $P = 2.1e\text{-}15$) and regulation of heart rate (GO:0002027, $P = 1.2e\text{-}07$). The subsequent clusters indicate further involvement in nerve cell regulatory processes (cluster no. 4), regulation of gene silencing by miRNA (cluster no. 1), and humoral immunity via IL-1 and IL-6 (cluster no. 7) (*SI Appendix*, Fig. S5). The entire list of clusters and gene enrichments is available in Dataset S6.

tRFs May Suppress Inflammation and Cholinergic-Associated TFs Alone or in Cooperation with miRs. Cellular responses to different stimuli are coordinated by cell type-specific transcriptional regulatory circuits. To facilitate understanding of the role of miRs and tRFs in regulating the transcriptional state of CD14$^+$ monocytes after stroke, we generated a monocyte-specific transcriptional interaction network of small RNAs targeting TFs (via *miRNeo*) (19), combined with differential expression of long and small RNAs from the PREDICT cohort. The gradually divergent targeting of these TFs by miRs and tRFs implied largely separate domains of regulation by these small RNA species (Fig. 5*C*). This notion was topologically strengthened by the fact that the force-directed network of all TFs active in CD14$^+$ monocytes self-segregated to form two distinct clusters of TFs, which were primarily targeted either by miRs or tRFs, including numerous TFs DE in stroke patient blood (Fig. 5 *D* and *E*). Among the implied TFs are proteins known for their influence on cholinergic genes, as well as their involvement in inflammation, such as STAT1 or KLF4 (27, 28). Notably, eight DE TFs were not

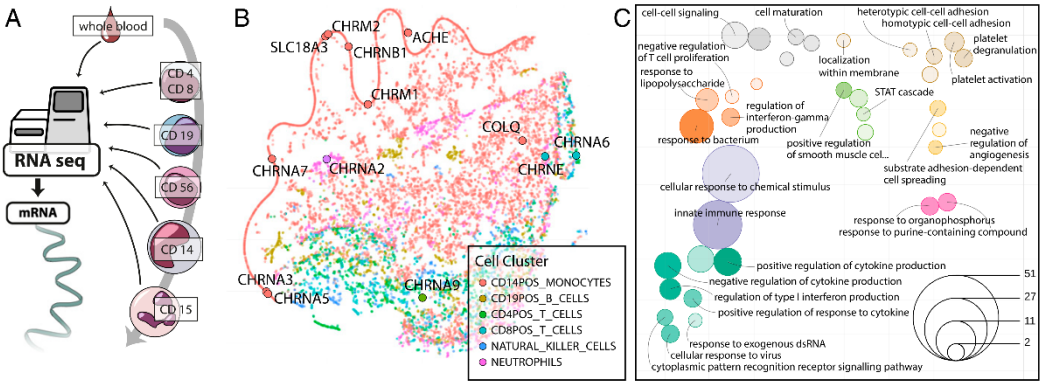

Fig. 4. Immune cell gene-expression clustering and long RNA pathways perturbed in stroke blood. (*A*) Published cell type-specific long RNA profiles (25) were used to visualize transcriptomes of T lymphocytes (CD4$^+$ T helper cells and CD8$^+$ T cytotoxic cells), B lymphocytes (CD19$^+$), NK cells (CD56$^+$), monocytes (CD14$^+$), and neutrophils (CD15$^+$). (*B*) t-SNE visualization of 15,032 genes on the basis of their expression in blood-borne immune cells extrapolated from transcriptional activities in regulatory circuits (25). Genes are colored by the cell type in which their expression was highest. Cholinergic core and receptor genes were mainly found in the CD14$^+$ monocytic compartment. (*C*) Enrichment of poststroke DE genes (log2FC > 1.4) in circulation- and immunity-related pathways, presented as t-SNE of GO terms by their shared genes (*SI Appendix, Expanded Methods*); color denotes t-SNE cluster, size denotes number of significant genes in term; deeper color indicates lower enrichment *P* value (all $P < 0.05$). Distance between terms indicates the number of shared genes between the GO terms, closer meaning more shared genes.

predicted to be targeted by any miR or tRF present in CD14$^+$ monocytes.

Stroke-Induced tRFs Show Evolutionarily Conserved Participation in Macrophage/Monocyte Responses to Inflammatory Stimuli. To test if the stroke-induced tRFs are involved in the inflammatory response of monocytes and macrophages, we subjected murine RAW 264.7 cells to LPS stimulation with or without dexamethasone suppression of their inflammatory reactions (Fig. 6*A*). By 18 h after LPS stimulation, qRT-PCR analysis after size-selection (for ≤50-nt fragments) detected pronounced up-regulation of the top six poststroke up-regulated tRFs (Fig. 6*B*). Moreover, dexamethasone suppression of the LPS response led to down-regulation of those tRFs, along with a diminished inflammatory response (*SI Appendix*, Fig. S6). Predicted targets of these molecules comprise members of mitogen-activated protein kinases (MAPK) and TNF receptor-associated factors (Dataset S7), further pointing toward their regulatory role in response to inflammatory stimuli. Notably, one of the top six stroke-perturbed tRFs, tRF-22-WE8SPOX52, is complementary to the 3′UTR sequence of murine Z-DNA binding protein Zbp1 and therefore a predicted regulator of the Zbp1 transcript and its immune system activity (Fig. 6*C*). To challenge the functional activity of tRF-22-WE8SPOX52 in murine RAW 264.7 macrophages, we overexpressed this tRF using single-stranded RNA (ssRNA) mimics (Fig. 6*D* and *SI Appendix*, Fig. S7), which significantly reduced the expression of its Zbp1 target compared to negative control, as quantified by long RNA-seq (Fig. 6*E*) and validated by qRT-PCR in an independent experiment (Fig. 6*F*).

Finally, we aimed to validate the functional implications of these findings in primary human cells. Therefore, we performed LPS stimulation experiments in magnetic-activated cell-sorted (MACS) CD14$^+$ monocytes from healthy volunteers and collected the cells at 6, 12, and 18 h after LPS addition (Fig. 6 *G* and *H* and *SI Appendix*, Fig. S8 *A* and *B* for 6- and 18-h timepoints). To further challenge the cholinergic link, we used nicotine as an immunosuppressive agent (*SI Appendix*, Fig. S8*C*) (29). LPS-stimulated primary CD14$^+$ cells presented significant up-regulation of four of the six stroke-induced tRFs at 12 h, an effect that was augmented by the addition of nicotine. Interestingly, at 18 h the tRF levels in the LPS + nicotine group were comparable to those of nonstimulated cells (*SI Appendix*, Fig. S8*B*). Together, these findings demonstrate evolutionarily conserved and cholinergic-regulated increases of stroke-induced tRFs under proinflammatory insults.

Discussion

To date, few studies have simultaneously assessed the joint impact of blood miR and tRF changes in human disease. Here we have discovered a stroke-induced decline of miRs and concomitant elevation of tRFs in whole blood, and demonstrated that this shift may be associated with the poststroke cholinergic blockade of immune function. To validate our RNA-seq findings of tRFs in a way that circumvents the ambiguous detection of full-length tRNA, we developed and used a size selection-based qRT-PCR test in an independent cohort of patients. Mining transcriptomic datasets identified CD14$^+$ monocytes as likely pivotal in the cholinergic control of immunity, demonstrated that the stroke-induced tRFs may target specific monocytic TFs, and showed that at least some of those tRFs may actively control processes linked to inflammatory responses. Moreover, several of the stroke-induced tRFs were also induced in LPS-exposed murine macrophages and in human CD14$^+$ primary cells and showed time-dependent nicotine- and dexamethasone-induced up-regulation/suppression, supporting the notion that the elevation of tRFs is an evolutionarily conserved response mechanism. Overexpression of tRF-22-WE8SPOX52 using ssRNA mimics led to the down-regulation of its Zbp1 target, which is involved in regulating inflammatory responses. This concept of integrated fine-tuning of poststroke immune responses opens new venues for stroke diagnostics and therapeutics.

The cholinergic antiinflammatory reflex plays a substantial role in regulating peripheral immune responses after CNS injury, along with the HPA axis and sympathetic signaling (3). Excessive cholinergic responses suppress pulmonary innate immunity, including macrophage and alveolar epithelial cell responses; this may facilitate the development of pneumonia (30), a major factor of nonrecovery (31). However, while reduced AChE

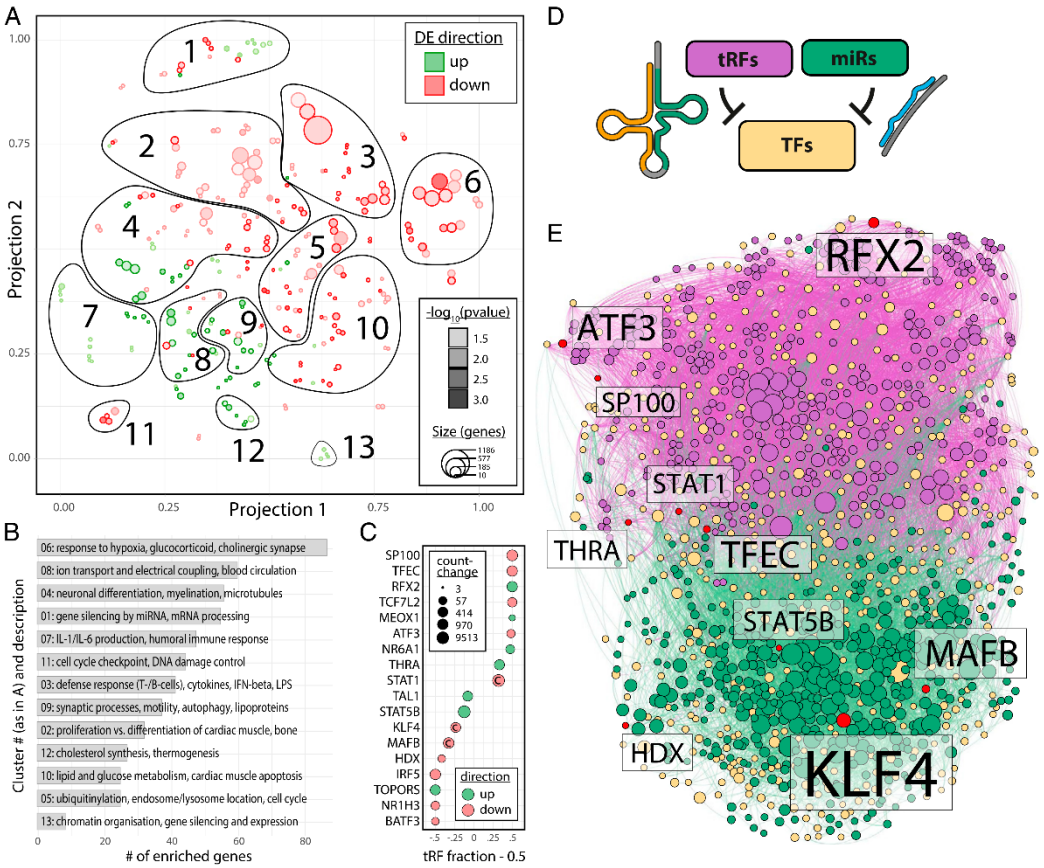

Fig. 5. GO enrichment of miR targets and perturbed pathways; divergent influence of miRs and tRFs in CD14⁺ TF regulatory circuits. (*A*) t-SNE visualization of GO terms enriched in the targets of miRs perturbed by stroke, performed separately for positively (green) and negatively (red) perturbed miRs, segregated into 13 functional clusters. Size of circles represents the number of genes in the respective GO term; depth of color represents enrichment *P* value (all $P < 0.05$). (*B*) Bar graph of clusters identified in *A* ordered by the number of enriched genes (Fisher's exact test, Benjamini–Hochberg adjusted $P < 0.05$) shows most pertinent processes with miR involvement. (*C*) The top 18 DE TFs in stroke patients' blood present a gradient of targeting by miRs and/or tRFs (left = 100% miR targeting, right = 100% tRF targeting; value shown as "tRF fraction − 0.5" to center on 50/50 regulation by miRs and tRFs). Size of points and color denote absolute count-change and direction of differential regulation, respectively. "C" marks TFs targeting cholinergic core or receptor genes. (*D*) Small RNA targeting of TFs active in CD14⁺ cells was analyzed using *miRNeo* (19). (*E*) Force-directed network of all TFs active in CD14⁺ monocytes self-segregates to form largely distinct TF clusters targeted by DE tRFs and miRs in stroke patients' blood. Yellow = TF, red = TF DE in stroke patients' blood, green = miR, purple = tRF. Size of node denotes activity toward targets.

activities in poststroke patients' serum associate with poor survival (32), stroke-induced immunosuppression may be brain-protective (2), calling for caution when considering therapeutic boosting of immune reaction in the periphery to limit infections. Therefore, an in-depth understanding and characterization of the molecular regulators of immune responses and the cholinergic pathway after CNS-injury is of utmost importance at both the system and mechanism levels.

System-Level Perturbations Associated with Ischemic Stroke. We identified CD14⁺ monocytes to be the most likely immune cell subpopulation for a transcriptional cholinergic response. Monocytes play established roles in responses to stroke, including prolonged monocytosis, deactivation, and functional impairment of circulating monocytes/macrophages observed in experimental models (33) and human patients (34). Moreover, stroke leads to overproduction of $CD14^{++}/CD16^{-}$ (classical) and $CD14^{++}/CD16^{+}$ (intermediate) monocytes with simultaneous decrease in $CD14^{+}/CD16^{++}$ (nonclassical) monocytes, which correlates with stroke-associated infection (35). Relatedly, immune cells in general, and monocytes in particular appear to be enriched in specific small RNA species (compare Fig. 3*C* and ref. 36), and several of the most highly perturbed small RNAs are abundantly expressed in monocytes (compare *SI Appendix*, Fig. S4 and ref. 37).

Our in-depth analysis of the pathways targeted by perturbed miRs supports a tie between stroke-induced changes and a cholinergic response. Both the identified clusters as well as the

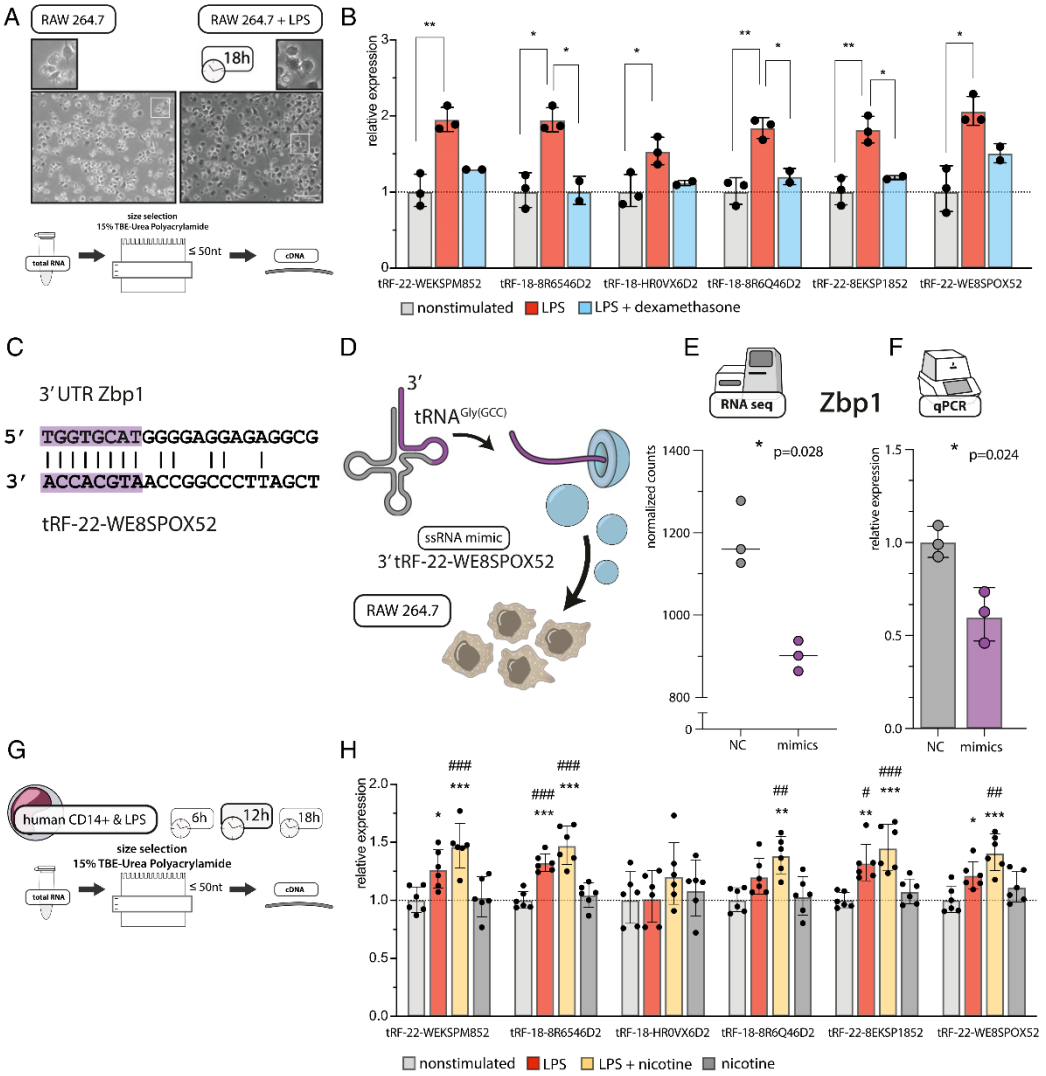

Fig. 6. tRF changes upon LPS stimulation of murine RAW 264.7 macrophages and human CD14$^+$ monocytes and tRF-mimic transfection. (*A*) LPS stimulation of RAW 264.7 murine macrophage cells induced clear morphologic changes within 18 h. Extracted RNA was subjected to size selection and cDNA synthesized from the ≤50-nt fraction alone. (Scale bar, 100 μm, magnification in the upper panel 2.5×) (*B*) LPS-stimulated RAW 264.7 cells show dexamethasone-suppressible elevated levels of poststroke induced tRFs. Normalized qRT-PCR values (using mmu-miR-30d-5p, mmu-let7d-5p as housekeeping transcripts) (*SI Appendix, Expanded Methods*), compared to unstimulated controls. Each dot represents two to four technical replicates, ANOVA with Tukey post hoc, $*P < 0.05$, $**P < 0.01$, bar graphs ±SD(lg). (*C*) Murine Zbp1 sequence carries an 8-nt-long fragment in the 3′UTR complementary to tRF-22-WE8SPOX52. (*D*) To test the miR-like mechanism of action, RAW 264.7 cells were transfected with ssRNA tRF-22-WE8SPOX mimics or negative control ssRNA, and RNA was extracted 24 h after transfection and subjected to polyA-selected RNA-seq (*E*) and qRT-PCR (*F*). (*E*) Long RNA-seq of cells transfected with ssRNA tRF-22-WE8SPOX52 mimics revealed significantly down-regulated expression of Z-DNA binding protein (Zbp1) as compared to negative control (NC). $*P < 0.05$, shown is adjusted *P* value of Wald test via DESeq2, bar graph ±SD. (*F*) qRT-PCR from an independent cell culture experiment confirmed the down-regulation of Zbp1 expression after ssRNA tRF-22-WE8SPOX52 mimic transfection (relative normalized expression using Gapdh as a housekeeping gene), $*P < 0.05$ one-way ANOVA, each dot represents a technical cell culture replicate, bar graph ±SD(lg). (*G*) MACS-sorted CD14$^+$ cells from healthy human donors were stimulated with LPS with or without addition of nicotine and collected 6, 12, and 18 h thereafter. Extracted RNA was subjected to size selection and cDNA synthesized from the ≤50-nt fraction. Timepoints 6 h and 18 h are shown in *SI Appendix*, Fig. S8. (*H*) At 12 h after LPS stimulation, human monocytes exhibited up-regulation of poststroke induced tRFs as compared to unstimulated controls or cells treated with nicotine alone. This reaction was boosted by the addition of nicotine. Shown is relative expression (hsa-miR-30d and hsa-let7d-5p were used as housekeeping transcripts) (*SI Appendix, Expanded Methods*) normalized to the nonstimulated group. Each dot represents one donor. ANOVA with Tukey post hoc, $*P < 0.05$, $**P < 0.01$, $***P < 0.001$ vs. nonstimulated cells; $^{\#}P < 0.05$, $^{\#\#}P < 0.01$, $^{\#\#\#}P < 0.001$ vs. cells upon addition of nicotine, bar graphs ±SD(lg).

genes enriched in each cluster may be further investigated for identifying the diverse mechanisms involved. A recent whole-blood microarray survey identified 15 miRs, 11 of which were replicated in our study, to be suppressed within less than 72 h in intracerebral hemorrhage patients compared to controls (38). Those miRs pointed toward the same processes we found, including inflammation and humoral immunity via JAK/STAT-activating cytokines, vascular integrity, and the cellular immune response (38).

Stroke is a sudden incident with rapid onset and drastic systemic changes within a short time frame. In the response to such immunologic emergencies, translational control is an important tool (39). That tRFs may be rapidly produced by regulated nuclease cleavage of preexisting tRNAs in a "burst-like" fashion makes them particularly appropriate for handling acute situations. Recent reports demonstrate production of 3′-tRFs by specific nucleases, and 3′- and 5′-tRNALeu fragments were shown to regulate T cell activation (40). Furthermore, tRFs can perform different molecular roles, including Ago-mediated suppression of target genes carrying complementary sequence motifs (13). At least two of the stroke-induced tRFs up-regulated after LPS stimulation show miR-like function: tRF-22-WE8S-POX52 regulates B cell growth via suppressing the expression of Replication Protein A1 (RPA1) (21) and a 17-nt-long analog of tRF-18-HR0VX6D2 limits cancer cell proliferation by impacting the cholinergic-regulating Notch signaling pathway (22). Interestingly, hsa-miR-1260b, identified in our study and by others as perturbed poststroke (41), differs from tRF-18-HR0VX6D2 by only 1 nt at position 9 and an additional nucleotide at the 3′-end (*SI Appendix*, Fig. S9), which indicates that hsa-miR-1260b may actually be a tRF (42), and calls for further investigation.

Our study identified two main factors that may lead to an overall decrease in transcript regulation by miRs after stroke. First, the majority of miRs perturbed in our patient collective were down-regulated, and second, the down-regulated miRs possessed significantly more targets than the up-regulated ones. For many processes regulated by these miRs, the resultant effect will hence be de-repression of targeted genes (Fig. 5*A*). Additionally, we have identified a stark dichotomy between the target sets of miRs and tRFs, indicating much complementarity and only little cooperative overlap of affected transcripts between those two small RNA species (Fig. 5*E*). However, these changes may still lead to a homeostatic functional cooperation. In summary, the poststroke "changing of the guards" in the small RNA response may lead to preferential de-repression of miR targets and concomitant repression of tRF targets, and the de-repression of miR targets may be as pivotal for regulating the initial inflammatory response and subsequent peripheral immunosuppression as the tRF elevation we identified.

Kinetically, stroke is characterized by an initial inflammatory response followed by immunosuppression facilitated by, among others, the cholinergic antiinflammatory reflex (3). Therefore, the time-dependent elevation of tRFs and Cholino-tRFs in particular may offer new mechanisms of homeostatic fine-tuning in response to cerebral ischemia. Furthermore, not only the peripheral but also the central immune response at the site of the injury is of great importance for stroke prognosis. Brain injury triggers activation of microglia and infiltration of peripheral immune cells, including monocyte-derived macrophages, which accumulate at the lesion site 3 to 7 d after stroke (35). Experimental evidence highlights essential roles of these cells in CNS-repair processes and neuronal protection (43, 44), and our own studies indicate small RNA-regulated cross-talk between neuronal and immunological regulation by JAK/STAT-related mechanisms (19).

Our present study presents tRFs as potential players in regulating the poststroke inflammatory responses. For example, KLF4, identified as down-regulated in our sequencing dataset, is involved in controlling the macrophage response to LPS (28) and the differentiation of monocytes toward an inflammatory phenotype (45). Therefore, a decrease in miRs targeting this TF may contribute to proinflammatory monocytic response observed in the initial phase of stroke. Similarly, MAFB is essential in facilitating the clearance of damage-associated molecular patterns (DAMPs) in the ischemic brain and, consequently, limiting the inflammatory response while supporting recovery (46). MAFB de-repression in peripheral immune cells may be a mechanism supporting monocyte infiltration of the brain. Conversely, STAT1 and ATF3 may be preferentially repressed due to their targeting by tRFs. STAT1 is essential in IFN- and IL-6–mediated inflammatory response, and ATF3 is similarly induced by IFNs and contributes to STAT activity via inhibition of STAT-dephosphorylating phosphatases (47, 48). Additionally, ATF3 down-regulates AChE expression during stress (49). Whether these processes contribute to body homeostasis after the damaging event, or rather to pathologic derailment of immune function, requires detailed kinetic studies of circulating monocytes and brain-infiltrating monocyte-derived macrophages, with simultaneous profiling of short and long transcripts.

Mechanistic Implications of tRF Regulation after Ischemic Stroke. To gain new insight into the regulation of inflammation by stroke-induced tRFs, we quantified the top six perturbed tRFs in RAW 264.7 murine macrophages and primary LPS-stimulated $CD14^+$ human monocytes. Both cell types responded to LPS by up-regulation of these tRFs within 12 to 18 h. Interestingly, dexamethasone prevented or subsequently down-regulated the increased expression of tRFs in the RAW 264.7 cells. To further seek cholinergic links of these stroke-regulated tRFs, we used nicotine as an immunosuppressive stimulus in LPS-stimulated human $CD14^+$ cells. Monocytes and macrophages express the cholinergic nicotinic α7 receptor, which after binding of ACh down-regulates the production of inflammatory cytokines (e.g., TNF-α) (29). In human $CD14^+$ cells, the levels of the top six stroke-induced tRFs were transiently elevated by the addition of nicotine at the 12-h timepoint (back to baseline by 18-h post-stimulation). Thus, the elevated levels of blood tRFs 2 d after ischemic stroke may reflect potentiated cholinergic signaling, which remains to be investigated in the clinical setting.

In human patients, the stroke response in blood is cell type- and time-specific. For example, day 2 postischemia features a transient increase in STAT3 phosphorylation of monocyte subsets, which is also detected in patients after major surgery (50). Conversely, STAT3 signaling causes immune stimulation in monocytes but is linked to immunosuppression in monocytic myeloid-derived suppressor cells (50). Therefore, the biological activities of stroke-induced tRFs are very likely also cell type- and context-specific. Our ssRNA tRF-22-WE8SPOX52 mimic experiments further support tRF involvement in the posttranscriptional regulation of genes implicated in inflammatory responses. Zbp1, which was significantly down-regulated under tRF-22-WE8SPOX52 overexpression, is a DAMP-sensor that induces IFN responses, programmed cell death, and NLRP3 inflammasome formation (51). The ZBP1 protein has often been linked to the response to viral infections, but some studies point to its role in the reaction to bacterial pathogens, where it may be involved in the induction of necroptosis (51). Incidentally, the ZBP1 transcript is also down-regulated in our long RNA-seq of patient blood (log2FC = −1.7, adjusted $P = 0.001$); the exact nature of the interaction of tRF-22-WE8SPOX52 and ZBP1 should be subject of future studies.

Limitations. We hypothesized that the tRFs identified in our study are of cellular origin and therefore reanalyzed the small RNA-seq data provided by Juzenas et al. (24) (GSE100467). While some studies identified an enrichment of tRFs in exosomes (40),

our reanalysis found the tRFs mostly in the cellular blood compartments. Although the main immune populations are included in the analyzed dataset, it should be noted that the tRFs identified in our study may also originate from immune cells not sorted/sequenced by Juzenas et al. (24). Additionally, considering the different roles of specific immune subpopulations, identifying the specific source of tRFs and their roles in immune function should be the goal of further investigations. For example, monocyte subsets are differentially regulated after stroke, and since these cells all express the CD14 marker (35), a higher cellular resolution is called for. Furthermore, tRFs are induced upon cellular stress (52), such that the sorting procedure may affect their expression, and they may reside in extracellular compartments (15, 53), calling for testing the impact of sample processing, RNA isolation, and sequencing techniques on the detectability of tRFs. Additionally, a method for the direct comparison of miR and tRF levels in the same sequencing experiment will be important for discerning the true difference in detected counts after alignment, possibly via spike-in procedures. The currently maturing technology of single-cell sequencing is an obvious candidate for achieving the goals of higher cellular resolution along with avoiding stressors associated with sample preparation, but its shallow sequencing depth is still an issue.

Given the sex-related differences in cholinergic responses (19, 54), the molecular regulators of cholinergic signaling and immunity should be investigated in detail in both males and females. However, to increase the consistency of our results, we only included male stroke patients, which is a further limitation of this study. Interestingly, the overall impact of stroke is greater in women, as their higher life expectancy is linked to increased stroke incidence in older adults and they face worse recovery prospects (55). Last, but not least, tRFs may have functions other than their miR-like activities; for example, tRNALeu-CAG fragments facilitate translation and ribosome biogenesis (12), whereas tRNAGly-, tRNAGlu-, tRNAAsp-, and tRNATyr-derived tRFs displace RNA-binding proteins leading to mRNA destabilization (11). Therefore, potential functions of stroke-perturbed tRFs other than Ago-mediated suppression of translation should be further examined.

Conclusion

While the specific roles of tRFs in regulating local neuroinflammatory responses and functional modulation of specific peripheral monocyte subsets remain to be elucidated, our findings point toward tRFs/miRs as homeostatic regulators of post-stroke immune responses and potential biomarkers for increased infection risk in these patients. The cumulative role of tRFs and miRs as general postdamage mediators of CNS-immune communication thus calls for seeking small RNAs, and tRFs in particular, as involved in other traumatic pathologies, such as spinal cord injury, traumatic brain injury, concussion, as well as neuroinflammatory brain diseases.

Materials and Methods

Expanded methods can be found in *SI Appendix*.

Clinical Cohort. PREDICT was a prospective multicenter study with sites in Germany and Spain (https://www.clinicaltrials.gov/, NCT01079728) (16) that analyzed 484 acute ischemic stroke patients. Patients underwent daily screenings for stroke-associated pneumonia, dysphagia, and inflammation markers and their clinical outcome was recorded 3 mo poststroke. To exclude very severe cases of stroke, we only considered for sequencing samples from patients with modified Rankin Scale (mRS) values of 3 and below at discharge from the hospital, leaving $n = 240$ relevant cases. Blood was collected into RNA stabilizing tubes (Tempus Blood RNA tubes, Applied Biosystems) on each day of hospitalization. Blood samples collected on the second day were subjected to small and long RNA-seq, with time from stroke occurrence to blood withdrawal varying between 0.94 and 2.63 d (average: 1.98 d). Blood samples from age- and ethnicity-matched healthy controls were obtained at matched circadian time from donors (ZenBio). These samples were collected from an FDA Regulated Blood Bank. All procedures, polices, forms and consents used in the donor screening, collection and manufacturing process were submitted to the FDA for review and approval through the Prior Approval Supplement process described in 21 CFR 601.12(b) (ZenBio).

RNA Extraction, Quality Control, and Sequencing. RNA was extracted from 3 mL of whole blood of 484 PREDICT patients using a Tempus Spin RNA isolation kit (Invitrogen, Thermo Fisher Scientific). Presequencing Bioanalyzer 6000 (Agilent) tests showed high RNA quality (RIN values 7.9 to 9.9, median 8.8). Libraries constructed from 600 ng total RNA of 43 samples were subjected to small RNA-seq (NEBNext Multiplex Small RNA library prep set for Illumina, New England Biolabs), and 24 of the small RNA-seq samples served for PolyA-selected long mRNA sequencing (1,000 ng total RNA per sample, TruSeq RNA library preparation kit;Illumina). Sequencing (24 or 12 samples per flow cell for small and long RNAs, respectively) was performed on the Illumina NextSeq 500 platform at the Hebrew University's Center for Genomic Technologies.

Alignment and Count Table Generation of RNA-Seq Reads. Quality control was performed using FastQC, v0.11.2 (56); more details can be found in *SI Appendix, Expanded Methods*. Flexbar (with parameters "-q TAIL -qf Sanger -qw 4 -min-read-length 16") (57) served for adapter trimming and quality-based filtering of all raw reads. Long RNA was aligned to the human reference transcriptome (ENSEMBL GRCh38 release 79) using salmon (58) with default parameters. Small RNA was aligned to miRBase v21 using miRExpress 2.1.4 (59) with default parameters but skipping adapter trimming for miR expression, and to the tRNA transcriptome using the MINTmap pipeline (60) with default parameters for tRF expression (using only reads mapping exclusively to the tRNA space). Raw gene-expression data of small and long RNA-seq and technical covariates of all experiments are available via the National Center for Biotechnology Information Gene Expression Omnibus database (accession no. GSE158312) (61).

Size Selection for tRF Quantification. Standard qRT-PCR methods do not allow to distinguish between full-length tRNA molecules and 3′-tRFs. To exclude longer RNA species in the qRT-PCR quantifications, we performed RNA size selection on 15% TBE-Urea-Polyacrylamide gels, selecting only RNA molecules ≤25 nt for validations in the clinical cohort and ≤50 nt for the assessment of tRF expression in LPS-stimulated RAW 264.7 cells and human $CD14^+$ monocytes. A detailed description can be found in *SI Appendix, Expanded Methods*.

Analysis of the Presence/Absence of Specific tRFs in Blood Compartments. In descriptive analysis of small RNA expression, a threshold (e.g., at least five counts in at least 80% of samples) is often used to define presence or absence of small RNAs. However, since this definition relies heavily on sequencing depth, and depth can vary widely even in methodically robust sequencing experiments depending on a large number of variables, we defined our own test for descriptive analysis of the presence or absence of lowly expressed small RNAs in each of the sample types. Briefly, this definition comprises estimation of a log-normal distribution on the expression profile of the small RNA across all samples in the individual cell types, and a statistical test to refute the null hypothesis that the distribution is in fact log-normal. For each small RNA, the distribution mean and SD of the expression values per cell type were estimated using the *fitdist* function of the R/fitdistrplus package (62). The count distribution was then tested against a log-normal distribution with the estimated mean and SD via the R implementation of the Kolmogorov–Smirnov test, with a cutoff of 0.1. The small RNA was defined as present if the test failed to reject the null hypothesis (see *SI Appendix*, Fig. S4 for examples). The code implementation is available at https://github.com/slobentanzer/stroke-trf.

LPS Stimulation of Murine Macrophages. Murine RAW 264.7 cells (ATCC TIB-71) cultured in Dulbecco's Modified Eagle's Medium supplemented with 10% fetal calf serum, 1% penicillin-streptomycin-amphotericin B, and 1% L-glutamine (all reagents from Biological Industries) were collected using a cell scraper and stimulated with LPS (from *Escherichia coli* 0127:B8, Sigma Aldrich) following a modified protocol (63). Briefly, 2e05 cells were stimulated with 100 ng/mL LPS ± 0.5 μM dexamethasone per well (Sigma Aldrich) in 12-well cell culture plates. Cells were collected in Tri-Reagent (Sigma Aldrich) 18 h after LPS stimulation and RNA was isolated using miRNeasy kit (Qiagen). For the size selection, 1 μg of total RNA was used and cDNA was synthesized from 500 pg of size-selected RNA using qScript microRNA cDNA

Synthesis Kit (Quanta Biosciences) and following standard protocol (for further details, see *SI Appendix, Expanded Methods*). Data presented in the report is derived from three independent experiments (two of them with dexamethasone treatment) with two to four technical replicates in each group.

Transfection Experiments with tRF-22-WE8SPOX52 Mimics, RNA-Seq, and qRT-PCR. Transfections were performed using HiPerFect transfection agent (Qiagen) following a standard protocol for transfecting RAW 264.7 macrophages. Briefly, 2e05 RAW 264.7 cells per well were seeded in 24-well plates and transfected using 6 μL HiPerFect reagent per well and 50 nM final ssRNA tRF-mimics: /5PHOS/rArU rCrCrC rArCrC rGrCrU rGrCrC rAmCmC rA, using NC5 /5PHOS/rGrC rGrArC rUrArU rArCrG rCrGrC rArArU mAmUrG (both from IDT) as negative control. Cells were collected after 24 h following the transfection in Tri-Reagent (Sigma Aldrich) and total RNA isolated using the miRNeasy kit (Qiagen). Two separate experiments were performed: 1) 180 ng RNA was subjected to long RNA-seq (KAPA stranded mRNA-seq kit, Roche) and 2) Zbp1 levels were quantified by qRT-PCR (relative expression normalized to Gapdh) after cDNA synthesis (qScript Kit; Quanta Biosciences) from 100 ng RNA.

Isolation and Ex Vivo Stimulation of Human Monocytes. This study was approved by the ethics committees of the Charité-Universitätsmedizin Berlin (MG Cohort: EA1/281/10). Peripheral blood mononuclear cells were separated from whole-blood anticoagulated with heparin by density gradient centrifugation over Ficoll (Biocoll separating solution, Biochrom). Untouched monocytes were isolated by using a commercially available Pan Monocyte Isolation Kit (Miltenyi Biotec). Cells (2e06 cells/mL) were cultured in RPMI medium 1640 (VWR), supplemented with 1% penicillin-streptomycin (Biochrom), 2 mM L-glutamine (Biochrom), and 10% autologous serum and stimulated with LPS (1 ng/mL, 0127:B8; Sigma) in the presence or absence of nicotine (300 μM, Sigma) for 6, 12, and 18 h at 37 °C. Unstimulated monocytes and monocytes stimulated with nicotine served as controls. TNF-α concentration was measured in cell culture supernatant by using a commercially available DuoSet ELISA kit (R&D Systems). Cells were collected in Tri-Reagent (Sigma Aldrich) and RNA was isolated using miRNeasy kit (Qiagen). For the size selection, 600 ng of total RNA (or maximum loading volume of 20 μL) were used and cDNA was synthesized from 500 pg of size-selected RNA using qScript microRNA cDNA Synthesis Kit (Quanta Biosciences) and following standard protocol (for further details, see *SI Appendix, Expanded Methods*).

Statistical Analysis. Data analysis was performed using R (v4.0.2), the code is available at https://github.com/slobentanzer/stroke-trf (including code for analyses of qRT-PCR data) (64). False-discovery rate correction was applied whenever applicable. qRT-PCR data were analyzed using Bio-Rad CFX Maestro software (Bio-Rad, v4.1.2433.1219) and plotted in GraphPad Prism 8.0 (GraphPad Prism Software).

Data Availability. Code data have been deposited in GitHub (https://github.com/slobentanzer/stroke-trf) (64). RNA sequencing data reported in this paper have been deposited in the Gene Expression Omnibus database, (accession no. GSE158312) (61).

ACKNOWLEDGMENTS. We thank Dr. Simonas Juzenas (Saarbrücken) and Prof. Andreas Keller (Saarbrücken/Stanford) for their support concerning the blood compartments RNA-sequencing dataset, and Dr. Iftach Shaked (San Diego) for fruitful discussions. This study was supported by the European Research Council Advanced Award 321501; the Israel Science Foundation Grant 1016/18; the Israeli Ministry of Science, Technology and Space Grant No. 53140 (to H.S.); the German Research Foundation (Exc257, TR84, SFB/TRR167) (to A.M. and C.M.); the Leducq Foundation (19CVD01); and the Einstein Foundation, Berlin (A-2017-406) (to A.M. and H.S.). Further support was provided by a NeuroCure visiting fellowship (to H.S.), as well as by Edmond and Lily Safra Center of Brain Science (ELSC) postdoctoral fellowships (to S.S.-T and K.W.). K.W. is a Shimon Peres Post-doctoral Fellow at the ELSC and S.L. received an ELSC fellowship for visiting PhD students.

1. C. O. Johnson *et al.*; GBD 2016 Stroke Collaborators, Global, regional, and national burden of stroke, 1990-2016: A systematic analysis for the Global Burden of Disease Study 2016. *Lancet Neurol.* **18**, 439–458 (2019).
2. U. Dirnagl *et al.*, Stroke-induced immunodepression: Experimental evidence and clinical relevance. *Stroke* **38** (suppl.(2), 770–773 (2007).
3. C. Meisel, J. M. Schwab, K. Prass, A. Meisel, U. Dirnagl, Central nervous system injury-induced immune deficiency syndrome. *Nat. Rev. Neurosci.* **6**, 775–786 (2005).
4. M. Rosas-Ballina *et al.*, Acetylcholine-synthesizing T cells relay neural signals in a vagus nerve circuit. *Science* **334**, 98–101 (2011).
5. L. V. Borovikova *et al.*, Vagus nerve stimulation attenuates the systemic inflammatory response to endotoxin. *Nature* **405**, 458–462 (2000).
6. I. Shaked *et al.*, MicroRNA-132 potentiates cholinergic anti-inflammatory signaling by targeting acetylcholinesterase. *Immunity* **31**, 965–973 (2009).
7. H. Soreq, Checks and balances on cholinergic signaling in brain and body function. *Trends Neurosci.* **38**, 448–458 (2015).
8. A. G. Torres, O. Reina, C. Stephan-Otto Attolini, L. Ribas de Pouplana, Differential expression of human tRNA genes drives the abundance of tRNA-derived fragments. *Proc. Natl. Acad. Sci. U.S.A.* **116**, 8451–8456 (2019).
9. S. Yamasaki, P. Ivanov, G. F. Hu, P. Anderson, Angiogenin cleaves tRNA and promotes stress-induced translational repression. *J. Cell Biol.* **185**, 35–42 (2009).
10. L. Huang, H. Guo, M. Cheng, Y. Zhao, X. Jin, The kinetic change of the serum angiogenin level in patients with acute cerebral infarction. *Eur. Neurol.* **58**, 224–227 (2007).
11. H. Goodarzi *et al.*, Endogenous tRNA-derived fragments suppress breast cancer progression via YBX1 displacement. *Cell* **161**, 790–802 (2015).
12. H. K. Kim *et al.*, A transfer-RNA-derived small RNA regulates ribosome biogenesis. *Nature* **552**, 57–62 (2017).
13. P. Kumar, J. Anaya, S. B. Mudunuri, A. Dutta, Meta-analysis of tRNA derived RNA fragments reveals that they are evolutionarily conserved and associate with AGO proteins to recognize specific RNA targets. *BMC Biol.* **12**, 78 (2014).
14. Q. Li *et al.*, tRNA-derived small non-coding RNAs in response to ischemia inhibit angiogenesis. *Sci. Rep.* **6**, 20850 (2016).
15. M. C. Hogg *et al.*, Elevation in plasma tRNA fragments precede seizures in human epilepsy. *J. Clin. Invest.* **129**, 2946–2951 (2019).
16. S. Hoffmann *et al.*; PREDICT Investigators, Stroke-induced immunodepression and dysphagia independently predict stroke-associated pneumonia—The PREDICT study. *J. Cereb. Blood Flow Metab.* **37**, 3671–3682 (2017).
17. P. Li *et al.*, Identification of circulating microRNAs as potential biomarkers for detecting acute ischemic stroke. *Cell. Mol. Neurobiol.* **35**, 433–447 (2015).
18. G. C. Jickling *et al.*, microRNA expression in peripheral blood cells following acute ischemic stroke and their predicted gene targets. *PLoS One* **9**, e99283 (2014).
19. S. Lobentanzer, G. Hanin, J. Klein, H. Soreq, Integrative transcriptomics reveals sexually dimorphic control of the cholinergic/neurokine interface in schizophrenia and bipolar disorder. *Cell Rep.* **29**, 764–777.e5 (2019).
20. V. Agarwal, G. W. Bell, J. W. Nam, D. P. Bartel, Predicting effective microRNA target sites in mammalian mRNAs. *eLife* **4**, e05005 (2015).
21. R. L. Maute *et al.*, tRNA-derived microRNA modulates proliferation and the DNA damage response and is down-regulated in B cell lymphoma. *Proc. Natl. Acad. Sci. U.S.A.* **110**, 1404–1409 (2013).
22. B. Huang, *et al.*, tRF/miR-1280 suppresses stem cell-like cells and metastasis in colorectal cancer. *Cancer Res.* **77**, 3194–3206 (2017).
23. M. I. Love, W. Huber, S. Anders, Moderated estimation of fold change and dispersion for RNA-seq data with DESeq2. *Genome Biol.* **15**, 550 (2014).
24. S. Juzenas *et al.*, A comprehensive, cell specific microRNA catalogue of human peripheral blood. *Nucleic Acids Res.* **45**, 9290–9301 (2017).
25. D. Marbach *et al.*, Tissue-specific regulatory circuits reveal variable modular perturbations across complex diseases. *Nat. Methods* **13**, 366–370 (2016).
26. W. Huang, B. T. Sherman, R. A. Lempicki, Systematic and integrative analysis of large gene lists using DAVID bioinformatics resources. *Nat. Protoc.* **4**, 44–57 (2009).
27. K. Shuai *et al.*, Interferon activation of the transcription factor Stat91 involves dimerization through SH2-phosphotyrosyl peptide interactions. *Cell* **76**, 821–828 (1994).
28. M. W. Feinberg *et al.*, Kruppel-like factor 4 is a mediator of proinflammatory signaling in macrophages. *J. Biol. Chem.* **280**, 38247–38258 (2005).
29. T. Fujii *et al.*, Expression and function of the cholinergic system in immune cells. *Front. Immunol.* **8**, 1085 (2017).
30. O. Engel *et al.*, Cholinergic pathway suppresses pulmonary innate immunity facilitating pneumonia after stroke. *Stroke* **46**, 3232–3240 (2015).
31. O. Finlayson *et al.*, Canadian Stroke Network; Stroke Outcome Research Canada (SORCan) Working Group, Risk factors, inpatient care, and outcomes of pneumonia after ischemic stroke. *Neurology* **77**, 1338–1345 (2011).
32. E. Ben Assayag *et al.*, Serum cholinesterase activities distinguish between stroke patients and controls and predict 12-month mortality. *Mol. Med.* **16**, 278–286 (2010).
33. L. McCulloch, A. Alfieri, B. W. McColl, Experimental stroke differentially affects discrete subpopulations of splenic macrophages. *Front. Immunol.* **9**, 1108 (2018).
34. X. Urra *et al.*, Monocyte subtypes predict clinical course and prognosis in human stroke. *J. Cereb. Blood Flow Metab.* **29**, 994–1002 (2009).
35. A. ElAli, N. Jean LeBlanc, The role of monocytes in ischemic stroke pathobiology: New avenues to explore. *Front. Aging Neurosci.* **8**, 29 (2016).
36. P. Leidinger, C. Backes, B. Meder, E. Meese, A. Keller, The human miRNA repertoire of different blood compounds. *BMC Genomics* **15**, 474 (2014).
37. S. Lobentanzer, "Small RNA dynamics in cholinergic systems," PhD dissertation, Goethe University, Frankfurt, Germany (2020).
38. X. Cheng *et al.*, MicroRNA and their target mRNAs change expression in whole blood of patients after intracerebral hemorrhage. *J. Cereb. Blood Flow Metab.* **40**, 775–786 (2019).
39. C. A. Piccirillo, E. Bjur, I. Topisirovic, N. Sonenberg, O. Larsson, Translational control of immune responses: From transcripts to translatomes. *Nat. Immunol.* **15**, 503–511 (2014).

40. N.-T. Chiou, R. Kageyama, K. M. Ansel, Selective export into extracellular vesicles and function of tRNA fragments during T cell activation. *Cell Rep.* **25**, 3356–3370.e4 (2018).
41. J. R. Tan *et al.*, Blood microRNAs in low or no risk ischemic stroke patients. *Int. J. Mol. Sci.* **14**, 2072–2084 (2013).
42. N. C. T. Schopman, S. Heynen, J. Haasnoot, B. Berkhout, A miRNA-tRNA mix-up: tRNA origin of proposed miRNA. *RNA Biol.* **7**, 573–576 (2010).
43. S. Wattananit *et al.*, Monocyte-derived macrophages contribute to spontaneous long-term functional recovery after stroke in mice. *J. Neurosci.* **36**, 4182–4195 (2016).
44. C. Cserép *et al.*, Microglia monitor and protect neuronal function through specialized somatic purinergic junctions. *Science* **367**, 528–537 (2020).
45. M. W. Feinberg *et al.*, The Kruppel-like factor KLF4 is a critical regulator of monocyte differentiation. *EMBO J.* **26**, 4138–4148 (2007).
46. T. Shichita *et al.*, MAFB prevents excess inflammation after ischemic stroke by accelerating clearance of damage signals through MSR1. *Nat. Med.* **23**, 723–732 (2017).
47. L. I. Labzin *et al.*, ATF3 is a key regulator of macrophage IFN responses. *J. Immunol.* **195**, 4446–4455 (2015).
48. D. Glal *et al.*, ATF3 sustains IL-22-induced STAT3 phosphorylation to maintain mucosal immunity through inhibiting phosphatases. *Front. Immunol.* **9**, 2522 (2018).
49. R. Heinrich *et al.*, ATF3 regulates the expression of AChE during stress. *Front. Mol. Neurosci.* **11**, 88 (2018).
50. A. S. Tsai *et al.*, A year-long immune profile of the systemic response in acute stroke survivors. *Brain* **142**, 978–991 (2019).
51. T. Kuriakose, T. D. Kanneganti, ZBP1: Innate sensor regulating cell death and inflammation. *Trends Immunol.* **39**, 123–134 (2018).
52. D. M. Thompson, R. Parker, Stressing out over tRNA cleavage. *Cell* **138**, 215–219 (2009).
53. P. M. Godoy *et al.*, Large differences in small RNA composition between human biofluids. *Cell Rep.* **25**, 1346–1358 (2018).
54. S. Shenhar-Tsarfaty *et al.*, Weakened cholinergic blockade of inflammation associates with diabetes-related depression. *Mol. Med.* **22**, 156–161 (2016).
55. M. J. Reeves *et al.*, Sex differences in stroke: Epidemiology, clinical presentation, medical care, and outcomes. *Lancet Neurol.* **7**, 915–926 (2008).
56. S. Andrews, FastQC: A quality control tool for high throughput sequence data. http://www.bioinformatics.babraham.ac.uk/projects/fastqc/ (2010).
57. J. T. Roehr, C. Dieterich, K. Reinert, Flexbar 3.0–SIMD and multicore parallelization. *Bioinformatics* **33**, 2941–2942 (2020).
58. R. Patro, G. Duggal, M. I. Love, R. A. Irizarry, C. Kingsford, Salmon provides fast and bias-aware quantification of transcript expression. *Nat. Methods* **14**, 417–419 (2017).
59. W. C. Wang *et al.*, miREXpress: analyzing high-throughput sequencing data for profiling microRNA expression. *BMC Bioinformatics* **10**, 328 (2009).
60. P. Loher, A. G. Telonis, I. Rigoutsos, MINTmap: Fast and exhaustive profiling of nuclear and mitochondrial tRNA fragments from short RNA-seq data. *Sci. Rep.* **7**, 41184 (2017).
61. K. Winek, S. Lobentanzer, H. Soreq, GEO submission. https://www.ncbi.nlm.nih.gov/geo/query/acc.cgi?acc=GSE158314. Deposited 21 September 2020.
62. M. L. Delignette-Muller, C. Dutang, fitdistrplus: An R package for fitting distributions. *J. Stat. Softw.* **64**, 1–34 (2015).
63. T. J. Bartosh, J. H. Ylostalo, Macrophage inflammatory assay. *Bio Protoc.* **4**, e1180 (2014).
64. S. Lobentanzer, GitHub repository. https://github.com/slobentanzer/stroke-trf. Deposited 17 April 2020.

Supplementary Material:

Expanded Methods:

Sequencing Quality Control
Small RNA was aligned using miRExpress and MINTmap. Total reads (after flexbar with quality control): 500,488,798. Reads per sample: 10,214,057 +/- (SD) 4,605,190. No significant difference between groups. Total miRNA: 284,749,858. miRNA hit / (hit+nohit): 56% +/- (SD) 4.4%. Total tRF (exclusive to tRNA space, see MINTmap documentation): 1,637,476. tRF (exclusive to tRNA space, see MINTmap documentation) hit / total reads: 3238 ppm +/- (SD) 1421 ppm. FastQC: All analyzed samples/bases showed exceptional quality. These metrics and FastQC results can be viewed at https://github.com/slobentanzer/stroke-trf.

At present, no standardized method exists to directly compare absolute counts derived from two separate alignments of the same sequencing experiment, as is the case here with the miRExpress and MINTmap alignments; MINTmap is a much more stringent pipeline (at least for the "exclusive tRNA space" used here). Future experiments should include a spike-in procedure or a similar approach to estimate absolute transcript numbers for each smRNA species, and to enable a better comparison between those absolute values.

Large RNA: Total reads (after flexbar with quality control): 880,069,396. Reads per sample: 36,669,558 +/-(SD) 4,543,364. No significant difference between groups. Mean mapping rate 89% +/- (SD) 2%. FastQC: All analyzed samples/bases showed exceptional quality. These metrics and FastQC results can be viewed at https://github.com/slobentanzer/stroke-trf.

Differential expression analysis
Differential expression was determined using the R/DESeq2 package (1) including the log2 fold change shrinkage estimation "apeglm" algorithm (2). Genes were considered differentially expressed at an adjusted p-value of < 0.05. The analysis was performed on the raw count tables (outliers already removed) with correction of covariates (age, batch, time2blood) in the model formula. Outliers were identified by sample clustering based on batch-corrected variance-stabilized expression, leading to exclusion of sample 4044 (stroke patient) in the small RNA sequencing experiment.

The count-change metric
The log-fold change metric is not ideally suited for assessing the potential impact of expression changes for individual small RNAs, because it does not reflect mean expression levels. We calculated the count-change for individual miRs and tRFs by combining base mean expression with the de-logarithmicized fold-change (from DESeq2 output).

$$CC = (BM \times 2^{LFC}) - BM$$

CC: countChange, BM: baseMean, LFC: log2-fold change

Small RNA targeting predictions
miR targeting was analyzed via our in-house database, *miRNeo*, as described (3). Briefly, the database unites 10 prediction algorithms and all available experimentally validated miR:gene interactions, and unites them in a scoring system. For all analyses in this manuscript, the cutoff score for consideration of a valid miR:gene interaction was ≥ 6.

Since no comprehensive tRF targeting predictions are available, we performed our own prediction based on all tRFs detected with more than 10 reads on average. We used the TargetScan 7.0 algorithm (4) to determine putative miR-like binding of any 7-nucleotide substring ("seed") of any tRF to any human transcript 3'-UTR. Hits were scored according to conserved branch length (BL) and probability of conserved targeting (PCT) across all 23 available species (5) and were entered into *miRNeo* (seed-gene targeting and tRF-seed association).

Gene set compilation of cholinergic and associated genes
We started out with a set of 28 cholinergic genes described in (6), targets including ACLY, CHAT, VAChT (aka SLC18A3), the 16 nicotinic and 5 muscarinic receptor subtypes, ACHE, BCHE, PRIMA1, and CHT (aka SLC5A7). In addition, we added several groups of genes known to be associated with

cholinergic functioning and of interest to our aims. These include: genes from the neurokine and neurotrophin signaling pathways; families of genes implicated in the development and differentiation of cholinergic cell types, including lim-homeobox transcription factors, bone morphogenetic protein family genes, and genes from the JAK-STAT pathway (see Data File S2)

miRs were considered Cholino-miRs if they were validated or predicted (with a score > 5/10) to target at least 5 transcripts on this list; tRFs were considered Cholino-tRFs if they contained a seed targeting evolutionarily conserved binding sites in at least 5 transcripts on this list (Figure S2 for empirical cumulative distribution function, ECDF plot); because of diverging numbers between miRs and tRFs we chose to use the higher (more stringent) threshold for miRs. Transcription factors were similarly associated with each transcript on the list, using the transcription factor activity derived from (7) in circulatory immune cells.

Permutation targeting analysis
Where appropriate, we determined permutation p-values via *miRNeo* targeting permutation. We determined a score for the test condition (e.g. by summing the individual targeting scores of all DE miRs towards cholinergic genes) and compared it to a null distribution consisting of permutated scores resulting from random substitution of test parameters (e.g. a random selection out of all genes the same size as the cholinergic test set), the p-value being the fraction of the null distribution at least as extreme as the real score.

Gene Ontology Analyses
We performed GO analyses on differentially expressed (DE) long RNA transcripts based on their DE p-value. GO analyses were performed using R/topGO as recommended by the authors, using the weighted method (8). Transcripts were ranked by p-value, and all DE transcripts (adjusted p-value < 0.05) with absolute log2 fold changes > 1.4 were tested against the background of the topmost two thousand transcripts. While GO enrichment analysis can be informative, interpretation and visualization of its results is not standardized and is often limited to presentation of top *X* terms by p-value. R/gsoap (9) is an analysis tool proposed to aid in interpretation of GO enrichment results via t-SNE display of similarity of terms based on the amount of shared significant genes. GO enrichment results were processed to fulfil gsoap input criteria and visualized using R/ggplot2 (10).

Pathways targeted by perturbed miRs
We determined target sets of positively and negatively DE miRs (separately) via *miRNeo* query with a threshold score of at least 6. The gene targets were ranked by the amount of miRs targeting each gene, yielding a range of 1-44 (mean 4.7 +/-SD 4.7) for positively regulated miRs, and a range of 1-155 (mean 13.5 +/-SD 15.6) for negatively regulated miRs, both resembling power law distributions. To account for possible biases in the underlying targeting dataset, targeting and scoring were then permutated for both sets with the same query and ranking, but randomized input miRs were selected from all mature miRs in the same length as the original DE set, for 10,000 times. Upon calculation of permutation p-values, we dismissed genes that were not targeted by the set of DE miRs significantly more than by the random permutation sets ($p < 0.05$). The larger negative-DE set in this analysis yielded a large number of highly enriched genes, such that a distinction by adjusted p-value was not possible in the top 2000 targeted genes. Thus, we repeated the analysis for negatively regulated miRs using a log2FoldChange threshold of -2, which reduced the amount of miRs to 82, and the range of miRs targeting each gene to 1-52, mean 5.8 +/-SD 6.1. This set was subjected to the same permutation approach and was used instead of the non-limited set in the p-value-based approach below.

The gene lists so derived were used in a GO analysis similar to the one described above, based on the following scorings: for positively regulated miRs, GO enrichment was based on *1)* the significantly targeted genes ($p < 0.05$) as a test set, and the (non-enriched, $p > 0.05$) genes as background; and *2)*, to identify the most-targeted genes, the top 200 genes (sorted by amount of distinct miRs targeting each gene (also $p < 0.05$)) served as a test set, with all other genes (starting from 201) as the background. For negatively regulated miRs, target genes were analyzed similarly, but the non-threshold significantly targeted genes were replaced by the -2 log2FoldChange threshold set in approach *1)*. The GO terms yielded by these four analyses were visualized and clustered using the R/gsoap-approach described above.

The resulting 13 clusters were manually annotated and organized on a canvas to better understand the relationships between the targeted gene sets of positively and negatively regulated miRs (Figure S5).

Few terms fell outside the area of these manually adjoined clusters due to little similarity with the clustered terms; these were disregarded in the further analyses (but are available in Data File S6). To discern the most relevant genes and seek putative hub genes in the stroke response, the clusters identified in the gsoap visualization were imported back into the R environment. Detection of significantly enriched genes in each cluster involved hypergeometric enrichment of each gene in each cluster versus all other clusters (background) via Fisher's exact test. The resultant p-values were corrected for multiple testing using the Benjamini-Hochberg method, and genes with an adjusted p-value < 0.05 were considered significantly enriched in the respective cluster (Data File S6), with a range of enriched genes per cluster from 8 to 84. The final 13 clusters were ranked by the total amount of enriched genes per cluster, and cross-checked for functional implications of enriched genes in each cluster using DAVID 6.8 (11).

PCR quantification of inflammatory markers after LPS stimulation and Zbp1 quantification.
LPS stimulation: 18h after LPS stimulation, cells were collected in Tri-Reagent (Sigma Aldrich, St. Louis, USA) and total RNA, including small RNAs, isolated using miRNeasy (Qiagen, Hilden, Germany). cDNA was synthesized from 100ng RNA using qScript™ cDNA Synthesis Kit (Quanta Biosciences, Beverly MA, USA). Expression of Cd14, Stat1, Tnfa and Il10 were assessed using PerfeCTa® SYBR® Green FastMix® (Quanta Biosciences, Beverly MA, USA) and normalized using Peptidylprolyl isomerase A (Ppia) and 18S ribosomal RNA genes as house-keeping.

ssRNA tRF-22-WE8SPOX52 mimics experiments: 24h after transfection of the mimics, cells were collected in TRI-Reagent (Sigma Aldrich, St. Louis, USA) and total RNA, including small RNAs, isolated using miRNeasy (Qiagen, Hilden, Germany). cDNA was synthesized from 100ng RNA using qScript™ cDNA Synthesis Kit (Quanta Biosciences, Beverly MA, USA), and expression of Zbp1 was assessed using PerfeCTa® SYBR® Green FastMix® (Quanta Biosciences, Beverly MA, USA) and normalized using Glyceraldehyde 3-phosphate dehydrogenase (Gapdh) as house-keeping. Primer sequences were obtained from the Primer Bank (12) and were as follows:

Cd14: **FORWARD** AGCACACTCGCTCAACTTTTC,
REVERSE GCCCAATTCAGGATTGTCAGAC
Stat1:**F** TCACAGTGGTTCGAGCTTCAG, **R** CGAGACATCATAGGCAGCGTG
Tnfa: **F** CCTGTAGCCCACGTCGTAG, **R** GGGAGTAGACAAGGTACAACCC
Il-10: **F** GCTCTTACTGACTGGCATGAG, **R** CGCAGCTCTAGGAGCATGTG
Ppia: **F** GAGCTGTTTGCAGACAAAGTTC, **R** CCCTGGCACATGAATCCTGG
18S rRNA: **F** CTCAACACGGGAAACCTCAC, **R** CGCTCCACCAACTAAGAACG
Gapdh: **F** ATCAAGAAGGTGGTGAA, **R** CTTACTCCTTGGAGGCCAT

PCR quantification of tRFs
First, we performed size selection of total RNA, to exclude molecules > 25 nt in case of human samples and > 50 nt in case of cell culture experiments with RAW 264.7 cells. 1 μg of RNA was loaded into 15% TBE-Urea-Polyacrylamide gel (Biorad, Hercules, USA) after mixing 1:1 with Gel Loading Buffer II (Thermo Fisher, Waltham, USA) and run at 200V for 40-50 minutes. When testing human CD14+ monocytes, 600 ng of RNA were loaded into the gel; in case of low total RNA concentrations (with minimum 21 ng/μl), we used the maximum accommodable volume of 20 μl. Gels were stained with SYBR Gold (Thermo Fisher, Waltham, USA) and visualized on a UV table to cut out the desired section. As size markers, miR marker and Low Range ssRNA ladder (both from New England Biolabs, Ipswitch, USA) were used. Excised gel fragments were incubated in 810μl 3M NaCl over-night at 4°C on a rotation stand. The supernatant was then transferred into a new Eppendorf and 1 volume of iso-propanol was added for 24h at -20°C. Then, RNA was precipitated.

RNA concentrations were measured using Bioanalyzer (Agilent, Santa Clara, USAμ) and cDNA was prepared from 500 pg (with exception of control samples 16 and 18 yielding low concentrations after size selection – here 250pg were used) using qScript™ microRNA cDNA Synthesis Kit (Quanta Biosciences, Beverly MA, USA) and diluted to 200 μl total. tRFs were quantified using quantitative reverse transcription PCR (qRT-PCR) with PerfeCTa® SYBR® Green FastMix®, Low ROX™ (Quanta Biosciences, Beverly MA, USA) and normalized to hsa-miR-30d-5p, hsa-let-7d-5p, hsa-miR-106b-3p and hsa-miR-3615 (human stroke patients) or mmu-miR-30d-5p, mmu-let-7d-5p for experiments with RAW 264.7 cells. In experiments with ssRNA tRF-22-WE8SPOX52 mimics, tRF-22-WE8SPOX52 levels were assessed without size-selection (measuring levels of the tRF and its parental tRNA molecule) and normalized to Snord47.

Primer sequences are listed below:
hsa/mmu-miR-30d-5p: TGTAAACATCCCCGACTGGAAG
hsa/mmu-let-7d-5p: AGAGGTAGTAGGTTGCATAGTT
hsa-miR-106b-3p: CCGCACTGTGGGTACTTGCTGC
hsa-miR-3615: TCTCTCGGCTCCTCGCGGCTC
tRF-22-WEKSPM852: TCGATCCCCGGCATCTCCACCA
tRF-22-WE8SPOX52 (and tRF-21-WE8SPOX5D): TCGATTCCCGGCCAATGCACC
tRF-18-8R6Q46D2: TCCCCGGCATCTCCACCA
tRF-22-8EKSP1852: TCAATCCCCGGCACCTCCACCA
tRF-18-8R6546D2: TCCCCGGCACCTCCACCA
tRF-18-HR0VX6D2: ATCCCACCGCTGCCACCA
Snord47 (Quanta Biosciences, Beverly MA, USA):
GTGATGATTCTGCCAAATGATACAAAGTGATATCACCTTTAAACCGTTCCATTTTATTTCTGAGG

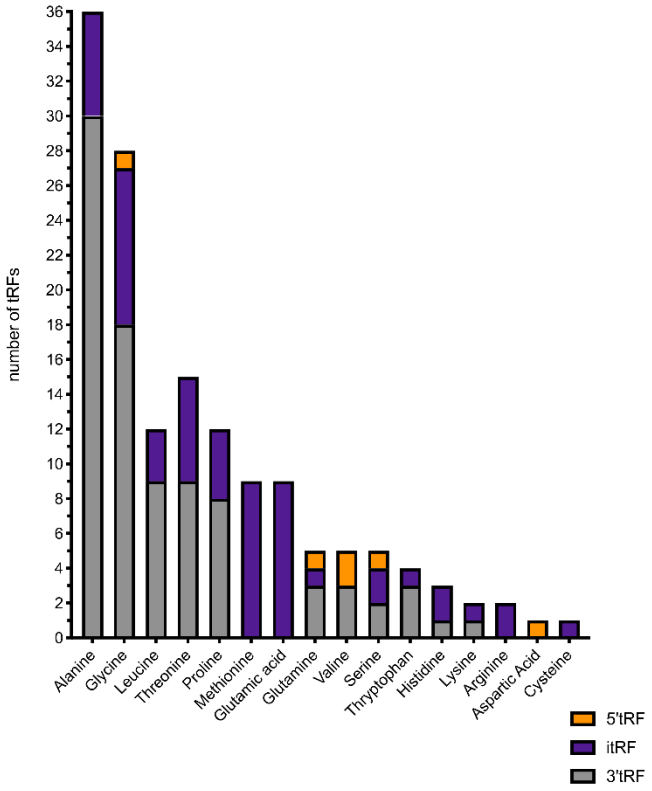

Figure S1
Analysis of types of DE tRFs indicates non-random cleavage of tRNA molecules.
Most DE tRFs were derived from tRNA-Ala (36) and 3'-tRFs were the most common type in the whole DE dataset.

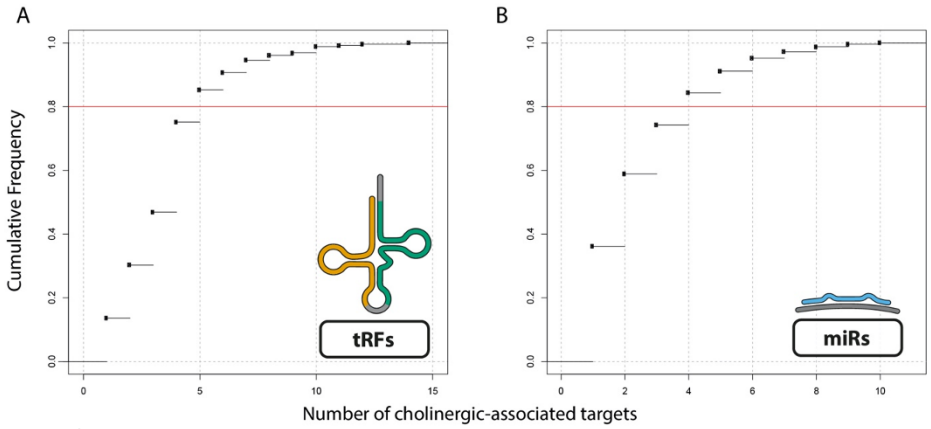

Figure S2
Cholinergic-associated small RNA empirical cumulative distribution function (ECDF) curves.
Cholinergic association was tested using *miRNeo* targeting data of miRs and tRFs.
To assess the best-suited threshold for defining cholinergic association, ECDFs were calculated for the number of cholinergic-associated (CA) genes targeted by each unique small RNA. A) Cumulative frequency of the number of CA genes targeted by tRFs. Threshold of 80% (red line) is passed at five CA genes targeted. B) Cumulative frequency of the number of CA genes targeted by miRs. Threshold of 80% (red line) is passed at four CA genes targeted.

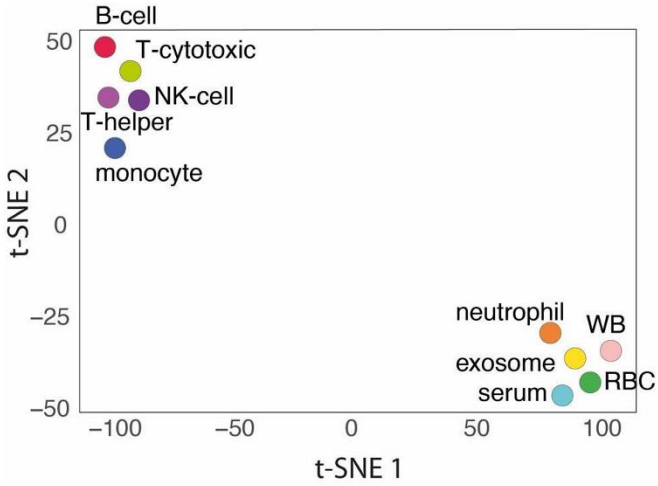

Figure S3
tRF profiles of blood compartments distinguish leukocyte subsets, excluding neutrophils, from erythrocytes and non-cellular compartments. t-SNE of specific blood compartments based on tRF expression, WB – whole blood, RBC – erythrocytes.

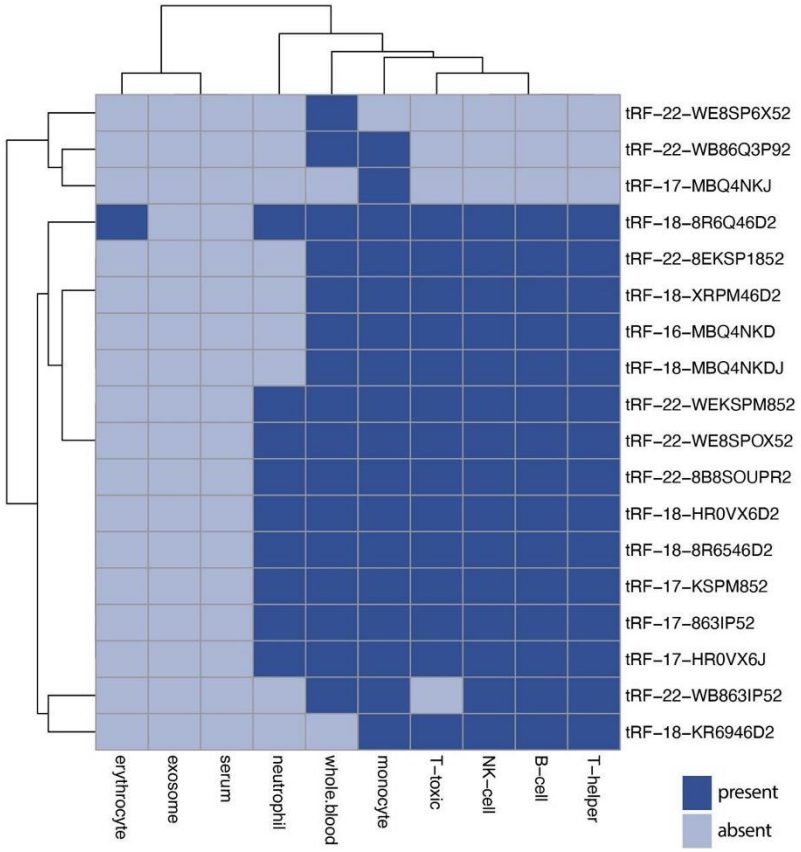

Figure S4
Most of top 20 stroke DE tRFs are present in immune cell compartments. Heatmap showing the presence/absence of the 20 most highly-perturbed tRFs in defined blood compartments.

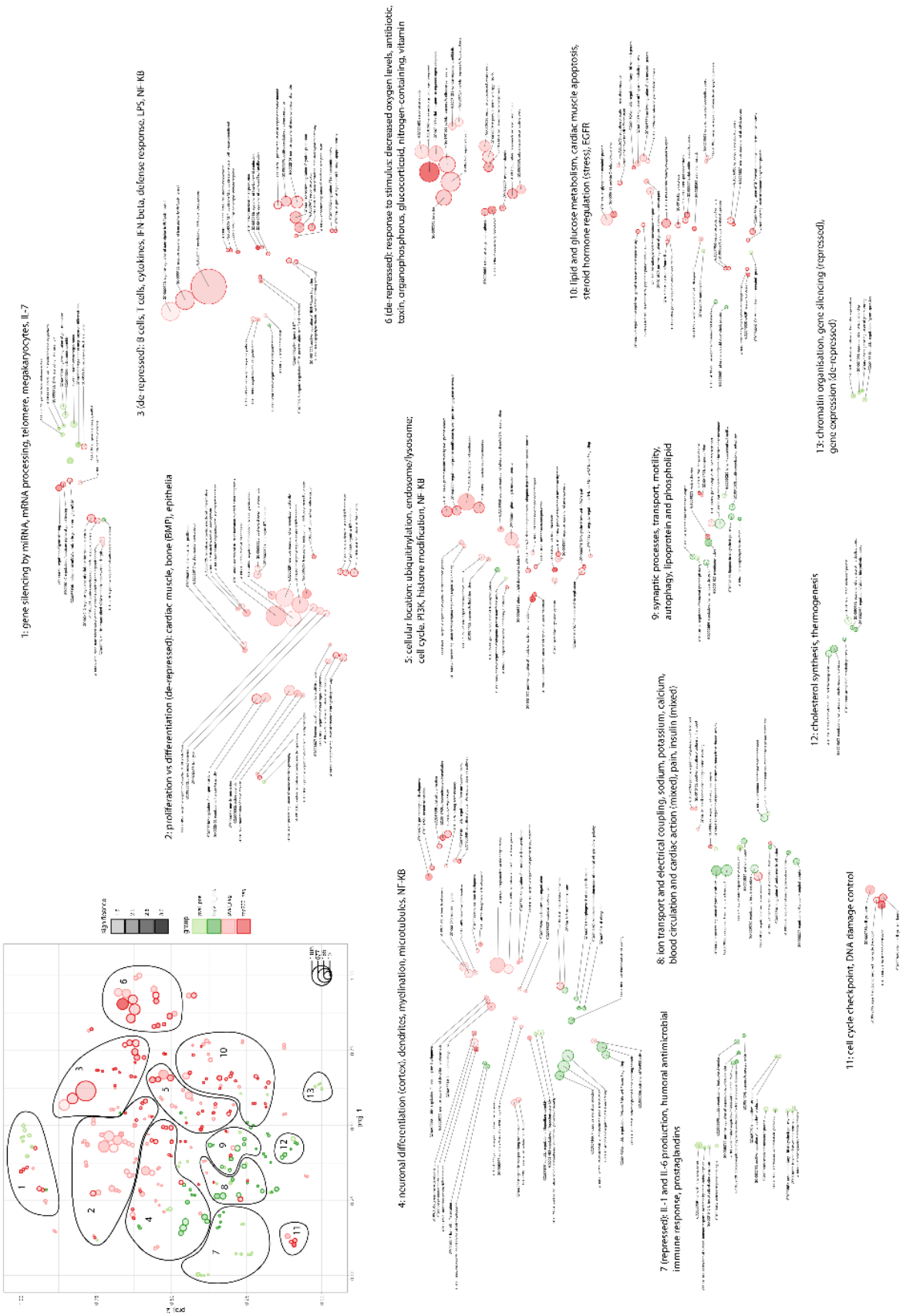
1: gene silencing by miRNA, mRNA processing, telomere, megakaryocytes, IL-7
3: (de repressed): B cells, T cells, cytokines, IFN beta, defense response, LPS, NF-KB
2: proliferation vs differentiation (de-repressed): cardiac muscle, bone (BMP), epithelia
6 (de-repressed): response to stimulus: decreased oxygen levels, antibiotic, toxin, organophosphorus, glucocorticoid, nitrogen-containing, vitamin
5: cellular location: ubiquitinylation, endosome/lysosome; cell cycle, PI3K, histone modification, NF-KB
10: lipid and glucose metabolism, cardiac muscle apoptosis, steriod hormone regulation (stress), EGFR
9: synaptic processes, transport, motility, autophagy, lipoprotein and phospholipid
4: neuronal differentiation (cortex), dendrites, myelination, microtubules, NF-KB
8: ion transport and electrical coupling, sodium, potassium, calcium, blood circulation and cardiac action (mixed), pain, insulin (mixed)
12: cholesterol synthesis, thermogenesis
13: chromatin organisation, gene silencing (repressed), gene expression (de-repressed)
7 (repressed): IL-1 and IL-6 production, humoral antimicrobial immune response, prostaglandins
11: cell cycle checkpoint, DNA damage control
significance
group

Figure S5 (on previous page)
Ontological enrichment and clustering of gene target sets of DE miRs show distinct perturbed pathways. Gene target sets of positively and negatively perturbed miRs were subjected to gene ontology analysis separately, based on two scoring systems: “pval,” based on enrichment p-value in targeting permutation, and “top200”, based on the top 200 genes with highest amounts of miRs targeting each gene. Resulting GO terms were visualized using R/gsoap and clustered based on their shared genes (upper left). Circle sizes represent the number of genes in each term, their color depth denotes p-value (all $p < 0.05$). The single clusters were manually screened and annotated regarding their functions (right side).

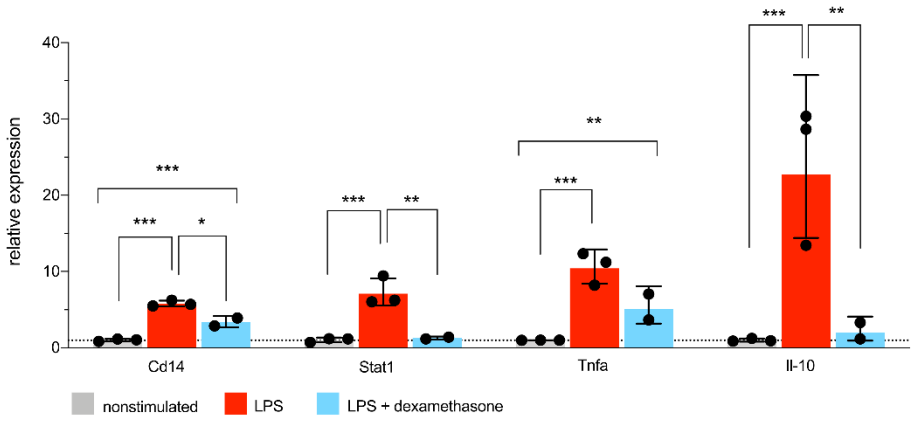

Figure S6
Upregulated inflammatory signaling molecules and cytokines in LPS-stimulated murine RAW 264.7 cells. A) Levels of cluster of differentiation 14 (Cd14), signal transducer and activator of transcription 1 (Stat1), tumor necrosis factor alpha (Tnfa) and interleukin 10 (Il-10) were measured with qRT-PCR using normalized expression (Ppia and 18SrRNA served as house-keeping), relative to the nonstimulated control group (line at mean normalized expression for the control group = 1), Each dot represents 2-4 technical replicates, ANOVA with Tukey post-hoc, * $p < 0.05$, ** $p < 0.01$, *** $p < 0.001$, bar graphs +/- SD(lg).

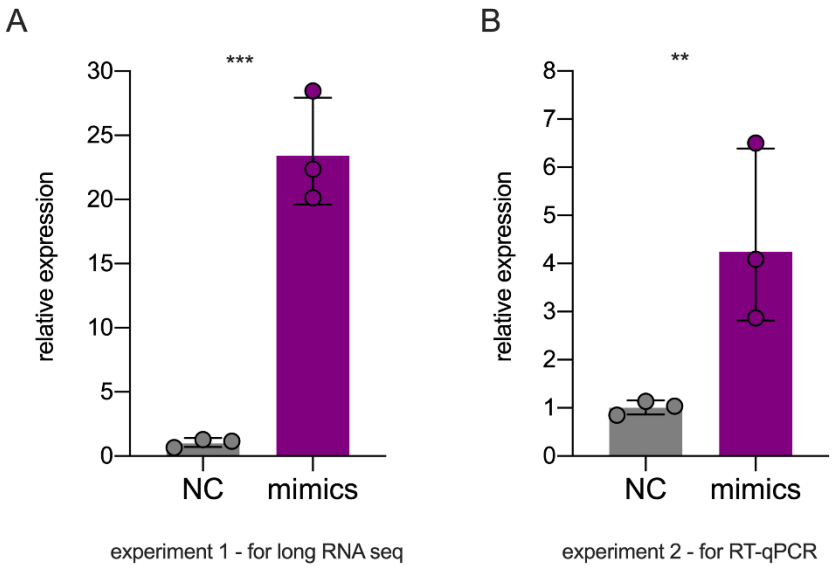

Figure S7
tRF-22-WE8SPOX52 expression in the ssRNA mimics transfection experiments. Shown is normalized expression of tRF-22-WE8SPOX52 and parental tRNA molecule (measurement without size selection) by qRT-PCR using Snord47 as house-keeping gene. A) Experiment 1 - samples subjected to long RNA sequencing. B) Experiment 2 - samples used for qRT-PCR measurements of Zbp1 expression. Each dot represents one technical replicate in the cell culture experiment. ** p< 0.01, *** p< 0.001, one-way ANOVA, bar graphs +/- SD(lg).

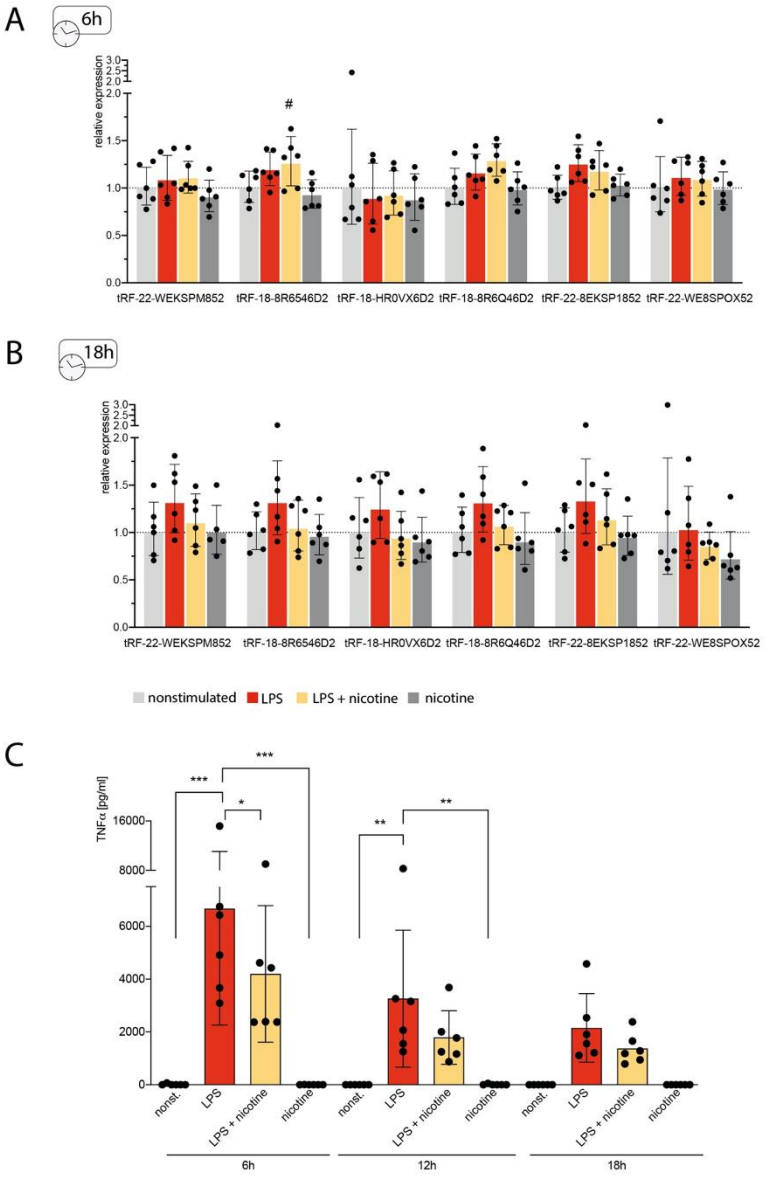

Figure S8
LPS stimulation of human CD14+ cells yields transient nicotine-affected tRF changes. The top 6 stroke-perturbed tRFs were quantified using qRT-PCR in human CD14+ cells following LPS stimulation with and without addition of nicotine; controls were nonstimulated cells and cells with nicotine alone (for setup, see Figure 6G in the main manuscript). A) Cells collected 6h after LPS stimulation showed significantly elevated tRF-18-8R6546D2 under LPS + nicotine exposure alone. B) At 18h after LPS

stimulation, none of the top 6 stroke-perturbed tRFs showed significant changes, including LPS +nicotine challenged cells which showed upregulation at the 12h time point (see Figure 6H in the main manuscript). LPS-stimulated cells still showed the highest expression of tRFs, albeit not significant when compared to other groups. $^{\#}p < 0.05$ when compared to nicotine-treated cells. Each dot represents one donor, one-way ANOVA with Tukey post-hoc; bar graphs +/- SD(lg). C) LPS-stimulation led to significantly elevated TNFα levels in the supernatant of CD14+ cells (measured by ELISA). * $p<0.05$, ** $p<0.01$, *** $p<0.001$, two-way ANOVA on the influence of group and time variable on the TNFα levels. $F(3, 60) = 23.53$, $p <0.0001$ for the main effect "group" (nonstimulated, LPS, LPS + nicotine and nicotine), $F(2,60) = 7.56$ $p = 0.0012$ for the main effect "time", $F(6, 60)$ $p=0.02$ for the interaction; with Dunnett's post-hoc performing comparisons LPS group vs. others; bar graph +/- SD.

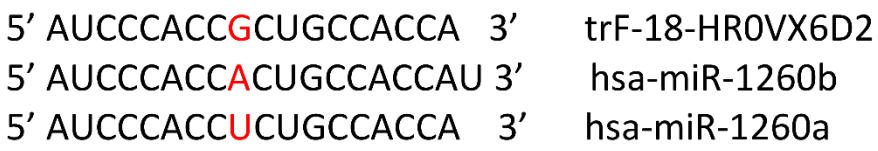

Figure S9
Sequence of tRF-18-HR0VX6D2 shows high similarities to two known miRs (13)
hsa-miR-1260b differs from tRF-18-HR0VX6D2 by one nucleotide at position 9 and an additional nucleotide at the 3'-end, has-miR-1260a differs from tRF-18-HR0VX6D2 only at position 9.

GO.ID	Term	Annotated	Significant	Expected	Rank in classic	classic	weight
GO:0001819	positive regulation of cytokine producti...	66	14	4.38	42	6E-05	0.00017
GO:0032479	regulation of type I interferon producti...	29	8	1.93	52	0.00039	0.00039
GO:0001818	negative regulation of cytokine producti...	51	11	3.39	51	0.00034	0.00057
GO:0009617	response to bacterium	95	18	6.31	35	2.5E-05	0.00059
GO:0045087	innate immune response	151	38	10.03	1	9.1E-15	0.00197
GO:0098586	cellular response to virus	15	5	1	65	0.00208	0.00208
GO:0046683	response to organophosphorus	22	6	1.46	68	0.00233	0.00233
GO:0002753	cytoplasmic pattern recognition receptor...	10	4	0.66	70	0.00284	0.00284
GO:0048661	positive regulation of smooth muscle cel...	16	5	1.06	72	0.00286	0.00286
GO:0060760	positive regulation of response to cytok...	16	5	1.06	73	0.00286	0.00286
GO:0014074	response to purine-containing compound	23	6	1.53	75	0.00299	0.00299
GO:0032649	regulation of interferon-gamma productio...	17	5	1.13	80	0.00384	0.00384
GO:0016525	negative regulation of angiogenesis	12	4	0.8	88	0.00603	0.00603
GO:0034446	substrate adhesion-dependent cell spread...	13	4	0.86	93	0.00827	0.00827
GO:0032496	response to lipopolysaccharide	46	8	3.06	96	0.00917	0.00917
GO:0009063	cellular amino acid catabolic process	14	4	0.93	100	0.01099	0.01099
GO:0031349	positive regulation of defense response	58	11	3.85	61	0.00109	0.01236
GO:0002576	platelet degranulation	22	5	1.46	102	0.01252	0.01252
GO:0010469	regulation of signaling receptor activit...	49	8	3.26	103	0.01340	0.01340
GO:0070887	cellular response to chemical stimulus	404	54	26.84	19	6.2E-09	0.01563
GO:0030168	platelet activation	32	6	2.13	111	0.01641	0.01641
GO:0034109	homotypic cell-cell adhesion	16	4	1.06	112	0.01802	0.01802
GO:0050731	positive regulation of peptidyl-tyrosine...	25	5	1.66	117	0.02152	0.02152
GO:0048469	cell maturation	17	4	1.13	118	0.02238	0.02238
GO:0097696	STAT cascade	17	4	1.13	119	0.02238	0.02356
GO:0043330	response to exogenous dsRNA	10	3	0.66	123	0.02429	0.02429
GO:0071695	anatomical structure maturation	18	4	1.2	127	0.02734	0.02734
GO:0050680	negative regulation of epithelial cell p...	19	4	1.26	139	0.03290	0.03290
GO:0007267	cell-cell signaling	146	11	9.7	649	0.37575	0.03503
GO:0001936	regulation of endothelial cell prolifera...	20	4	1.33	145	0.03907	0.03907
GO:0006906	vesicle fusion	20	4	1.33	146	0.03907	0.03907
GO:0007160	cell-matrix adhesion	20	4	1.33	147	0.03907	0.03907
GO:0030856	regulation of epithelial cell differenti...	12	3	0.8	151	0.04041	0.04041
GO:0034113	heterotypic cell-cell adhesion	12	3	0.8	152	0.04041	0.04041
GO:0042130	negative regulation of T cell proliferat...	12	3	0.8	153	0.04041	0.04041
GO:0051668	localization within membrane	12	3	0.8	154	0.04041	0.04041

Table S1
Post-stroke DE genes are enriched in circulation- and immunity- related pathways.
Full list of GO terms used for generation of tSNE in Figure 4 (main manuscript).

References:

1. M. I. Love, W. Huber, S. Anders, Moderated estimation of fold change and dispersion for RNA-seq data with DESeq2. *Genome Biol.* **15** (2014).
2. A. Zhu, J. G. Ibrahim, M. I. Love, Heavy-tailed prior distributions for sequence count data: removing the noise and preserving large differences. *Bioinformatics* **35**, 2084–2092 (2019).
3. S. Lobentanzer, G. Hanin, J. Klein, H. Soreq, Integrative Transcriptomics Reveals Sexually Dimorphic Control of the Cholinergic/Neurokine Interface in Schizophrenia and Bipolar Disorder. *Cell Rep.* **29**, 764-777.e5 (2019).
4. V. Agarwal, G. W. Bell, J. W. Nam, D. P. Bartel, Predicting effective microRNA target sites in mammalian mRNAs. *Elife* **4** (2015).
5. R. C. Friedman, K. K. H. Farh, C. B. Burge, D. P. Bartel, Most mammalian mRNAs are conserved targets of microRNAs. *Genome Res.* **19**, 92–105 (2009).
6. H. Soreq, Checks and balances on cholinergic signaling in brain and body function. *Trends Neurosci* **38**, 448–458 (2015).
7. D. Marbach, *et al.*, Tissue-specific regulatory circuits reveal variable modular perturbations across complex diseases. *Nat. Methods* **13**, 366–370 (2016).
8. A. Alexa, J. Rahnenfuhrer, T. Lengauer, Improved scoring of functional groups from gene expression data by decorrelating GO graph structure. *Bioinformatics* **22**, 1600–1607 (2006).
9. T. Tokar, C. Pastrello, I. Jurisica, GSOAP: a tool for visualization of gene set over-representation analysis. *Bioinformatics* (2020) https:/doi.org/10.1093/bioinformatics/btaa001.
10. H. Wickham, *ggplot2: Elegant Graphics for Data Analysis* (Springer-Verlag, 2016).
11. D. W. Huang, B. T. Sherman, R. A. Lempicki, Systematic and integrative analysis of large gene lists using DAVID bioinformatics resources. *Nat. Protoc.* **4**, 44–57 (2009).
12. X. Wang, A. Spandidos, H. Wang, B. Seed, PrimerBank: A PCR primer database for quantitative gene expression analysis, 2012 update. *Nucleic Acids Res.* **40**, D1144–D1149 (2012).
13. N. C. T. Schopman, S. Heynen, J. Haasnoot, B. Berkhout, A miRNA-tRNA mix-up: tRNA origin of proposed miRNA. *RNA Biol.* **7**, 573–576 (2010).

8.3 Study 3

Journal of Neuroimmunology 355 (2021) 577568

Contents lists available at ScienceDirect

Journal of Neuroimmunology

journal homepage: www.elsevier.com/locate/jneuroim

Efficacy and safety of intratracheal IFN-γ treatment to reverse stroke-induced susceptibility to pulmonary bacterial infections

Sandra Jagdmann [a], Daniel Berchtold [b], Birgitt Gutbier [c], Martin Witzenrath [c,d], Andreas Meisel [b,e,f,g], Christian Meisel [a,h], Claudia Dames [a,b,*]

[a] Charité – Universitätsmedizin, Corporate member of Freie Universität Berlin, Humboldt-Universität zu Berlin, Berlin Institute of Health, Institute for Medical Immunology, Augustenburger Platz 1, Berlin 13353, Germany
[b] Charité – Universitätsmedizin, Corporate member of Freie Universität Berlin, Humboldt-Universität zu Berlin, Berlin Institute of Health, Department of Experimental Neurology, Charitéplatz 1, Berlin 10117, Germany
[c] Charité – Universitätsmedizin, Corporate member of Freie Universität Berlin, Humboldt-Universität zu Berlin, Berlin Institute of Health, Division of Pulmonary Inflammation, Charitéplatz 1, Berlin 10117, Germany
[d] Charité – Universitätsmedizin, Corporate member of Freie Universität Berlin, Humboldt-Universität zu Berlin, Berlin Institute of Health, Department of Infectious Diseases and Respiratory Medicine, Charitéplatz 1, Berlin 10117, Germany
[e] Charité – Universitätsmedizin, Corporate member of Freie Universität Berlin, Humboldt-Universität zu Berlin, Berlin Institute of Health, Center for Stroke Research Berlin, Charitéplatz 1, Berlin 10117, Germany
[f] Charité – Universitätsmedizin, Corporate member of Freie Universität Berlin, Humboldt-Universität zu Berlin, Berlin Institute of Health, Neurocure Cluster of Excellence, Charitéplatz 1, Berlin 10117, Germany
[g] Charité – Universitätsmedizin, Corporate member of Freie Universität Berlin, Humboldt-Universität zu Berlin, Berlin Institute of Health, Department of Neurology, Charitéplatz 1, Berlin 10117, Germany
[h] Labor Berlin-Charité Vivantes, Sylter Str. 2, Berlin 13353, Germany

ARTICLE INFO

Keywords:
Immunomodulation
IFN-γ
MCAo
Lung
Stroke-associated pneumonia

ABSTRACT

Stroke-induced immunosuppression contributes to the development of stroke-associated pneumonia (SAP). Experiments in mice demonstrated that apoptosis of IFN-γ producing cells and reduced IFN-γ secretion resulted in impaired immune responses and the development of pneumonia after middle cerebral artery occlusion (MCAo). In the present study, we investigated the efficacy of intratracheal IFN-γ treatment to prevent SAP and demonstrated that modest benefits on pulmonary cytokine response in IFN-γ treated stroke mice did not prevent spontaneously developing infections and even slightly reduced bacterial clearance of aspirated pneumococci. Our results suggest that pulmonary IFN-γ treatment is not an effective preventive measure for SAP.

1. Introduction

Pneumonia is the most frequent severe complication after stroke increasing morbidity, mortality and length of hospitalization (Armstrong and Mosher, 2011). Previous studies identified various risk factors contributing to the development of pneumonia during the acute phase of stroke including greater severity of neurologic impairment, old age, diabetes mellitus and dysphagia (Sellars et al., 2007). There is evidence from clinical and experimental settings that stroke-induced immunosuppression, due to overactivation of stress pathways, increases the risk of developing pulmonary infections after stroke (Dirnagl et al., 2007; Hoffmann et al., 2017; Huang et al., 2019; McCulloch et al., 2017; Meisel et al., 2005; Prass et al., 2003; Shi et al., 2018; Wong et al., 2011). Over the last decade, clinical studies investigated antibiotic treatment in acute stroke patients to prevent SAP (Emsley and Hopkins, 2008; Westendorp et al., 2015). In summary, antibiotic treatment of acute stroke patients is capable of reducing urinary but not pulmonary infections and does not improve stroke outcome, particularly in severely affected patients. Rising antibiotic resistance sparked the interest of research on immunomodulatory therapy to improve pulmonary immune

Abbreviation: BAL, Bronchoalveolar lavage; BALF, Bronchoalveolar lavage fluid; i.n., intranasal; i.p., intraperitoneal; i.t., intratracheal; IRF-1, IFN regulatory factor-1; LPS, lipopolysaccharide; MCAo, middle cerebral artery occlusion; NF-κB, nuclear factor 'kappa-light-chain-enhancer' of activated B-cells; NK cells, Natural killer cells; SAP, stroke-associated pneumonia; SD, standard deviation; WT, wild type.

* Corresponding author at: Augustenburger Platz 1, 13353 Berlin, Germany.
E-mail addresses: sandra.jagdmann@charite.de (S. Jagdmann), daniel.berchtold@charite.de (D. Berchtold), birgitt.gutbier@charite.de (B. Gutbier), martin.witzenrath@charite.de (M. Witzenrath), andreas.meisel@charite.de (A. Meisel), chr.meisel@charite.de (C. Meisel), claudia.dames@charite.de (C. Dames).

https://doi.org/10.1016/j.jneuroim.2021.577568
Received 30 October 2020; Received in revised form 1 April 2021; Accepted 1 April 2021
Available online 3 April 2021

response and prevent SAP. In an experimental stroke model, it was shown that a diminished IFN-γ production mainly by T cells and invariant natural killer T cells (iNKT) in the blood and visceral organs as well as stroke-induced apoptosis of IFN-γ producing immune cells in lymphatic organs mainly contributes to the development of SAP (Prass et al., 2003; Wong et al., 2011). Investigation of lung immunity also showed significantly reduced IFN-γ level in lung tissue but not bronchoalveolar lavage fluid (BALF) 72 h after experimental stroke (Farris et al., 2019).

IFN-γ is an important component of the early host defense against infectious diseases (Schroder et al., 2004). Therefore, IFN-γ could become an alternative to antibiotic treatment after stroke. Experiments in mice confirmed that preventive IFN-γ treatment improves bacterial clearance of *Legionella pneumophila*, *Toxoplasma gondii*, *Listeria monocytogenes* and *Mycobacterium tuberculosis* (Khor et al., 1986; Kiderlen et al., 1984; McCabe et al., 1984; Skerrett and Martin, 1994). However, the efficacy and safety of local IFN-γ treatment to reverse stroke-induced susceptibility to pulmonary bacterial infections has not been investigated so far.

Findings in patients demonstrated that SAP is caused by both Gram-positive and Gram-negative bacteria. Investigations of tracheal aspirate cultures, sputum cultures and blood cultures identified *Enterobacteriaceae* (*Klebsiella pneumoniae*, *Escherichia coli)*, *Staphylococcus aureus*, *Pseudomonas aeruginosa*, *Acinetobacter baumanii* and *Streptococcus pneumoniae (S. pneumoniae)* as the most common organisms in stroke patients (Kishore Amit et al., 2018). Stroke patients develop SAP within the first week after stroke onset (Kishore et al., 2019). In line with clinical observations, experimental stroke in mice also results in spontaneously developing pneumonia within 3 days after stroke (Prass et al., 2003). To improve the reproducibility of pneumonia in mice, an aspiration-induced pneumococcal pneumonia after stroke was established, demonstrating that MCAo in mice leads to an increased susceptibility to aspiration-induced *S. pneumoniae* infections (Mracsko et al., 2017; Prass et al., 2006). Here, we tested the hypothesis that IFN-γ treatment reconstitutes the pulmonary immune response and prevents spontaneous pneumonia as well as improves the clearance of induced pneumococcal pneumonia after experimental stroke. We found that intratracheal (i.t.) IFN-γ treatment enhanced pro-inflammatory immune responses in naïve mice and had no adverse effects on infarct size development after experimental stroke. However, the stimulatory properties of IFN-γ treatment were less pronounced in stroke mice and therefore did not significantly reduce spontaneously developing infections or aspiration-induced pneumococcal pneumonia after stroke.

2. Methods

2.1. Animals and housing

12 weeks old male C57Bl/6 J (Janvier, Saint Berthevin, France) mice were housed in cages with chip bedding and environmental enrichment on a 12 h light/dark cycle with *ad libitum* access to standard chow and water. Experiments were performed in accordance with the European directive on the protection of animals used for scientific purposes and all other applicable regulations and approved by the relevant authority, Landesamt für Gesundheit und Soziales, Berlin, Germany.

2.2. Experimental stroke

60 min focal cerebral ischemia was induced by transient middle cerebral artery occlusion (MCAo) according to standard operating procedures of the laboratory (Engel et al., 2011). In brief, the mice were anesthetized with 1.5% isoflurane (Forene, Abbott, Wiesbaden Germany) in 1:2 mixtures of O_2/N_2O. A silicon monofilament (Doccol, MA, USA) was inserted into the common carotid artery and advanced until the origin of the middle cerebral artery. After 60 min, the filament was removed. The infarct size was determined by hematoxylin staining. Animals without infarcts were excluded from the study.

2.3. Bronchoscopy-guided application of IFN-γ

IFN-γ application was performed as described elsewhere (Dames et al., 2014). In brief, mice were anesthetized by intraperitoneal (i.p.) injection of Midazolam (5.0 mg/kg body weight, Roche Pharma AG, Grenzach-Whylen, Germany) and Medetomidin (0.5 mg/kg body weight, Orion Cooperation, Espoo, Finland). Under visual control, the bronchoscope (Polydiagnost, Pfaffenhofen, Germany) was introduced into the trachea and advanced until the bifurcation. IFN-γ (PeproTech GmbH, Hamburg, Germany) diluted in solvent at given concentrations or solvent were applied by using a microsprayer (Penn-Century, PA, USA). Anesthesia was antagonized subcutaneously with Flumazenil (0.5 mg/kg body weight, Inresa, Freiburg, Germany) and Atipamezol (5.0 mg/kg body weight, Orion Cooperation, Espoo, Finland).

2.4. Nasal inoculation with S. pneumoniae on d4 after experimental stroke

Mice were treated one day before and at the day of MCAo i.p. with Marbofloxacin (5.0 g/kg body weight, Vétoquinol GmbH, Ravensburg, Germany) to prevent spontaneously developing infections after experimental stroke. For *S. pneumoniae* infection mice were anesthetized and antagonized as described under IFN-γ application. A suspension of 10,000 colony-forming units (CFU) in 20 µl (serotype 3, PN36, NCTC 7978) was applied intranasal (i.n.). To ensure aspiration, mice were fixed in a vertical position head up for 15 min.

2.5. Microbiological investigations

Bronchoalveolar lavage (BAL) was performed as described elsewhere (Sun et al., 2017). The lungs were homogenized in 500 µl PBS. BALF and lung were serially diluted and plated on LB-Agar. After 18 h incubation at 37 °C, the colonies were counted and CFU per ml tissue/liquid calculated.

2.6. Analysis of cytokines in BALF and plasma

Cytokines in BALF and plasma were measured by commercially available MILLIPLEX Multiplex Assays using Luminex xMAP technology (Merk Millipore, Darmstadt, Germany).

2.7. Analysis of leukocytes in lung and spleen by flow cytometry

Lung cells and splenocytes were isolated as described elsewhere (Engel et al., 2015) and stained with the following anti-mouse monoclonal antibodies for 20 min at 4 °C in the dark: CD45 PerCP, CD11b APC-Cy7, NK1.1 PE, CD19 FITC, CD3 APC, CD4 A700, CD8 PB, Gr1 PE, CD11b PE-Cy7, F4/80 APC, Siglec F APC-Cy7, CD11c PB (Biolegend, San Diego, USA or BD Bioscience, Heidelberg, Germany). Cell phenotyping was performed on LSRII flow cytometer using FACS Diva software (BD Bioscience, Heidelberg, Germany) and analyzed using FlowJo software (Tree Star Inc). Leukocytes were analyzed as follows: Neutrophils in spleen and lung ($CD45+/CD11b^{high}/Gr1^{high}$), Lymphocytes in spleen and lung (B cells: CD45+/CD11b−/CD19+; T cells: CD45+/CD11b−/CD3+; NK cells: CD45+/NK1.1+/CD3−; NKT cells: CD45+/NK1.1+/CD3+), alveolar macrophages (CD45+/Gr1−/SiglecF+/CD11c+), macrophages in spleen (CD45+/Gr1−/CD11b+/CD11c−).

2.8. Analysis of leukocytes in BALF

Cytocentrifuge preparations of BALF samples were used for differential cell counting after May-Grünwald-Giemsa staining. The percentage of neutrophils, macrophages and lymphocytes was determined by examining 200 to 400 cells on 2 cytospins per sample and used to

calculate absolute numbers of leukocyte subsets using the total cell count per ml BALF.

2.9. Isolation and ex vivo stimulation of BALF and lung cells

BALF cells (100,000 cells/ml) and single-cell suspension (2×10^6 cells/ml) of isolated lung cells were diluted in Roswell park memorial institute medium (RPMI) (Biochrom GmbH, Berlin, Germany) with 10% FCS, 100 U/ml Penicillin/Streptomycin, L-Alanyl-ι-Glutamine (Biochrom GmbH, Berlin, Germany) and stimulated with 1 μg/ml lipopolysaccharide (LPS) (O55:B5, Sigma) for 12 h at 37 °C. Commercially available enzyme-linked immunosorbent assay (eBioscience, San Diego, USA) were used to analyze IL-6 and TNF-α concentrations in cell culture supernatant.

2.10. Statistics

Statistical analysis was performed using Prism 6.0 Software (GraphPad, San Diego, USA). Comparison between groups was performed using one-tailed Mann-Whitney, Kruskal-Wallis test followed by Dunn's test for multiple comparison or two-way ANOVA and Bonferroni's multiple comparisons test. Values were given as mean ± standard deviation (SD). *P*-values of $p \leq 0.05$ were considered as statistically significant.

3. Results

3.1. IFN-γ dose escalation in naïve mice

To test the efficacy of different IFN-γ doses on cytokine secretion and leukocyte recruitment in lung and blood, naïve mice were treated i.t. with 1 μg, 10 μg or 50 μg IFN-γ or solvent as control. Even 12 h after local treatment 3–8% of the applied IFN-γ were still detectable in BALF (Fig. 1 A). Already 1 μg IFN-γ was sufficient to induce a maximum IP-10 secretion in BALF, whereas TNF-α increased dose-dependently (Fig. 1 B—C). Only small amounts (0.01%) of the applied IFN-γ translocated from the airways into the blood, sufficient to induce detectable plasma levels of IP-10 but not of TNF-α 12 h after treatment (Fig. 1 D—F). Analysis of leukocytes in lung showed a significant increase of pulmonary lymphocytes in mice treated with 10 μg or 50 μg IFN-γ and neutrophils in mice treated with 50 μg IFN-γ (Fig. 1 G). Cellular composition of BALF showed no impact of i.t. IFN-γ treatment on neutrophil counts, but slightly diminished absolute macrophage numbers. Application of 50 μg IFN-γ led to a non-significant reduction of lymphocytes in BALF (Fig. 1H). Analysis of relative leukocyte composition of BALF showed a non-significant reduction of macrophages in mice treated with 1 μg, 10

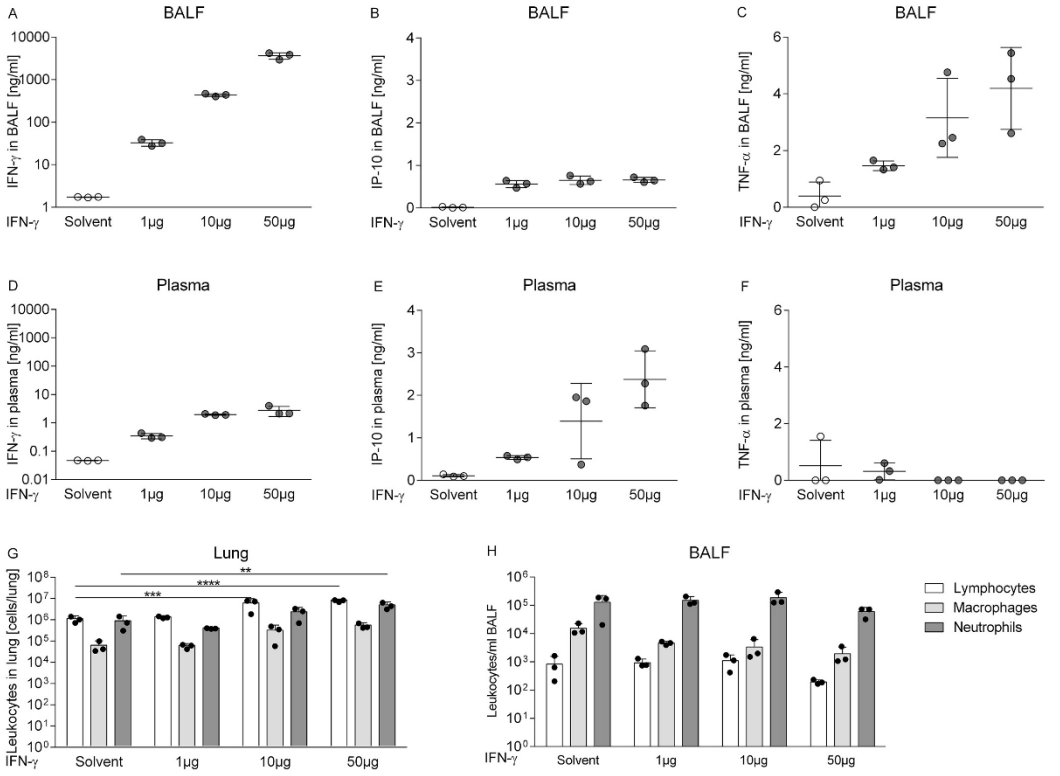

Fig. 1. Increased cytokine level and cell recruitment 12 h after IFN-γ treatment in naïve mice. Cytokines in BALF and plasma as well as cellularity of lung and BALF analyzed 12 h after i.t. application of solvent or IFN-γ in naïve mice indicate that IFN-γ (A, D) is capable of inducing IP-10 and TNF-α secretion in lavage (B, C) and IP-10 in plasma (E) as well as recruit lymphocytes and granulocytes to the lung (G) in a dose dependent manner, whereas alveolar macrophages and lymphocytes are slightly decreasing in BALF (H). Data from one experiment are shown as scatter plots (A-F) or as bars (G-H) with mean ± SD ($n = 3$) using two-way ANOVA and Dunn's multiple comparison compared to solvent treated mice as reference group; ** indicates $p < 0.01$; *** $p < 0.001$; **** $p < 0.0001$.

µg and 50 µg IFN-γ as well as a slightly decreased lymphocytes in mice treated with 50 µg IFN-γ. Since IFN-γ treatment had no effect on neutrophil numbers, the reduction of macrophages and lymphocytes resulted in significantly increased percentage of neutrophils (Fig. S1).

In order to assess the functionality of lung and BALF cells upon IFN-γ or solvent treatment, cells of naïve mice were isolated 12 h after application, stimulated with LPS for additional 12 h, and production of IL-6 and TNF-α measured in culture supernatants. IFN-γ increased IL-6 and TNF-α secretion by lung cells upon LPS stimulation in a dose-dependent manner (Fig. 2 A-B). In contrast, IFN-γ treatment did not augment the cytokine secretion by BAL cells upon LPS stimulation (Fig. 2 C—D).

3.2. Efficacy and safety of IFN-γ treatment after experimental stroke

In order to analyze whether local IFN-γ application is efficient and safe after experimental stoke, mice were treated with solvent or 1 µg IFN-γ one day after MCAo and infarct maturation as well as pro-inflammatory cytokine response in BALF and plasma were quantified and compared to solvent or 1 µg IFN-γ treated naïve mice (Fig. 3A). Infarct size and pro-inflammatory cytokines in plasma including IL-6, KC and TNF-α did not significantly differ between solvent and IFN-γ treated stroke mice 12 h after application (Fig. 3 B—C). Analysis of IFN-γ levels in BALF from stroke animals showed no endogenous IFN-γ secretion in solvent treated mice, whereas administration of exogenous IFN-γ one day after ischemia resulted in significantly increased IFN-γ levels in BALF within 12 h (Fig. S2A). We also determined whether IFN-γ treatment is able to increase IL-12 secretion, which in turn may induce the secretion of endogenous IFN-γ by T and NK cells. IFN-γ treatment resulted in a significant increase of IL-12p40 in naïve but not in MCAo mice (Fig. S2B). These data indicate that IFN-γ treatment is unlikely to induce endogenous IFN-γ production *via* IL-12 in stroke mice. Pro-inflammatory Cytokines in BALF including IL-6, KC and TNF-α and cellular composition of the lung indicated no impact of IFN-γ treatment compared to solvent treated MCAo mice. Notably, we found non-significantly elevated neutrophil counts in lung and IL-6 and KC cytokine levels in BALF as an indirect indicator of spontaneous bacterial infections in several solvent treated stroke mice (Fig. 3 D-E). *Ex vivo* LPS stimulation of lung single cell suspensions revealed that IFN-γ is capable to significantly increase TNF-α secretion by cells isolated from naïve mice. In contrast, IFN-γ treatment did not result in significantly increased TNF-α secretion by lung cells isolated from MCAo mice. Additionally, TNF-α level were significantly diminished upon LPS stimulation in MCAo mice compared to naïve mice. Interestingly, overall IL-6 level in supernatant of LPS stimulated lung cells from both MCAo groups were higher than those found in naïve mice. IFN-γ was capable of inducing in trend increased IL-6 levels upon LPS stimulation after experimental stroke (Fig. 3 F).

3.3. Impact of IFN-γ treatment on spontaneously developing infections after experimental stroke

To investigate the impact of IFN-γ treatment on spontaneously developing infections, MCAo mice were treated with IFN-γ or solvent one day after stroke onset. Naïve mice served as healthy controls. Infarct size and bacterial burden in BALF ($p = 0.1734$) and lung ($p = 0.2440$) determined 2 days after treatment (Fig. 4 A) were slightly reduced in IFN-γ treated mice but did not significantly differ between both MCAo groups (Fig. 4 B—D). Regression analysis revealed no correlation between infarct size and bacterial burden in lung (Solvent: $r = 0.08353$, $p = 0.8186$; IFN-γ: $r = 0.1394$; $p = 0.7009$) (Fig. 4 E), indicating even minor strokes may cause severe pulmonary infections. Since IFN-γ is an immunostimulatory cytokine, we analyzed the effect of IFN-γ treatment on pro-inflammatory cytokine levels in BALF and plasma during spontaneous pulmonary infection after stroke. 48 h after application, 0.6% of the applied IFN-γ concentration was still detectable in BALF and significantly elevated compared to solvent treated mice but failed to induce IP-10, IL-6, KC, MIP-1α or TNF-α secretion in BALF or plasma (Fig. 4 F-G). Flow cytometric analysis of pulmonary and peripheral leukocytes revealed that solvent treated mice showed a moderate increase of neutrophils in lavage, probably as a consequence of the slightly higher bacterial burden compared to IFN-γ treated mice (Fig. 4 H). Both

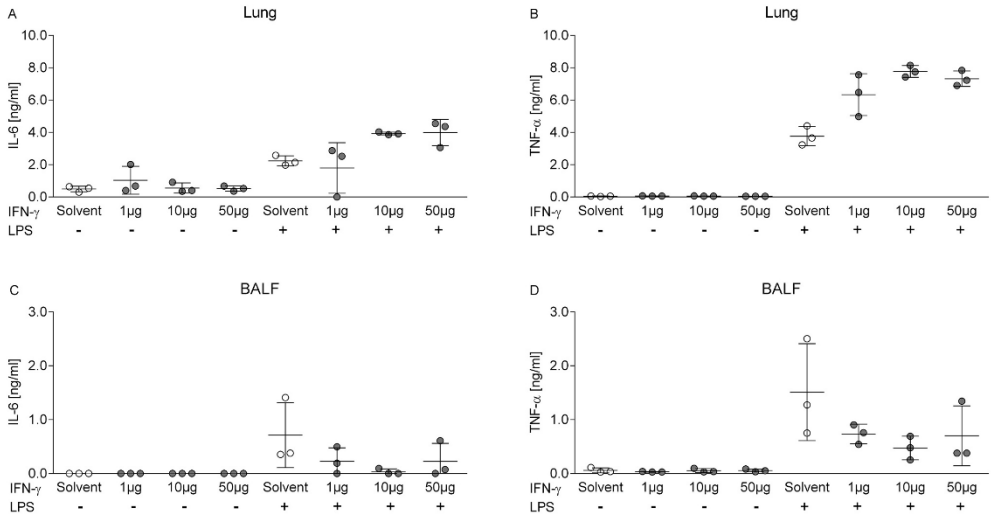

Fig. 2. IFN-γ treatment of naïve mice enhanced cytokine secretion by lung but not BAL cells upon *ex vivo* LPS stimulation. Lung and BAL cells were isolated 12 h after solvent or IFN-γ treatment and stimulated *ex vivo* with LPS for 12 h. IFN-γ improved functionality of lung cells indicated by increasing IL-6 (A) and TNF-α level (B) in cell culture supernatants. In contrast, IFN-γ application decreased IL-6 (C) and TNF-α level (D) in supernatant of LPS stimulated BAL cells. Data from one experiment ($n = 3$) are shown as scatter plots with mean ± SD.

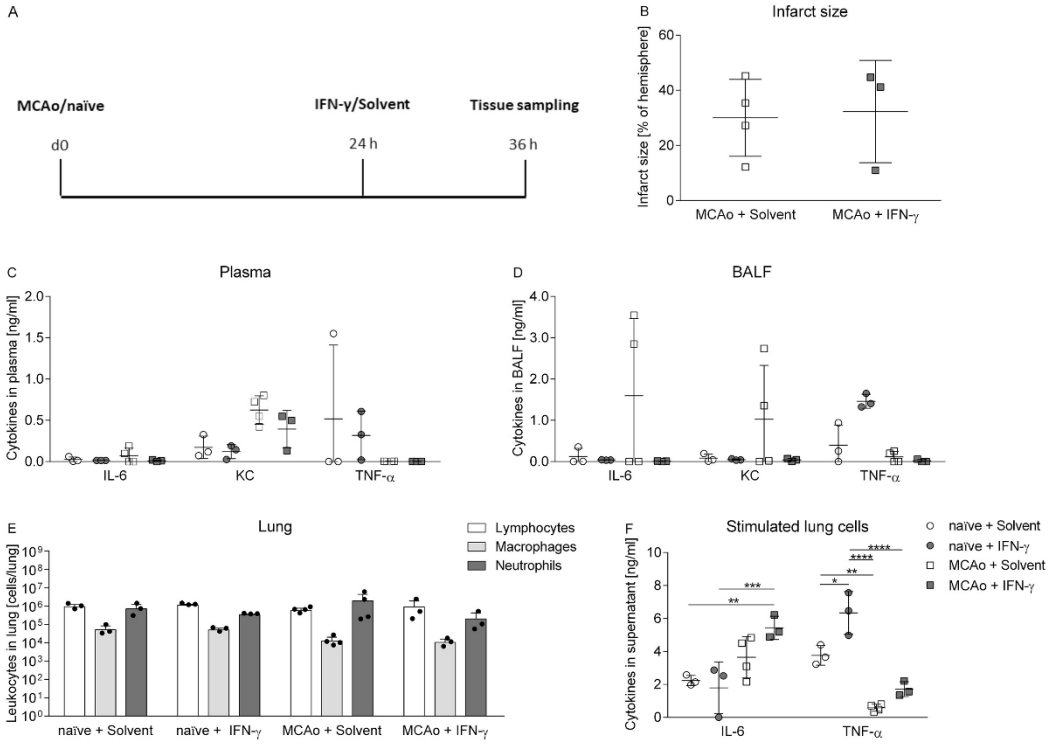

Fig. 3. Lower pro-inflammatory status in IFN-γ treated stroke mice. Experimental setup (A). IFN-γ applied 24 h after stroke had no impact on infarct size (B), pro-inflammatory cytokine secretion in plasma (C) and BALF (D) or leukocyte recruitment in the lung 12 h after treatment (E). *Ex vivo* LPS stimulated lung cells isolated from MCAo mice secreted significantly increased IL-6 level compared to lung cells isolated from healthy mice, whereas TNF-α could only slightly be induced by IFN-γ treatment after experimental stroke compared to naïve mice (F). Data from one experiment are shown as scatter plots (B—D, F) or bars (E) with mean ± SD ($n = 3$–4) and analyzed using one-tailed Mann-Whitney test (B) or two-way ANOVA and Bonferroni's multiple comparisons test (C—F); * indicates $p < 0.05$;** $p < 0.01$; *** $p < 0.001$; **** $p < 0.0001$.

MCAo groups showed the characteristic post stroke lymphopenia in lung and spleen. IFN-γ treatment had no impact on leukocyte composition in lung and spleen (Fig. 4 I-J).

3.4. IFN-γ treatment in a model of induced pneumococcal pneumonia after experimental stroke

To determine the effect of IFN-γ in a model of aspiration-induced pneumococcal pneumonia after stroke, mice were treated with i.t. IFN-γ at day three and i.n. infected with 10,000 CFU *S. pneumoniae* at day four after MCAo. Two days after infection infarct size, pathogen clearance, cellular composition of lung, spleen and BALF as well as cytokine secretion in BALF and plasma were examined (Fig. 5 A). Infarct size and bacterial burden in BALF ($p = 0.6$) did not differ between IFN-γ and solvent treated mice (Fig. 5 B—C), whereas IFN-γ treated mice showed slightly increased bacterial burden in the lung ($p = 0.2$) (Fig. 5 D). IFN-γ had no effect on IP-10 or cytokines in BALF and plasma during spontaneous pneumonia after stroke, but slightly induced IP-10 in BALF and significantly increased IP-10 levels in plasma during the course of induced pneumococcal pneumonia. Additionally, IL-6 levels were significantly increased in BALF from IFN-γ compared to solvent treated mice, while cytokines in plasma did not differ significantly (Fig. 5 *E*-F). Analysis of cellular composition revealed significantly increased lymphocytes in spleen and BALF as well as not significantly increased neutrophil counts in BALF and slightly reduced macrophages in lungs of IFN-γ compared to solvent treated mice during the course of a pneumococcal pneumonia (Fig. 5 G-I). In contrast, IFN-γ had no effect on cellularity in BALF, lung and spleen in the model of spontaneously developing infections.

4. Discussion

The main finding of the present study is that pulmonary administration of IFN-γ in stroke mice is safe, having no effect on infarct size and marginally improves pulmonary cytokine response. However, local immunostimulation with IFN-γ did not result in clinically meaningful reconstitution of lung antibacterial defense after experimental stroke and thus did not lead to significant prevention of spontaneous as well as *S. pneumoniae*-induced pneumonia in mice.

Pneumonia is the most frequent, severe medial complication after stroke and affects 7–22% of all stroke patients within the first few days after stroke (Chamorro et al., 2007). Dysphagia and aspiration were identified as the most commonly risk factors (Hoffmann et al., 2017; Holas et al., 1994; Perry and Love, 2001; Smithard et al., 1996). Furthermore, it was shown that central nervous system injuries, like stroke, induce a long lasting immunosuppression *via* overactivation of

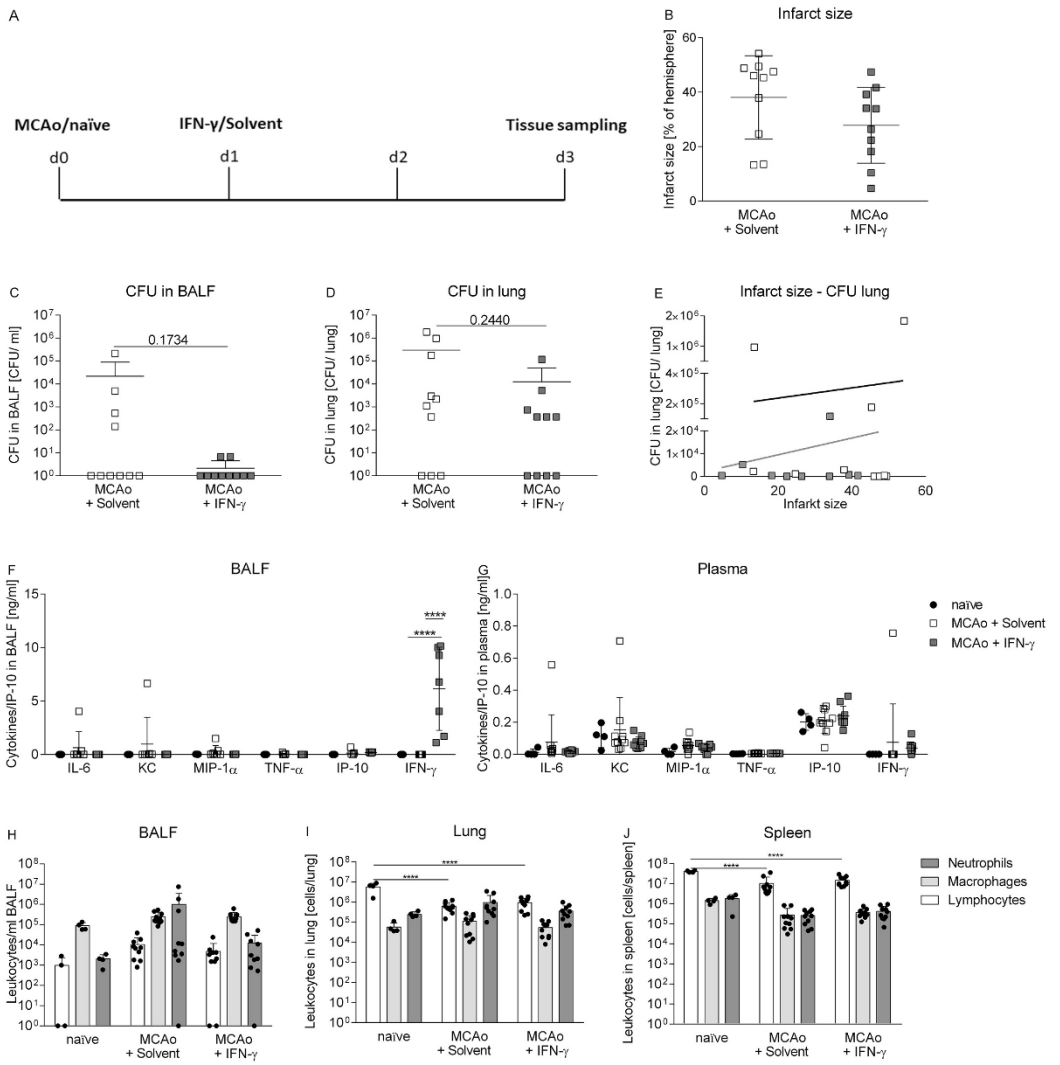

Fig. 4. IFN-γ slightly reduced the frequency of spontaneously developing infections after experimental stroke. Experimental setup (A). IFN-γ applied one day after stroke onset had no negative impact on infarct size and slightly reduced bacterial burden in BALF ($p = 0.1734$) and lung ($p = 0.2440$) investigated 2 days after treatment (B—D). IFN-γ was not capable of inducing pro-inflammatory cytokines in BALF and plasma (F-G) or leukocyte recruitment in BALF and lung (H—I). Splenic leukocytes were also not influenced by IFN-γ treatment (J). Regression analysis between infarct size and bacterial burden in lung showed no correlation for solvent ($r = 0.08353$; $p = 0.8186$) or IFN-γ treated mice ($r = 0.1394$; $p = 0.7009$) using two tailed Pearson Correlation (E). Data from 3 experiments ($n = 4$–10) are shown as scatter plots (B-G) or bars (H-J) and analyzed using one-tailed Mann-Whitney test for analysis of infarct size and bacterial burden (B—D) or two-way ANOVA with Bonferroni's multiple comparisons for cytokine analysis and cellularity (F-J). Values are given as mean ± SD; **** indicates $p < 0.0001$.

stress pathways, thereby contributing to the development of infections after stroke (Meisel et al., 2005). Overactivation of the sympathetic nervous system, parasympathetic nervous system and hypothalamic-pituitary-adrenal axis results in a decrease of inflammatory cytokines including IFN-γ as well as stroke-induced apoptosis of IFN-γ producing lymphocytes contributing to the development of SAP (Meisel et al., 2005; Prass et al., 2003; Santos Samary et al., 2016). IFN-γ is essential for the cellular response to viral and microbial pathogens as it promotes phagocytosis in macrophages, upregulation of chemokine and cytokine expression and stimulation of antigen presentation in B cells, macrophages and dendritic cells. (Boehm et al., 1997; Murray, 1988; Schroder et al., 2004). IFN-γ induces the expression of the pro-inflammatory chemokine IP-10 playing an important role in T cell migration and stimulation of monocytes and NK cells (Neville et al., 1997). Studies in

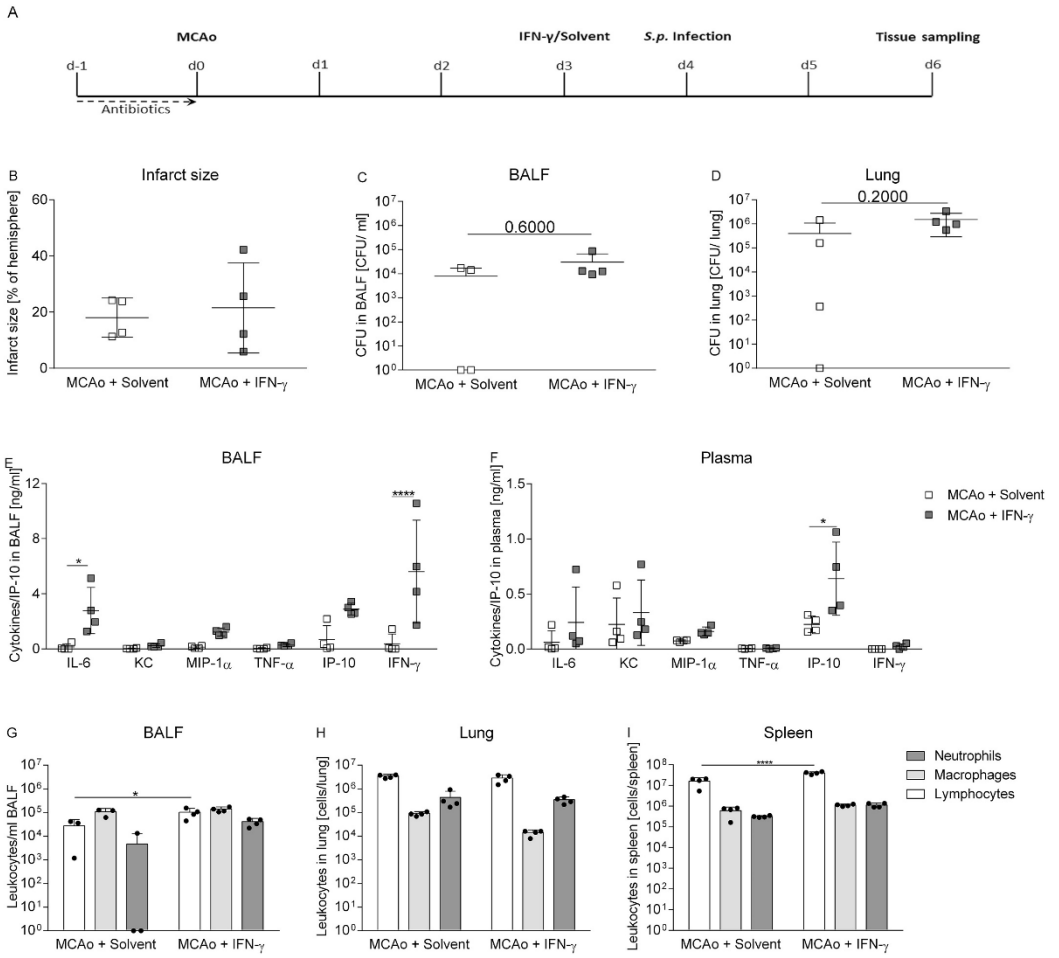

Fig. 5. IFN-γ treatment slightly reduced clearance of aspirated pneumococci after experimental stroke. MCAo mice were infected i.n. with *S. pneumoniae* one day after solvent or IFN-γ treatment, which was performed on day 3 after MCAo. Infarct size, bacterial burden in lung and BALF, cytokines in plasma and BALF as well as cellularity in spleen, lung and BALF were investigated two days after infection (A). IFN-γ treatment had no negative effect on infarct size (B) and bacterial burden in BALF ($p = 0.6000$) (C) but slightly increased bacterial burden in lung ($P = 0.2000$) (D). IFN-γ was able to slightly induce IP-10 in BALF and significantly increase IP-10 in plasma. Analysis of pro-inflammatory cytokine response showed significant increased IL-6 concentration in BALF from IFN-γ compared to solvent treated mice, whereas cytokines in plasma did not differ between both groups (E, F). Lymphocytes in spleen and BALF were significantly increased and neutrophils in BALF slightly increased in IFN-γ treated compared to the control group. Macrophages in lung were tended to diminish in IFN-γ compared to solvent treated mice. In contrast, macrophages in BALF and spleen, neutrophils in lung and spleen as well as lymphocytes in lung were unaffected by IFN-γ treatment (G-I). Data from one experiment are shown ($n = 3$–4 per group) as scatter plots or bars using one-tailed Mann-Whitney test for infarct analysis (B) and for analysis of bacterial burden (C—D) or using two-way ANOVA and Bonferroni's multiple comparisons test (*E*-I) . Values are given as mean ± SD; * indicates $p < 0.05$.

mice showed that the lack of IFN-γ led to increased mortality and diminished elimination of i.n. induced *Legionella pneumophila* infection (Shinozawa et al., 2002). Similar findings were reported in a mouse model of pulmonary *Klebsiella pneumoniae* infection (Moore et al., 2002). Additionally, IFN-γ treatment was tested in clinical studies demonstrating that different diseases such as tuberculosis, *Mycobacterium avium* complex infections, scleroderma and fungal infections in immunosuppressed patients were successfully treated with recombinant IFN-γ or adenovirus vectors expressing IFN-γ (Miller et al., 2009). In proof-of-principle clinical studies, immunomodulatory therapy was already tested in septic patients with temporary immunosuppression demonstrating that IFN-γ and GM-CSF treatment successfully reconstituted immune function and improved the clinical course (Döcke et al., 1997; Meisel et al., 2009). These data suggest that local IFN-γ application could prevent development of SAP.

Several studies suggest that IFN-γ contributes to brain damage and neurodegeneration after experimental stroke. Myelin basic protein promotor-IFN-γ-transgenic mice showed significantly increased infarct volumes compared to wild type (WT) littermates (Lambertsen et al., 2004). Additionally, application of IFN-γ neutralizing antibody 24 h, 48

h, 72 h after stroke led to significantly decreased infarct volume compared to controls (Seifert et al., 2014). Furthermore, it was shown that splenic-derived IFN-γ contributes to increased IFN-γ protein level in injured brain at 72 h following MCAo and splenectomy significantly decreased IFN-γ level (Seifert et al., 2012). To prevent systemic effects worsening neurological outcome, we opted for a local, pulmonary IFN-γ treatment under visual control using bronchoscopy. Although IFN-γ translocated partially from lung into the blood having measurable systemic effects, we found no negative impact on infarct size development, indicating local application after experimental stroke is safe and therefore basically suitable for the treatment of SAP.

Data on local pulmonary IFN-γ treatment in mice are scarce. Therefore, we established an IFN-γ dose suitable for treatment of SAP. Mice treated with 10 μg or 50 μg IFN-γ showed an intolerance and impaired medical condition. In addition, we observed excessive TNF-α level and IFN-γ level in BAL 12 h post-application. It has been described that an exaggerated secretion of TNF-α and IFN-γ can lead to pathological processes including increased oxidative and nitrosative stress, cytotoxicity and tissue injury (Malaviya et al., 2017; Peteranderl and Herold, 2017; Tracey and PDA, 1994). Hence, high IFN-γ concentrations resulted in an unbalanced, overshooting inflammatory response and were therefore unsuitable for treatment. In contrast, application of 1 μg IFN-γ was sufficient to induce IP-10 and TNF-α in BALF as well as dose-dependently enhance IL-6 and TNF-α secretion by LPS stimulated lung cells, suggesting that 1 μg IFN-γ could be suitable for prevention of SAP in mice. Interestingly, we observed that IFN-γ pretreatment of LPS stimulated BALF cells showed no improved TNF-α and IL-6 secretion. TNF-α is mainly expressed by macrophages (Bazzoni and Beutler, 1996), whereas IL-6 can be released by several immune cells including macrophages, monocytes and T cells as well as from epithelial cells and endothelial cells in response to inflammatory stimuli and tissue damage (Choy and Rose-John, 2017; Crestani et al., 1994). We observed that i.t. IFN-γ application in naïve mice changes the cellular composition of BALF including a decrease of percentage of macrophages. In contrast, macrophages in lung tissue were unaffected by IFN-γ treatment, suggesting that differences in cellular composition of lung and BALF seemed to contribute to the contrary cytokine response to LPS stimulation. Finally, the underlying mechanisms for the observed differences are not conclusively clarified.

Whereas IFN-γ application significantly enhanced pulmonary cytokine response to LPS by lung cells isolated from naïve mice, IFN-γ treatment resulted only in a minor increase of TNF-α secretion by lung cells isolated from MCAo mice. These data indicate, that local IFN-γ administration may not fully reconstitute stroke-induced impaired cytokine responses in lung and peripheral blood which have been demonstrated already previously after experimental stroke (Engel et al., 2015). LPS stimulated blood cells showed diminished TNF-α secretion 12 h and 2 days after stroke compared to sham operated mice. Blockade of the sympathetic nervous system by propranolol treatment prevented the reduction of TNF-α secretion (Prass et al., 2003). *Ex vivo* stimulation of lung cells with LPS confirmed an impaired TNF-α response, whereas vagotomy performed 5 days before MCAo reversed the effect suggesting also a role of cholinergic signaling in impaired TNF-α secretion after stroke (Engel et al., 2015). Stroke mice without pulmonary infections showed significantly diminished cytokine levels including TNF-α, IL-1ß, IL-17A, IL-27, IL-1α in the lung compared to sham mice 72 h after surgery (Farris et al., 2019). An impaired TNF-α response to LPS was also shown in patients with trauma- or sepsis-associated immunosuppression. It was demonstrated that increased IL-10 and TGF-β1 levels in septic patients contribute to monocyte deactivation and consequently to LPS tolerance. PBMCs isolated from septic patients were pretreated with or without IFN-γ and stimulated with LPS. IFN-γ treatment resulted in significantly enhanced TNF-α response to LPS, but the response was significantly lower than pretreated naïve PBMCs (Döcke et al., 1997). A clinical study demonstrated that stroke patients also showed increased serum levels of IL-10 and TGF-β1 (Jiang et al., 2017) suggesting that these anti-inflammatory cytokines could also contribute to an impaired TNF-α response, which cannot be completely reconstituted by IFN-γ treatment. Furthermore, *in vitro* experiments demonstrated that IFN-γ treatment regulates TNF-α expression at the transcriptional level by the transcription factors IFN regulatory factor-1 (IRF-1) and IRF-8 (Vila-del Sol et al., 2008). Stroke leads to an overactivation of the cholinergic signaling (Engel et al., 2015), whereby acetylcholine interacts with the nicotinic acetylcholine receptors on macrophages and alveolar epithelial cells and blocks the nuclear factor 'kappa-light-chain-enhancer' of activated B-cells (NF-κB) signaling, resulting in diminished TNF-α expression (Ren et al., 2017). IRF-1 and NF-κB were shown to interact and synergistically activate transcription, suggesting that IRF-1 and IRF-2 cannot increase TNF-α transcription without NF-κB (Drew et al., 1995; Saura et al., 1999). IL-6 secretion by lung cells upon LPS stimulation was also described to be impaired after experimental stroke (Engel et al., 2015). In the present study, we observed significantly increased IL-6 secretion upon *ex vivo* LPS stimulation of lung cells from IFN-γ treated MCAo mice, suggesting that IFN-γ is capable of reconstituting IL-6 response after experimental stroke by NF-κB and IRF-1 independent mechanisms. IFN-γ is not only able to prime macrophages for an enhanced and more rapid pro-inflammatory cytokine response to pathogens, but also to an increased IL-12 secretion by macrophages, which in turn can increase the release of IFN-γ by NK cells and induces the differentiation of $CD4^+$ cells into IFN-γ producing Th1 cells (Ma et al., 2015). Treatment of murine macrophages with recombinant IFN-γ resulted in induction of IL-12 mRNA expression beginning after 12 h (Yoshida et al., 1994). In line with this observation, we found significantly increased IL-12p40 levels in BALF of naïve mice 12 h after i.t. IFN-γ administration suggesting that IFN-γ treatment may induce endogenous IFN-γ production *via* IL-12 in immunocompetent hosts. However, clinical studies showed significantly decreased IL-12p70 levels in the serum of stroke patients compared to healthy controls one day after stroke onset (Vogelgesang et al., 2010). Additionally, analysis of blood plasma of stroke patients demonstrated significantly increased expression levels of miRNA-21 (Lin et al., 2016), which was shown to inhibit IL-12p35 expression resulting in diminished IL-12 production (Lu et al., 2009). In contrast to naïve mice, we found that applied IFN-γ was not capable of inducing pulmonary IL-12 production in stroke mice. Whether this effect involves miRNA-21 dependent mechanisms remains to be investigated. Our data indicate that IFN-γ treatment did not result in an induction of endogenous IFN-γ production *via* IL-12 in stroke mice.

In our experimental stroke model, we previously demonstrated that suppression of systemic immunity including decreased number of lymphocytes in blood and spleen along with diminished TNF-α and IFN-γ level in blood starting 12 h after stroke onset with a maximum at day 3 (Prass et al., 2003). In addition, pulmonary immunity was shown to be impaired 24 h and 72 h after experimental stroke in mice (Farris et al., 2019). Consequently, pulmonary infections were observed between day 2 and 5 in mice as well as in patients (Kishore et al., 2019; Prass et al., 2003). These data indicate that immunostimulatory therapy has to be applied early after stroke onset in order to be successful. Therefore, we decided to apply IFN-γ one day after MCAo to prevent spontaneous infections. We found that pulmonary IFN-γ treatment only slightly reduced the frequency of spontaneously developing infections after experimental stroke. Experiments in mice already demonstrated that IFN-γ plays an important role in the immune response against pulmonary infections. IFN-γ-deficient mice showed a diminished clearance of aspirated *Klebsiella pneumonia* or *Legionella pneumophila* due to an impaired neutrophil and lymphocyte recruitment as well as reduced pro-inflammatory cytokines and increased IL-10 responses (Moore et al., 2002; Yoshida et al., 2001). Additionally, *Pseudomonas aeruginosa* pneumonia treated with a recombinant adenovirus encoding murine IFN-γ improved pathogen clearance in a TNF-α independent manner (Lei et al., 1997). Although IFN-γ treatment in the present study showed an immunostimulatory effect, the pulmonary immune response was not sufficient to prevent spontaneously developing infection after

experimental stroke.

In order to mimic aspiration-induced pneumococcal pneumonia, we infected mice intranasally with *S. pneumoniae* serotype 3 at day 4 after MCAo. Stroke mice instilled with pneumococci serotype 2 developed severe pulmonary infections, whereas sham operated mice and naïve mice were able to clear inoculated bacteria (Jagdmann et al., 2020; Prass et al., 2006). In this study, we found that IFN-γ treatment on day 3 after stroke onset did not improve the course of pneumococcal pneumonia after experimental stroke. The beneficial role of IFN-γ in *S. pneumoniae* defense is still under debate. Whereas the LD (lethal dose) 50% of *S. pneumoniae* serotype 2 in IFN-γ deficient C57BL6/J mice was 20-fold lower compared to WT controls (Rubins and Pomeroy, 1997), IFN-γ-receptor deficient 129/Sv/Ev mice infected with serotype 3 showed a diminished bacterial burden and due to improved inflammatory infiltrates and pathogen clearing (Rijneveld et al., 2002). It is well known that mouse strains differ in their susceptibility to infections (Gingles et al., 2001; Kadioglu and Andrew, 2005; Schulte-Herbrüggen et al., 2006) and pneumococcal serotypes vary in pathogenicity (Trzciński et al., 2015). Therefore, it is likely that infection route, mouse strain and pneumococcal serotype determine whether IFN-γ supports or impairs pulmonary pneumococcal defense. However, different *in vivo* experiments provide evidence that IFN-γ treatment has a negative effect on the course of a pneumococcal pneumonia using the A66.1 strain, a mouse-passaged derivative of the clinical isolate A66 NCTC 7978 (Gor et al., 2005), used in this study. IFN-γ treatment was shown to diminish phagocytosis of alveolar macrophages resulting in an impaired bacterial clearance of i.n. inoculated *S. pneumoniae* strain A66.1. *In vitro* experiments confirmed the reduced uptake of bacteria by macrophages after IFN-γ exposition (Sun and Metzger, 2008). It is well known that IFN-γ induces the expression of three chemokines, CXCL9, CXCL10, and CXCL11, that all bind to the chemokine receptor CXCR3 (Loetscher et al., 1996; Metzemaekers et al., 2018). Experiments in CXCR3 KO mice demonstrated a reduced bacterial burden, attenuated inflammation, less lung tissue damage and significantly improved survival upon i.n. *S. pneumoniae* strain A66.1 infection compared to WT littermates (Seyoum et al., 2011). In summary, these data suggest that excessive increased IFN-γ levels could be harmful and result in an impaired clearance of *S. pneumoniae* strain A66.1. In the present study, we observed significantly increased lymphocytes in spleen and BALF as well as slightly increased neutrophils in BAL of IFN-γ treated stroke mice. Furthermore, pneumococcal infection resulted in a significant increased IL-6 response in IFN-γ compared to solvent treated mice. These beneficial immune responses contradict the increased susceptibility to *S. pneumoniae*. The responsible mechanism for the observed effects on the course of induced pneumococcal pneumonia after experimental stroke remains unknown and reflects the importance of pathogen identification in mice and human.

In line with clinical observations (Johnston et al., 1998; Katzan et al., 2003; Meisel et al., 2005) not all mice suffered from spontaneous post stroke infections. Since experimental stroke is close to the situation in patients, the variability in onset and bacterial load as well as pathogen spectrum result in a high demand of animals to achieve clear effects. In contrast, aspiration-induced pneumococcal pneumonia is much more reproducible, since every mouse is infected with a defined dose of a known bacterial strain.

One limitation of the study is that we only tested single IFN-γ administration. Since repetitive inhalation of IFN-γ might be more effective, further investigations are required. The crucial limitation is the lack of experimental replicates leading to a relatively small sample size in the IFN-γ dose escalation and in the IFN-γ treatment of the pneumococcal pneumonia after stroke. Since IFN-γ doses exceeding 10 μg were absolutely intolerable and the IFN-γ treatment of a pneumococcal pneumonia worsened the clinical course of the infection, further experiments would have represented a disproportionate violation of the animal welfare rights and were therefore not justifiable. Therefore, small to moderate effects are associated with insufficient power to detect differences between the treatment groups. Larger sample sizes would be required to achieve sufficient statistical power and draw definite conclusions. However, our assumption that IFN-γ administration has no major beneficial effect seems reasonable.

5. Conclusions

In summary, our findings suggest that i.t. IFN-γ treatment in experimental stroke is safe having no negative impact on infarct size. Although IFN-γ resulted in beneficial effects on the pulmonary immune response in healthy mice and in part also in spontaneous SAP, our data suggest that IFN-γ i.t. treatment is not effective for prevention or early treatment of SAP.

Funding

This work was supported by the German Research Foundation [SFB-TRR84, SFB-TRR167], Einstein Foundation [A-2017-406], Leducq Foundation [19CVD01] and German Ministry of Education and Research (BMBF) in the framework of the CAPSyS (01ZX1304B) and SYMPATH (01ZX1906A) project. The sponsor was not involved in study design and preparation of the article.

Declaration of Competing Interest

None.

Acknowledgements

We would like to thank Susanne Metzkow, Sabine Kolodziej, Claudia Muselmann-Genschow and Denise Barthel for their excellent technical assistance and we would like to acknowledge the assistance of the BIH Cytometry Core.

Appendix A. Supplementary data

Supplementary data to this article can be found online at https://doi.org/10.1016/j.jneuroim.2021.577568.

References

Armstrong, J.R., Mosher, B.D., 2011. Aspiration pneumonia after stroke: intervention and prevention. The Neurohospitalist. 1, 85–93.
Bazzoni, F., Beutler, B., 1996. The tumor necrosis factor ligand and receptor families. N. Engl. J. Med. 334, 1717–1725.
Boehm, U., Klamp, T., Groot, M., Howard, J.C., 1997. Cellular responses to interferon-γ. Annu. Rev. Immunol. 15, 749–795.
Chamorro, Á., Urra, X., Planas, Anna M., 2007. Infection after acute ischemic stroke. Stroke. 38, 1097–1103.
Choy, E., Rose-John, S., 2017. Interleukin-6 as a multifunctional regulator: inflammation, immune response, and fibrosis. J. Scleroderma Rel. Disord. 2, 1–5.
Crestani, B., Cornillet, P., Dehoux, M., Rolland, C., Guenounou, M., Aubier, M., 1994. Alveolar type II epithelial cells produce interleukin-6 in vitro and in vivo. Regulation by alveolar macrophage secretory products. J. Clin. Invest. 94, 731–740.
Dames, C., Akyüz, L., Reppe, K., Tabeling, C., Dietert, K., Kershaw, O., et al., 2014. Miniaturized bronchoscopy enables unilateral investigation, application, and sampling in mice. Am. J. Respir. Cell Mol. Biol. 51, 730–737.
Dirnagl, U., Klehmet, J., Braun Johann, S., Harms, H., Meisel, C., Ziemssen, T., et al., 2007. Stroke-induced Immunodepression. Stroke. 38, 770–773.
Döcke, W.D., Randow, F., Syrbe, U., Krausch, D., Asadullah, K., Reinke, P., et al., 1997. Monocyte deactivation in septic patients: restoration by IFN-gamma treatment. Nat. Med. 3, 678–681.
Drew, P.D., Franzoso, G., Becker, K.G., Bours, V., Carlson, L.M., Siebenlist, U., et al., 1995. NF kappa B and interferon regulatory factor 1 physically interact and synergistically induce major histocompatibility class I gene expression. J. Interf. Cytokine Res. 15, 1037–1045.
Emsley, H.C.A., Hopkins, S.J., 2008. Acute ischaemic stroke and infection: recent and emerging concepts. The Lancet Neurol. 7, 341–353.
Engel, O., Kolodziej, S., Dirnagl, U., Prinz, V., 2011. Modeling stroke in mice - middle cerebral artery occlusion with the filament model. J. Vis. Exp.
Engel, O., Akyuz, L., da Costa Goncalves, A.C., Winek, K., Dames, C., Thielke, M., et al., 2015. Cholinergic pathway suppresses pulmonary innate immunity facilitating pneumonia after stroke. Stroke. 46, 3232–3240.

Farris, B.Y., Monaghan, K.L., Zheng, W., Amend, C.D., Hu, H., Ammer, A.G., et al., 2019. Ischemic stroke alters immune cell niche and chemokine profile in mice independent of spontaneous bacterial infection. Immunity, Inflammation and Disease. 7, 326–341.
Gingles, N.A., Alexander, J.E., Kadioglu, A., Andrew, P.W., Kerr, A., Mitchell, T.J., et al., 2001. Role of genetic resistance in invasive pneumococcal infection: identification and study of susceptibility and resistance in inbred mouse strains. Infect. Immun. 69, 426.
Gor, D.O., Ding, X., Briles, D.E., Jacobs, M.R., Greenspan, N.S., 2005. Relationship between surface accessibility for PpmA, PsaA, and PspA and antibody-mediated immunity to systemic infection by Streptococcus pneumoniae. Infect. Immun. 73, 1304–1312.
Hoffmann, S., Harms, H., Ulm, L., Nabavi, D.G., Mackert, B.-M., Schmehl, I., et al., 2017. Stroke-induced immunodepression and dysphagia independently predict stroke-associated pneumonia - the PREDICT study. J. Cereb. Blood Flow Metab. 37, 3671–3682.
Holas, M.A., DePippo, K.L., Reding, M.J., 1994. Aspiration and relative risk of medical complications following stroke. Arch. Neurol. 51, 1051–1053.
Huang, Y.-Y., Li, X., Li, X., Sheng, Y.-Y., Zhuang, P.-W., Zhang, Y.-J., 2019. Neuroimmune crosstalk in central nervous system injury-induced infection and pharmacological intervention. Brain Res. Bull. 153, 232–238.
Jagdmann, S., Dames, C., Berchtold, D., Winek, K., Weitbrecht, L., Meisel, A., et al., 2020. Impact of key nicotinic AChR subunits on post-stroke pneumococcal pneumonia. Vaccines (Basel) 8.
Jiang, C., Kong, W., Wang, Y., Ziai, W., Yang, Q., Zuo, F., et al., 2017. Changes in the cellular immune system and circulating inflammatory markers of stroke patients. Oncotarget. 8, 3553–3567.
Johnston, K.C., Li, J.Y., Lyden, P.D., Hanson, S.K., Feasby, T.E., Adams, R.J., et al., 1998. Medical and neurological complications of ischemic stroke: experience from the RANTTAS trial. RANTTAS Investigators. Stroke. 29, 447–453.
Kadioglu, A., Andrew, P.W., 2005. Susceptibility and resistance to pneumococcal disease in mice. Briefings Funct. Gen. 4, 241–247.
Katzan, I.L., Cebul, R.D., Husak, S.H., Dawson, N.V., Baker, D.W., 2003. The effect of pneumonia on mortality among patients hospitalized for acute stroke. Neurology. 60, 620.
Khor, M., Lowrie, D.B., Coates, A.R., Mitchison, D.A., 1986. Recombinant interferon-gamma and chemotherapy with isoniazid and rifampicin in experimental murine tuberculosis. Br. J. Exp. Pathol. 67, 587–596.
Kiderlen, A.F., Kaufmann, S.H.E., Lohmann-Matthes, M.-L., 1984. Protection of mice against the intracellular bacterium listeria monocytogenes by recombinant immune interferon. Eur. J. Immunol. 14, 964–967.
Kishore Amit, K., Vail, A., Jeans Adam, R., Chamorro, A., Di Napoli, M., Kalra, L., et al., 2018. Microbiological etiologies of pneumonia complicating stroke. Stroke. 49, 1602–1609.
Kishore, A.K., Jeans, A.R., Garau, J., Bustamante, A., Kalra, L., Langhorne, P., et al., 2019. Antibiotic treatment for pneumonia complicating stroke: recommendations from the pneumonia in stroke consensus (PISCES) group. Eur Stroke J. 4, 318–328.
Lambertsen, K.L., Gregersen, R., Meldgaard, M., Clausen, B.H., Heibøl, E.K., Ladeby, R., et al., 2004. A role for interferon-gamma in focal cerebral ischemia in mice. J. Neuropathol. Exp. Neurol. 63, 942–955.
Lei, D., Lancaster Jr., J.R., Joshi, M.S., Nelson, S., Stoltz, D., Bagby, G.J., et al., 1997. Activation of alveolar macrophages and lung host defenses using transfer of the interferon-gamma gene. Am. J. Phys. 272, L852–L859.
Lin, S.P., Ye, S., Chen, X.H., Jiang, H.L., Mao, H.F., Chen, M.T., et al., 2016. Increased expression of microRNA-21 in peripheral blood mediates the down-regulation of IFN-γ and increases the prevalence of stroke-associated infection. J. Neurol. Sci. 366, 235–239.
Loetscher, M., Gerber, B., Loetscher, P., Jones, S.A., Piali, L., Clark-Lewis, I., et al., 1996. Chemokine receptor specific for IP10 and mig: structure, function, and expression in activated T-lymphocytes. J. Exp. Med. 184, 963–969.
Lu, T.X., Munitz, A., Rothenberg, M.E., 2009. MicroRNA-21 is up-regulated in allergic airway inflammation and regulates IL-12p35 expression. J. Immunol. 182, 4994.
Ma, X., Yan, W., Zheng, H., Du, Q., Zhang, L., Ban, Y., et al., 2015. Regulation of IL-10 and IL-12 production and function in macrophages and dendritic cells. F1000Res. 4. F1000 Faculty Rev-465.
Malaviya, R., Laskin, J.D., Laskin, D.L., 2017. Anti-TNFα therapy in inflammatory lung diseases. Pharmacol. Ther. 180, 90–98.
McCabe, R.E., Luft, B.J., Remington, J.S., 1984. Effect of murine interferon gamma on murine toxoplasmosis. J. Infect. Dis. 150, 961–962.
McCulloch, L., Smith, C.J., McColl, B.W., 2017. Adrenergic-mediated loss of splenic marginal zone B cells contributes to infection susceptibility after stroke. Nat. Commun. 8, 15051.
Meisel, C., Schwab, J.M., Prass, K., Meisel, A., Dirnagl, U., 2005. Central nervous system injury-induced immune deficiency syndrome. Nat. Rev. Neurosci. 6, 775–786.
Meisel, C., Schefold, J.C., Pschowski, R., Baumann, T., Hetzger, K., Gregor, J., et al., 2009. Granulocyte-macrophage colony-stimulating factor to reverse sepsis-associated immunosuppression: a double-blind, randomized, placebo-controlled multicenter trial. Am. J. Respir. Crit. Care Med. 180, 640–648.
Metzemaekers, M., Vanheule, V., Janssens, R., Struyf, S., Proost, P., 2018. Overview of the mechanisms that May contribute to the non-redundant activities of interferon-inducible CXC chemokine receptor 3 ligands. Front. Immunol. 8.
Miller, C.H.T., Maher, S.G., Young, H.A., 2009. Clinical use of interferon-gamma. Ann. N. Y. Acad. Sci. 1182, 69–79.
Moore, T.A., Perry, M.L., Getsoian, A.G., Newstead, M.W., Standiford, T.J., 2002. Divergent role of gamma interferon in a murine model of pulmonary versus systemic *Klebsiella pneumoniae* infection. Infect. Immun. 70, 6310.
Mracsko, E., Stegemann-Koniszewski, S., Na, S.Y., Dalpke, A., Bruder, D., Lasitschka, F., et al., 2017. A mouse model of post-stroke pneumonia induced by intra-tracheal inoculation with Streptococcus pneumoniae. Cerebrovasc. Dis. 43, 99–109.
Murray, H.W., 1988. Interferon-gamma, the activated macrophage, and host defense against microbial challenge. Ann. Intern. Med. 108, 595–608.
Neville, L.F., Mathiak, G., Bagasra, O., 1997. The immunobiology of interferon-gamma inducible protein 10 kD (IP-10): a novel, pleiotropic member of the C-X-C chemokine superfamily. Cytokine Growth Factor Rev. 8, 207–219.
Perry, L., Love, C.P., 2001. Screening for dysphagia and aspiration in acute stroke: a systematic review. Dysphagia. 16, 7–18.
Peteranderl, C., Herold, S., 2017. The impact of the interferon/TNF-related apoptosis-inducing ligand signaling Axis on disease progression in respiratory viral infection and beyond. Front. Immunol. 8.
Prass, K., Meisel, C., Höflich, C., Braun, J., Halle, E., Wolf, T., et al., 2003. Stroke-induced immunodeficiency promotes spontaneous bacterial infections and is mediated by sympathetic activation reversal by Poststroke T helper cell type 1–like Immunostimulation. J. Exp. Med. 198, 725.
Prass, K., Braun Johann, S., Dirnagl, U., Meisel, C., Meisel, A., 2006. Stroke propagates bacterial aspiration to pneumonia in a model of cerebral ischemia. Stroke. 37, 2607–2612.
Ren, C., Tong, Y.-L., Li, J.-C., Lu, Z.-Q., Yao, Y.-M., 2017. The protective effect of alpha 7 nicotinic acetylcholine receptor activation on critical illness and its mechanism. Int. J. Biol. Sci. 13, 46–56.
Rijneveld, A.W., Lauw, F.N., Schultz, M.J., Florquin, S., Te Velde, A.A., Speelman, P., et al., 2002. The role of interferon-gamma in murine pneumococcal pneumonia. J. Infect. Dis. 185, 91–97.
Rubins, J.B., Pomeroy, C., 1997. Role of gamma interferon in the pathogenesis of bacteremic pneumococcal pneumonia. Infect. Immun. 65, 2975–2977.
Santos Samary, C., Pelosi, P., Leme Silva, P., Rieken Macedo Rocco, P., 2016. Immunomodulation after ischemic stroke: potential mechanisms and implications for therapy. Crit. Care 20, 391.
Saura, M., Zaragoza, C., Bao, C., McMillan, A., Lowenstein, C.J., 1999. Interaction of interferon regulatory factor-1 and nuclear factor kappaB during activation of inducible nitric oxide synthase transcription. J. Mol. Biol. 289, 459–471.
Schroder, K., Hertzog, P.J., Ravasi, T., Hume, D.A., 2004. Interferon-γ: an overview of signals, mechanisms and functions. J. Leukoc. Biol. 75, 163–189.
Schulte-Herbrüggen, O., Klehmet, J., Quarcoo, D., Meisel, C., Meisel, A., 2006. Mouse strains differ in their susceptibility to poststroke infections. Neuroimmunomodulation. 13, 13–18.
Seifert, H.A., Leonardo, C.C., Hall, A.A., Rowe, D.D., Collier, L.A., Benkovic, S.A., et al., 2012. The spleen contributes to stroke induced neurodegeneration through interferon gamma signaling. Metab. Brain Dis. 27, 131–141.
Seifert, H.A., Collier, L.A., Chapman, C.B., Benkovic, S.A., Willing, A.E., Pennypacker, K. R., 2014. Pro-inflammatory interferon gamma signaling is directly associated with stroke induced neurodegeneration. J. NeuroImmune Pharmacol. 9, 679–689.
Sellars, C., Bowie, L., Bagg, J., Sweeney, M.P., Miller, H., Tilston, J., et al., 2007. Risk factors for chest infection in acute stroke. Stroke. 38, 2284–2291.
Seyoum, B., Yano, M., Pirofski, L.A., 2011. The innate immune response to Streptococcus pneumoniae in the lung depends on serotype and host response. Vaccine. 29, 8002–8011.
Shi, K., Wood, K., Shi, F.-D., Wang, X., Liu, Q., 2018. Stroke-induced immunosuppression and poststroke infection. Stroke Vascul. Neurol. 3, 34.
Shinozawa, Y., Matsumoto, T., Uchida, K., Tsujimoto, S., Iwakura, Y., Yamaguchi, K., 2002. Role of interferon-gamma in inflammatory responses in murine respiratory infection with legionella pneumophila. J. Med. Microbiol. 51, 225–230.
Skerrett, S.J., Martin, T.R., 1994. Intratracheal interferon-gamma augments pulmonary defenses in experimental legionellosis. Am. J. Respir. Crit. Care Med. 149, 50–58.
Smithard, D.G., O'Neill, P.A., Park, C., Morris, J., Wyatt, R., England, R., et al., 1996. Complications and outcome after acute stroke. Stroke. 27, 1200–1204.
Sun, K., Metzger, D.W., 2008. Inhibition of pulmonary antibacterial defense by interferon-γ during recovery from influenza infection. Nat. Med. 14, 558–564.
Sun, F., Xiao, G., Qu, Z., 2017. Murine bronchoalveolar lavage. Bio Protoc. 7, e2287.
Tracey, M.D.K.J., PDA, Cerami, 1994. Tumor necrosis factor: A pleiotropic cytokine and therapuetic target. Annu. Rev. Med. 45, 491–503.
Trzciński, K., Li, Y., Weinberger, D.M., Thompson, C.M., Cordy, D., Bessolo, A., et al., 2015. Effect of serotype on pneumococcal competition in a mouse colonization model. mBio. 6, e00902–e00915.
Vila-del Sol, V., Punzón, C., Fresno, M., 2008. IFN-γ-induced TNF-α expression is regulated by interferon regulatory factors 1 and 8 in mouse macrophages. J. Immunol. 181, 4461.
Vogelgesang, A., May, V.E., Grunwald, U., Bakkeboe, M., Langner, S., Wallaschofski, H., et al., 2010. Functional status of peripheral blood T-cells in ischemic stroke patients. PLoS One 5, e8718.
Westendorp, W.F., Vermeij, J.-D., Zock, E., Hooijenga, I.J., Kruyt, N.D., Bosboom, H.J.L. W., et al., 2015. The preventive antibiotics in stroke study (PASS): a pragmatic randomised open-label masked endpoint clinical trial. Lancet 385, 1519–1526.
Wong, C.H., Jenne, C.N., Lee, W.Y., Léger, C., Kubes, P., 2011. Functional innervation of hepatic iNKT cells is immunosuppressive following stroke. Science. 334, 101–105.
Yoshida, A., Koide, Y., Uchijima, M., Yoshida TO, 1994. IFN-gamma induces IL-12 mRNA expression by a murine macrophage cell line, J774. Biochem. Biophys. Res. Commun. 198, 857–861.
Yoshida, K., Matsumoto, T., Tateda, K., Uchida, K., Tsujimoto, S., Iwakura, Y., et al., 2001. Protection against pulmonary infection with Klebsiella pneumoniae in mice by interferon-gamma through activation of phagocytic cells and stimulation of production of other cytokines. J. Med. Microbiol. 50, 959–964.

Supplement

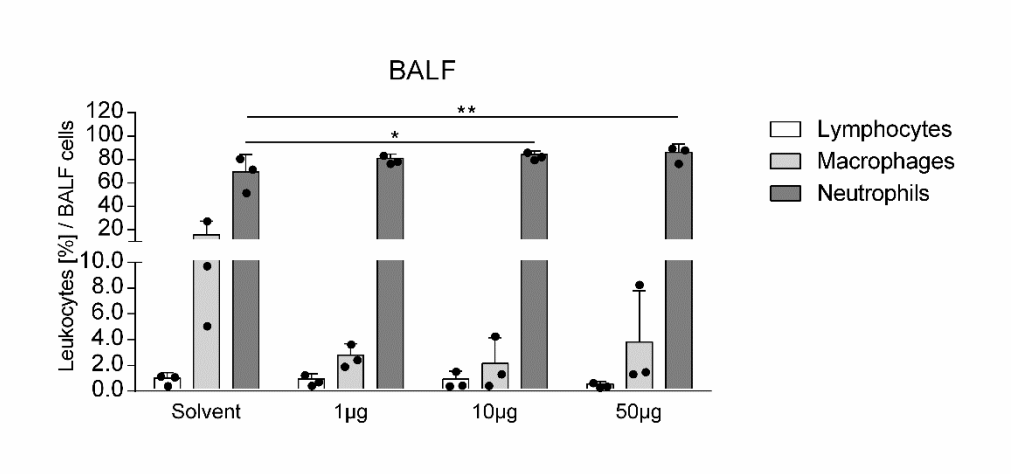

Figure S1: IFN-γ treatment changed cellular composition of BALF extracted from naïve mice. Cellularity of BALF analyzed 12 h after solvent or IFN-γ application in naïve mice indicate that IFN-γ resulted in a loss of macrophages and therefore a percentage increase of neutrophils in BALF. Data are shown as bars with mean ± SD (n=3) using two-way ANOVA and Dunn´s multiple comparison compared to solvent treated mice as reference group; * indicates $p<0.05$; ** $p<0.01$

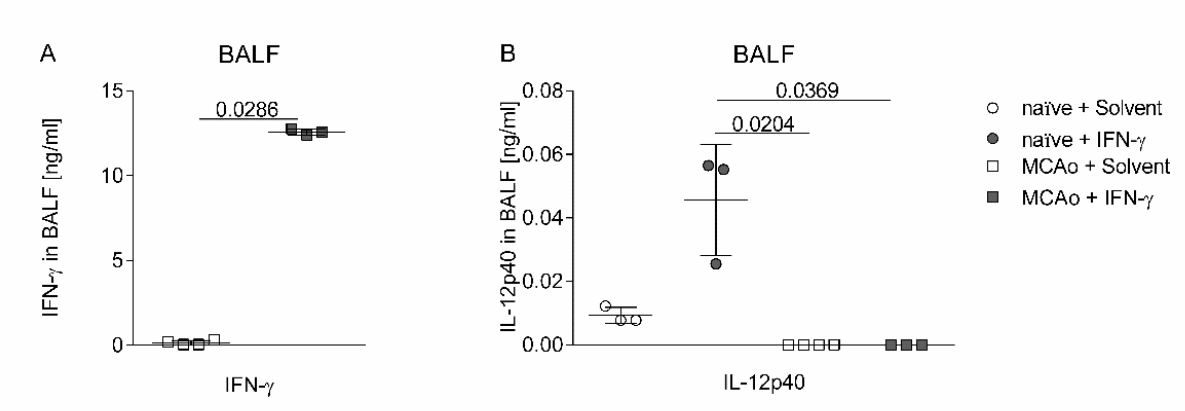

Figure S2: Induction of pulmonary IL-12p40 by IFN-γ treatment in naïve but not in MCAo mice. Analysis of IFN-γ levels in BALF of stroke mice revealed no endogenous IFN-γ secretion in solvent treated mice 36 h after stroke onset. In contrast, IFN-γ treatment one day after MCAo resulted in significantly increased IFN-γ levels in BALF within 12 h (A). IL-12p40 levels in lavage fluid were analyzed 12 h after i.t. application of solvent or IFN-γ in naïve mice and compared to stroke mice 36 h after MCAo. IFN-γ significantly increased IL-12p40 secretion in naïve but not stroke mice (B). Data from one experiment (n=3-4) are shown as scatter plots using Mann Whitney test or one-way ANOVA and Dunn´s multiple comparison.

9 CURRICULUM VITAE

Mein Lebenslauf wird aus datenschutzrechtlichen Gründen in der elektronischen Version meiner Arbeit nicht veröffentlicht.

10 PUBLICATION LIST

Jagdmann, S.; Berchtold, D.; Gutbier, B.; Witzenrath, M.; Meisel, A.; Meisel, C.; Dames, C. Efficacy and safety of intratracheal IFN-γ treatment to reverse stroke-induced susceptibility to pulmonary bacterial infections. *Journal of Neuroimmunology* **2021**, 355, 577568, doi:https://doi.org/10.1016/j.jneuroim.2021.577568. IF (2020): 3.125

Weitbrecht, L.; Berchtold, D.; Zhang, T.; **Jagdmann, S.**; Dames, C.; Winek, K.; Meisel, C.; Meisel, A. CD4(+) T cells promote delayed B cell responses in the ischemic brain after experimental stroke. *Brain Behav Immun* **2021**, *91*, 601-614, doi:10.1016/j.bbi.2020.09.029. IF (2020): 6.633

Winek, K.; Lobentanzer, S.; Nadorp, B.; Dubnov, S.; Dames, C.; **Jagdmann, S.**; Moshitzky, G.; Hotter, B.; Meisel, C.; Greenberg, D.S.; Shifman, S.; Klein, J.; Shenhar-Tsarfaty, S.; Meisel, A.; Soreq, H. Transfer RNA fragments replace microRNA regulators of the cholinergic poststroke immune blockade. *Proceedings of the National Academy of Sciences* **2020**, 10.1073/pnas.2013542117, 202013542, doi:10.1073/pnas.2013542117. IF (2019): 9.412

Schneider, B.; Glass, Ä.; **Jagdmann, S.**; Hühns, M.; Claus, J.; Zettl, H.; Dräger, D.-L.; Maruschke, M.; Hakenberg, O.W.; Erbersdobler, A.; Zimpfer, A. Loss of Mismatch-repair Protein Expression and Microsatellite Instability in Upper Tract Urothelial Carcinoma and Clinicopathologic Implications. *Clinical Genitourinary Cancer* **2020**, https://doi.org/10.1016/j.clgc.2020.03.006, doi:https://doi.org/10.1016/j.clgc.2020.03.006. IF (2019): 2.534

Binder, F.; Ryll, R.; Drewes, S.; **Jagdmann, S.**; Reil, D.; Hiltbrunner, M.; Rosenfeld, U.M.; Imholt, C.; Jacob, J.; Heckel, G.; Ulrich, R.G. Spatial and Temporal Evolutionary Patterns in Puumala Orthohantavirus (PUUV) S Segment. *Pathogens* **2020**, *9*, 548, doi:10.3390/pathogens9070548. IF (2019): 3.405

Jagdmann, S.; Dames, C.; Berchtold, D.; Winek, K.; Weitbrecht, L.; Meisel, A.; Meisel, C. Impact of Key Nicotinic AChR Subunits on Post-Stroke Pneumococcal Pneumonia. *Vaccines (Basel)* **2020**, *8*, doi:10.3390/vaccines8020253. IF (2019): 4.086

Straková, P.; **Jagdmann, S.**; Balčiauskas, L.; Balčiauskienė, L.; Drewes, S.; Ulrich, R.G. Puumala Virus in Bank Voles, Lithuania. *Emerg Infect Dis* **2017**, *23*, 158-160, doi:10.3201/eid2301.161400. IF (2016): 8.969

11 AKNOWLEDGMENT | DANKSAGUNG

Mein herzlichster Dank gilt an erster Stelle Dr. Christian Meisel und Prof. Dr. Andreas Meisel für die Unterstützung, Betreuung und das Vertrauen in den letzten Jahren. Vielen Dank vor allem für das spannende Thema, die kontinuierlichen Ermutigungen, die kritischen und produktiven Diskussionen, aber auch die wissenschaftliche Expertise.

Weiterhin bedanken möchte ich mich bei Prof. Dr. Hans-Dieter Volk, der mir die Möglichkeit gab, meine Dissertation am Institut für Medizinische Immunologie der Charité anzufertigen. Danken möchte ich ebenfalls Dr. Desirée Kunkel für die Einweisung und Unterstützung bei den FACS-Analysen. Vielen Dank an Prof. Dr. Ulrich Dirnagl, dass ich alle *in vivo* Experimente im Institut für experimentelle Neurologie durchführen konnte und an die Mitglieder der ExpNeuro für die Einweisungen in die Labore und Geräte.

Ebenfalls bedanken möchte ich mich bei Prof. Dr. Wolfgang Kummer für die Bereitstellung des α9/10 nAChR KO Maus Stamms, aber auch für die interessanten und anregenden Gespräche auf Kongressen. Vielen Dank an Prof. Dr. Hermona Soreq, dass ich Teil des spannenden Projekts „Transfer RNA fragments replace microRNA regulators of the cholinergic poststroke immune blockade“ sein durfte. Danken möchte ich außerdem Prof. Dr. Martin Witzenrath und Birgitt Gutbier für die Hilfe bei den Infektionsexperimenten.

Ein großer Dank gilt auch der AG Meisel, insbesondere Claudia, Daniel, Susanne und Kasia für die tatkräftige Unterstützung bei den umfangreichen *in vivo* Experimenten. Vielen Dank an Sabine und CMG für die Unterstützung bei den Infarktanalysen und den qRT-PCRs. Danke aber auch an Luis für die statistischen Ratschläge und an Andi für die Korrektur meiner Arbeit.

Ich bedanke mich auch bei den Mitarbeitern der AG Sawitzki und der AG Scheibenbogen für die Diskussion von Daten und Problemen, aber auch für die unterhaltsamen Mittagspausen und „Kuchenrunden“.

Ganz besonders danken möchte ich meiner Familie und meinen Freunden für die unvorstellbare Unterstützung, den Rückhalt und die vielen aufmunternden Worte während meiner gesamten Promotionszeit. Vielen Dank an meine Eltern, Großeltern, meinem Bruder Patrick und meiner Schwägerin Lisa. Vor allem möchte ich noch meinem Freund Jan danken, für die konstruktive Unterstützung und stetige Motivation. Ohne euch wäre die Erstellung meiner Dissertation nicht möglich gewesen. Danke, dass ihr an meiner Seite seid!